



LIBRARY
Michigan State
University

This is to certify that the

thesis entitled

Configurational Bias Monte Carlo Simulations of Phase Segregation in Networked Block Copolymers

presented by
Kent Ivan Palmer

has been accepted towards fulfillment of the requirements for

M.S. degree in Chemical Engineering

00

Maior professor

O-7639

MSU is an Affirmative Action/Equal Opportunity Institution

PLACE IN RETURN BOX to remove this checkout from your record. TO AVOID FINES return on or before date due. MAY BE RECALLED with earlier due date if requested.

DATE DUE	DATE DUE	DATE DUE
	•	
	·	

11/00 c/CIRC/DateDue.p65-p.14

Configurational Bias Monte Carlo Simulations of Phase Segregation in Networked Block Copolymers

Ву

Kent Ivan Palmer

A THESIS

Submitted to
Michigan State University
in partial fulfillment of the requirements
for the degree of

MASTER OF SCIENCE

Department of Chemical Engineering

2000

ABSTRACT

Configurational Bias Monte Carlo Simulations of Phase Segregation in Networked Block Copolymers

Ву

Kent Ivan Palmer

Crosslinked block copolymers are used as adhesives in fiber-reinforced composite materials manufactured for automotive applications. Good adhesion between the polymer matrix and fibers in the interphase region is required for the structural integrity of these materials. Experimental evidence indicates that superior adhesion is obtained when phase segregation occurs between the two matrix phase block copolymers. It is desirable to predict the conditions under which phase segregation is expected to occur. Configurational-bias Monte Carlo simulations of networked, two-component, trifunctional block copolymers were carried out to examine phase segregation in these materials. The effects of three principal parameters on phase segregation were examined: the weight fractions of the two components, the crosslink length, and the ratio of the square-well interactions. The molecular simulation results confirmed trends observed in laboratory measurements.

To my wife, Tiffany And my parents, Robert and Judy Palmer.

ACKNOWLEDGMENTS

I would like to thank my advisor Dr. Christian M. Lastoskie. His guidance, patience and support are deeply appreciated.

Thanks to Dr. Lawrence T. Drzal and Dr. Carl T. Lira for their insight and support as committee members.

Thanks also to Dr. Juan J. DePablo and Dr. Fernando Escobedo for the use of their Fortran Code. Their studies provided a helpful tool for this work.

I am also grateful to Robert Dombrowski for providing a second view, thought provoking discussions and making many hours in the lab bearable.

I thank the Chemical Engineering Department at Michigan State University for their support, as well as the opportunity to perform this work and advance my education.

TABLE OF CONTENTS

LIST OF TABLES	VII
LIST OF FIGURES	VIII
LIST OF FIGURES	VIII
LIST OF ABBREVIATIONS	XII
LIST OF ABBREVIATIONS	XII
1. INTRODUCTION	1
2. GENERAL BACKGROUND	3
2.1 Previous Experimental Work	
3. THEORTICAL CONSIDERATIONS	7
3.1 FLORY-HUGGINS THEORY	
4. METHODS	13
4.1 EXPERIMENTAL SETUP	18
4.2.2 CALCULATED RDF CURVES	20
5. RESULTS & DISCUSSION	22
5.1 GENERAL OBSERVATIONS	
5.1.2 RDF Behavior due to Square-Well model	24
5.2 Effect of Hard Segment Content	
5.2.2 Tone 301, 65% hard segment content	28
5.2.3 TONE 301 CONCLUSION	29
5.2.5 Tone 305, 50% hard segment content	
5.2.6 TONE 305, 63% HARD SEGMENT CONTENT	34
5.2.7 TONE 305 CONCLUSION	35
5.2.8 TONE 310, 13% HARD SEGMENT CONTENT	3 <i>6</i>
5.2.9 Tone 310, 37% hard segment content	

5.2.10 Tone 310, 50% hard segment content	40
5.2.11 TONE 310 CONCLUSION	41
5.3 EFFECT OF TONE SIZE	
5.3.2 50% HARD FRACTION	42
5.3.3 High Hard Fraction	42
5.4 EFFECT OF CROSS-LINKING	
5.4.2 Tone 310, 38% Hard Fraction, Incomplete Cross-Linking	45
5.4.3 Tone 310, 50% Hard Fraction, Incomplete Cross-Linking	47
5.5 EFFECT OF ε-RATIOS	
5.5.2 & RATIO OF 10	51
5.5.3 Node-Node Distribution for varying & ratios	52
5.7 COMMENT ON QUALITATIVE ANALYSIS	
6. CONCLUSIONS	60
7. RECOMMENDATIONS FOR FUTURE WORK	61
APPENDIX A	63
APPENDIX B	76
APPENDIX C	78
APPENDIX D	79
APPENDIX E	82
RIRLIOGRAPHY	80

LIST OF TABLES

TABLE 3-1 THEORETICAL AND EXPERIMENTAL PHASE SEGREGATION RESULTS	
TABLE 4-1 FULLY CROSS-LINKED SYSTEM SPECIFICATIONS	16
TABLE 4-2 PARTIALLY CROSS-LINKED SYSTEM PARAMETERS	17
TABLE 5-1 SUMMARY OF LENGTH OF RUNS	23
TABLE 5-2 SUMMARY OF PHASE SEGREGATION OBSERVED	. 55
TABLE D-1 SUMMERY OF AVERAGE ENERGY PER SITE	79
TABLE D-2 SUMMERY OF SYSTEM PACKING FRACTIONS	80
TABLE D-3 CROSS-LINK LENGTH AND PACKING FRACTION CORRELATION	. 81

LIST OF FIGURES

FIGURE 4-1. REPRESENTATION OF VARYING TONE SIZES IN MODEL 13
FIGURE 4-2. REPRESENTATION OF VARYING CROSS-LINK LENGTH 14
FIGURE 4-3. FULLY EXTENDED FULLY CROSS-LINKED SYSTEM15
FIGURE 5-1. GENERAL RDF, TONE 305, 17% HARD CONTENT, ε-RATIO = 0.1
FIGURE 5-2. RDF, TONE 301, 50% HARD CONTENT, ε-RATIO = 0.1 26
FIGURE 5-3. RDF, TONE 301, 65% HARD CONTENT, ε-RATIO = 0.1 28
FIGURE 5-4. RDF, TONE 305, 17% HARD CONTENT, ε-RATIO = 0.1 30
FIGURE 5-5. RDF, TONE 305, 50% HARD CONTENT, ε-RATIO = 0.1
FIGURE 5-6. RDF, TONE 305, 63% HARD CONTENT, ε-RATIO = 0.1
FIGURE 5-7. RDF, TONE 310, 13% HARD CONTENT, ε -RATIO = 0.1
FIGURE 5-8. RDF, TONE 310, 37% HARD CONTENT, ε -RATIO = 0.1
FIGURE 5-9. RDF, TONE 310, 50% HARD CONTENT, ε -RATIO = 0.140
FIGURE 5-10. RDF, TONE 305, 50% HARD CONTENT, ε-RATIO = 0.1, INCOMPLETE CROSS-LINKING43
FIGURE 5-11. RDF, TONE 310, 38% HARD CONTENT, ε–RATIO = 0.1, INCOMPLETE CROSS-LINKING45
FIGURE 5-12. RDF, TONE 310, 50% HARD CONTENT, ε–RATIO = 0.1, INCOMPLETE CROSS-LINKING47
FIGURE 5-13. RDF, TONE 310, 50% HARD CONTENT, ε–RATIO = 1 49
FIGURE 5-14. RDF, TONE 310, 50% HARD CONTENT, ε–RATIO = 10 51
FIGURE 5-15. NODE-NODE RDF, TONE 310, 50% HARD SEGMENT WITH VARYING ε-RATIOS52
FIGURE 5-16. SNAPSHOT: TONE 301, 50% HARD SEGMENT CONTENT 53

FIGURE 5-17. SNAPSHOT: TONE 301, 65% HARD SEGMENT CONTENT 54
FIGURE 5-18. EFFECT OF CONSTANT TONE SIZE FOR TONE 310 56
FIGURE 5-19. EFFECT OF CONSTANT TONE SIZE FOR TONE 30557
FIGURE 5-20. EFFECT OF CONSTANT HARD SEGMENT CONTENT - 50% 58
FIGURE 5-21. CORRELATION OF CROSS-LINK LENGTH WITH PACKING FRACTION
FIGURE A-1. RDF, TONE 301, 50% HARD CONTENT, ε-RATIO = 0.1, DIFFERENT CHAINS
FIGURE A-2. RDF, TONE 301, 50% HARD CONTENT, ε-RATIO = 0.1, SAME CHAINS
FIGURE A-3. RDF, TONE 301, 65% HARD CONTENT, ε-RATIO = 0.1, DIFFERENT CHAINS
FIGURE A-4. RDF, TONE 301, 65% HARD CONTENT, ε-RATIO = 0.1, SAME CHAINS64
FIGURE A-5. RDF, TONE 305, 17% HARD CONTENT, ε-RATIO = 0.1, DIFFERENT CHAINS
FIGURE A-6. RDF, TONE 305, 17% HARD CONTENT, ε-RATIO = 0.1, SAME CHAINS
FIGURE A-7. RDF, TONE 305, 50% HARD CONTENT, ε-RATIO = 0.1, DIFFERENT CHAINS
FIGURE A-8. RDF, TONE 305, 50% HARD CONTENT, ε-RATIO = 0.1, SAME CHAINS66
FIGURE A-9. RDF, TONE 305, 63% HARD CONTENT, ε-RATIO = 0.1, DIFFERENT CHAINS67
FIGURE A-10. RDF, TONE 305, 63% HARD CONTENT, ε-RATIO = 0.1, SAME CHAINS
FIGURE A-11. RDF, TONE 310, 13% HARD CONTENT, ε-RATIO = 0.1, DIFFERENT CHAINS68
FIGURE A-12. RDF, TONE 310, 13% HARD CONTENT, ε-RATIO = 0.1, SAME

FIGURE A-13. RDF, TONE 310, 37% HARD CONTENT, ε -RATIO = 0.1, DIFFERENT CHAINS69
FIGURE A-14. RDF, TONE 310, 37% HARD CONTENT, ε-RATIO = 0.1, SAME CHAINS
FIGURE A-15. RDF, TONE 310, 50% HARD CONTENT, ε-RATIO = 0.1, DIFFERENT CHAINS
FIGURE A-16. RDF, TONE 310, 50% HARD CONTENT, ε-RATIO = 0.1, SAME CHAINS70
FIGURE A-17. RDF, TONE 305, 50% HARD CONTENT, ε-RATIO = 0.1, INCOMPLETE CROSS-LINK, DIFFERENT CHAINS71
FIGURE A-18. RDF, TONE 305, 50% HARD CONTENT, ε-RATIO = 0.1, INCOMPLETE CROSS-LINK, SAME CHAINS71
FIGURE A-19. RDF, TONE 310, 38% HARD CONTENT, ε-RATIO = 0.1, INCOMPLETE CROSS-LINK, DIFFERENT CHAINS72
FIGURE A-20. RDF, TONE 310, 38% HARD CONTENT, ε-RATIO = 0.1, INCOMPLETE CROSS-LINK, SAME CHAINS72
FIGURE A-21. RDF, TONE 310, 50% HARD CONTENT, ε-RATIO = 0.1, INCOMPLETE CROSS-LINK, DIFFERENT CHAINS73
FIGURE A-22. RDF, TONE 310, 50% HARD CONTENT, ε-RATIO = 0.1, INCOMPLETE CROSS-LINK, SAME CHAINS73
FIGURE A-23. RDF, TONE 310, 50% HARD CONTENT, ε-RATIO = 1, DIFFERENT CHAINS74
FIGURE A-24. RDF, TONE 310, 50% HARD CONTENT, ε-RATIO = 1, SAME CHAINS74
FIGURE A-25. RDF, TONE 310, 50% HARD CONTENT, ε-RATIO = 10, DIFFERENT CHAINS75
FIGURE A-26. RDF, TONE 310, 50% HARD CONTENT, ε-RATIO = 10, SAME CHAINS75
FIGURE E-1. SNAPSHOT: TONE 305, 17% HARD SEGMENT CONTENT 82 FIGURE E-2. SNAPSHOT: TONE 305, 50% HARD SEGMENT CONTENT 83
FIGURE E-3. SNAPSHOT: TONE 305, 50% HARD SEGMENT CONTENT 83

FIGURE E-4. SNAPSHOT: TONE 310, 13% HARD SEGMENT CONTENT 8:	5
FIGURE E-5. SNAPSHOT: TONE 310, 37% HARD SEGMENT CONTENT 8	6
FIGURE E-6. SNAPSHOT: TONE 310, 50% HARD SEGMENT CONTENT 8	7

LIST OF ABBREVIATIONS

Symbol Definition

g(r) radial distribution function

H(r) pair number at radius r

H_{SUM} total number of pairs

k_B Boltzmann constant

MC Monte Carlo

N number of sites in system

N_{rdf} number of times radial distribution function called

p acceptance probability

P pressure

r radius

R_{in} inner radius of shell

R_{out} out radius of shell

T temperature

ΔU change in internal energy

U(r) interaction energy of a given radius

V_{BOX} simulation box volume

GREEK

 β inverse product of k_B and T

ε square-well potential depth

- λ maximum limit of energy well range
- σ site diameter

1. INTRODUCTION

Cross-linked, or networked, polymers are found in a larger variety of materials, including thermoplastics, thermosetting resins and elastomers. They find application in traditional fields like the textile and automotive industries, as well as newer areas such as biomedical applications. The automotive industry is the largest U.S. consumer of elastomeric polyurethanes (Kroschwitz, 1997), which belong to the family of cross-linked block co-polymers. Within this industry cross-linked polyurethanes are used in such applications as adhesives in fiber reinforced composite materials (e.g., bumper beams) and sealing materials (e.g., gasket applications). Studies (Dawson & Shortall, 1982; Kau, Baer, & Huber, 1989; Schwarz, Critchfield, Tackett, & Tarin, 1979; Yang & Lee, 1987) have shown that good adhesion between the polymer matrix and fibers in the interphase region is required for structural integrity of these composite and sealing materials. Agrawal and Drzal (1995a, 1995b, 1996) investigated the adhesion between polyurethane and glass using both experimental methods and adapted Flory-based thermodynamic calculations. Their study sought to identify correlations between the polyurethane structure and adhesion to glass surfaces. They were able to identify phase segregation as a major controlling factor of adhesion. The polyurethanes in their study consisted of varying diisocyanate content and three triols, the latter differentiated by their molecular weight. Both increased diisocyanate content and triol molecular weight where shown to increase the degree of phase segregation, and this in turn favored adhesion. Since phase segregation affects adhesion, it is of interest to investigate the phase segregation behavior in the matrix phase. The aim of this work is to investigate, using

molecular modeling, the effect of three principle parameters on phase segregation in the polymer matrix:

- 1. Hard Fraction Content
- 2. Cross-Link Length (or Tone molecular weight)
- 3. Ratio of interaction potentials

These parameters will be investigated by using isobaric-isothermal (NPT) Monte Carlo (MC) simulations to equilibrate fully cross-linked polymer networks. A further feature of this work is molecular simulations of dense, highly cross-linked systems. These results can then be compared with experimental data. Previous Flory-base calculations have had to resort to phase diagrams to investigate block copolymers. The work of this will investigate if molecular modeling provides an efficient method to predict phase segregation behavior.

2. GENERAL BACKGROUND

2.1 Previous Experimental Work

As part of their work on polyurethane-glass adhesion Agrawal and Drzal's work (1995a, 1995b, 1996) prepared polymers using polycaprolactone-based triol, toluene diisocyanate (TDI), and 1-4-butane diol (BDO) as chain extender. The triols varied in molecular weight and were identified by their trade names, in order of decreasing molecular weight, as Tone 0310, Tone 0305 and Tone 0301. The triol name refers to the Union Carbide trade name Tone®.

Agrawal and Drzal adopted Macosko's (1989) terminology of referring to TDI and BDO as hard segment and the triol component as soft segment. These descriptions refer to the high and low glass transition temperatures of the hard and soft segments respectively. Hard segment related transition temperatures obtained by Agrawal and Drzal (1995a) through differential scanning calorimetry experiments revealed that higher hard copolymer content increased the degree of phase segregation at a greater rate in the case of higher molecular weight soft segments than lower molecular weight segments. Tensile and iosipescu shear experiments also showed that higher tone molecular weight increased the degree of phase segregation. Near-infrared spectroscopy and Fourier transform infrared spectroscopy indicated that hard segment content also increased phase segregation development.

Additional experiments by Agrawal and Drzal (1995b), conducted with angular dependent X-ray photoelectron spectroscopy (ADXPS), detected an inter-phase region between the glass substrate and polyurethane matrix. ADXPS data showed that both the

composition and phase segregation of the matrix influenced the composition of the interphase region. To investigate the inter-phase region in terms of its surface free energy they conducted calculations using a method described by Eberhardt (1966) combined with an additive function proposed discussed by Van Krevelen (1990). These were compared with calculations based on contact angle measurements.

Agrawal and Drzal compared these calculations with data obtained from block-shear measurements and found a linear relationship between the polar surface free energy component and adhesion values. This higher polar surface free energy component was observed in phase-separated polyurethanes in which phase segregation had lead to butanediol/butandediol-derived moeities preferentially segregating to the polyurethane surface. This observation lead Agrawal and Drzal to conclude that "the mechanism of adhesion between the polyurethanes and the glass surface could be through the formation of an interphase region in which hydrogen bonding between the butanediol-rich interphase region and the hydroxylated glass surface places a key role." (1996) Experiments with pretreated glass furthermore lead them to assume that the effect of ionic or covalent bonding at the polyurethane/glass interphase was negligible.

2.2 Previous Network Simulation

Binder's (1995) review of work in molecular polymer simulations describes three methods of modeling cross-linked polymers.

The first system is a randomly linked (Duering, Kremer, & Grest, 1991; Grest & Kremer, 1990a, 1990b; Lay, Sommer, & Blumen, 1999; Plischke & Barsky, 1998; Schulz & Sommer, 1992; Sommer, 1994; Sommer, Schulz, & Trautenberg, 1993) network. This

structure is created by randomly cross-linking an equilibrated melt and most closely resembles radiation cross-linked or vulcanized polymers. A quantitative description in this case is difficult though due to variations in parameters such as cross-link length, chain length, and dangling chain ends.

The second type is an end-linked network. In this case an equilibrated monodisperse melt is kinetically cross-linked at the ends, either by defining a certain percentage of chain ends as multi-functional sites which can bond with more than two sites (Duering, Kremer, & Grest, 1993, 1994; Grest, Kremer, & Duering, 1992, 1993; Kenkare, Hall, & Khan, 1999; Kenkare, Smith, Hall, & Khan, 1998) or using cross linkers (Hölzl,

Trautenberg, & Göritz, 1997; Trautenberg, Sommer, & Göritz; 1995). The advantage of this system is that all cross-links have the same length.

While the two types described consist of partially connected networks, the third type represents the most idealized system, the fully connected network. This network type provides the highest degree parameter control. Fully connected networks have both been used to study simple networks (Escobedo & de Pablo, 1996, 1997a), as well as gel swelling behavior (Escobedo & de Pablo, 1997a, 1997b) by including solvent molecules in the latter case.

Lay et al. (1999) and Escobedo and de Pablo (1996, 1997a, 1997b) conducted computer simulations specifically involving fully connected structures. Lay et al. conducted lattice-based bond-fluctuation MC moves on stochastically cross-linked diblock copolymers to investigate structural behavior based on A-B repulsion parameters. These results were compared with those of a cross-linked homopolymer and networks with a diamond topology, both with comparable cross-link density. This was accomplished by

randomly cutting cross-linking strands in the diamond topology case. They observed that the fully connected lattice required a higher number of dangling ends than the randomly linked structure to show similar results.

Escobedo and de Pablo conducted athermal and square-well NPT MC moves on a defect-free continuum diamond-like structure. They investigated P-V behavior and attractive interaction effects on system packing fraction. As part of their work they developed and examined the capability of extended continuum configurational-bias (ECCB) (Escobedo & de Pablo, 1995b), "cluster" (Escobedo & de Pablo, 1997b), "hole" (Escobedo & de Pablo, 1995b) and 'slab' (Escobedo & de Pablo, 1995a) moves to handle cross-linked networks with trifunctional and tetrafunctional nodes. The importance of their work lies among other things in the methods developed to simulate highly cross-linked polymer networks.

In general, research of fully connected networks has been limited to homopolymers, whereas randomly linked systems have been used in copolymer research.

3. THEORTICAL CONSIDERATIONS

3.1 FLORY-HUGGINS THEORY

Agrawal and Drzal performed Flory-Huggins theory (Flory, 1953) based calculations and compared these results with experimental observations. This theory is the most commonly used theoretical approach to polymer blends (Nath, McCoy, Curro, & Saunders, 1995) and uses a dimensionless quantity, the Flory interaction parameter χ , to describe the interaction energy between the polymers.

$$\chi = \frac{V_R}{R * T} (\delta_H - \delta_S) \tag{1}$$

Eq. (1) shows that the Flory interaction parameter χ is a function of a reference volume V_R , temperature T, the universal gas constant R and solubility parameters δ_S and δ_H for soft and hard segments respectively. The solubility difference in polymers is the important driving force for phase segregation (Macosko, 1989). This solubility difference can be estimated using χ (Van Krevelen, 1990).

Agrawal and Drzal obtained χ -values using both a group contribution method (Van Krevelen, 1990) and listed values. Phase segregation occurs when χ exceeds the critical interaction parameter χ_C . The critical interaction parameter is described by Eq. (2):

$$\chi_C = \frac{1}{2} \left[\frac{1}{\sqrt{N_A}} + \frac{1}{\sqrt{N_B}} \right] \tag{2}$$

 N_A and N_B represent the number of polymer repeat units. Equations (1) and (2) predict that phase segregation will occur as the solubility difference between solubility

parameters increases and as chain lengthy increases. The Flory-Huggins method of using χ and χ_C to predict phase segregation applies to polymer blends.

Polyurethanes being block copolymers necessitated Agrawal and Drzal to resort to phase diagrams developed by Benoit and Hadziioannou (1988) for multiblock copolymers to obtain χ_C . These calculations allowed Agrawal and Drzal to predict phase segregation occurrence.

TABLE 3-1 THEORETICAL AND EXPERIMENTAL PHASE SEGREGATION RESULTS

Tone Polymer	Hard Segment	Phase Segregation		
	(Wt%)	Flory Theory	Experiment	
310	22	no	no	
310	37	yes	no	
310	47	yes	maybe	
310	51	yes	yes	
310	67	yes	yes	
305	36	no	no	
305	47	yes	no	
305	60	yes	yes	
305	68	yes	yes	
301	47	no	no	
301	61	no	no	
301	68	no	no	

Note. Flory Theory results are taken from Agrawal & Drzal, 1995b. Experimental results are taken from Agrawal & Drzal 1996.

Table 3-1 shows the results obtained by Agrawal & Drzal. They observed good qualitative agreement between Flory-Huggins calculations and experimental results, though differences regarding the onset of phase segregation were observed.

Theoretical work using modified Flory-Huggins theories have been conducted by de Gennes (1979) and Vargas and Barbosa (1998). Their work predicts that partial phase segregation occurs at a transition temperature, total phase segregation being prevented due to the cross-linking.

3.2 MOLECULAR SIMULATIONS

The development of rudimentary computers during Word War II first made molecular simulations possible. Molecular modeling manipulates models of comparatively small number of molecules to create different configurations, termed ensembles. The averages of these ensembles are comparable to observed experimental properties, which themselves are an average of behavior at the molecular level behavior.

These averages can be calculated either as time averages, as in the Molecular Dynamic (MD) approach, or as ensemble averages, as in the Monte Carlo (MC) approach. Both MD and MC represent the two main areas of molecular simulation. MD solves the classical equations of motion of the system particles. The resulting molecular mechanical properties are time averaged. MC simulations create a large number of system configurations. The weighted contribution of each configuration to the ensemble average is determined by its occurrence probability. MC allows more efficient equilibration than MD, whereas MD allows the collection of kinetic data.

MC simulations ensembles are generated by moving an arbitrarily chosen particle to a randomly determined location. The trial move is then accepted or rejected according to an importance sampling scheme proposed by Metropolis, Rosenbluth, Rosenbluth, Teller and Teller (1953). In this scheme Eq. (3) produces an acceptance probability p.

$$p = \exp(-\beta \Delta U) \tag{3}$$

In Eq. (3) ΔU is the change in energy between the two ensembles, β the inverse of the product of the Boltzmann constant k_B and absolute temperature T (i.e. $1/[k_BT]$). A generated random number is then compared with p. If the random number is smaller than p the move is accepted. This method is sufficient for small molecules. The probability of moving a whole molecule successfully using the method by Metropolis et al. (1953) decreases as the molecule size increases. This lead to work by Rosenbluth and Rosenbluth (1955) with polymer configurations, which provided the basis for the configurational-bias (CB) MC method developed by Siepman and Frenkel (1992).

Further work by de Pablo, Laso and Suter (1992) was able to expand this concept to the continuum environment. They termed their method the continuum configuration-bias (CCB) MC. Both CBMC and CCBMC involve cutting of a randomly chosen polymer chain end and regrowing the end site by site. In dense systems only relatively short molecule segments can be successfully regrown using CBMC and CCBMC, thus making simulation of chain middle segments difficult and unlikely. Both CB methods can not be applied to ring polymers.

The Crank-shaft move allows the movement of a single middle chain site and has been used successfully by various authors (Kumar, Vacatello, & Yoon, 1988; Li & Chiew,

1994). Escobedo and de Pablo (1995b) devised a method by which an arbitrary section of a chain molecule, including intra-chain and trifunctional segments, can be cut and regrown with chain closure assured. They termed this method extended continuum configurational bias (ECCB) MC. This method is used in this work to equilibrate the system thermally. The 'slab' method developed by Escobedo and de Pablo (1995a) is used to equilibrate the system mechanically. In this case the volume move is performed by arbitrarily selecting a slab of the simulation box, changing its width and repositioning the sites within the slab to satisfy connectivity restraints.

4. METHODS

4.1 EXPERIMENTAL SETUP

Simulations were conducted on 2 types of systems. Both systems consisted of strings of sphere, each sphere referred to as a "site" and representing a 90 g/mol molecular weight unit. These sites were created using the "united atom" model, according to which intra-molecular structures and interactions are combined into an overall structure represented by a sphere of a given diameter. The experimental basis for this research was the work conducted by Agrawal & Drzal (1995a, 1995b, 1996), hence the model is based on the polyurethane copolymers used in their work. For this work butane diol [HO-CH₂-CH₂-CH₂-CH₂-CH₂-OH] was represented by one sphere and toluene diisocyanate [CH₃(C₄H₃)(NCO)₂] was represented by two spheres.

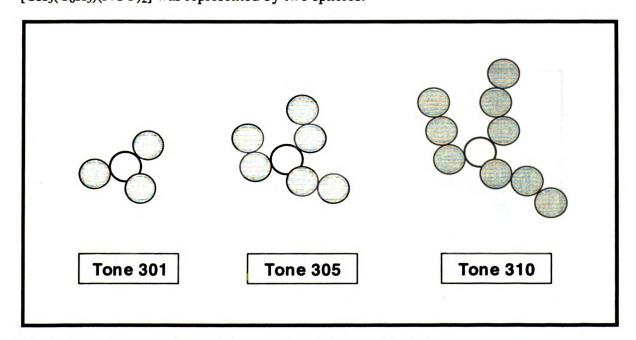


Figure 4-1. Representation of varying Tone sizes in Model

The polycaprolactone-based triols of varying molecular weight were modeled according to Figure 4-1. The sites with three neighbors are termed nodes. For the purpose of this work the Tone 0301, Tone 0305 and Tone 0310 polymers are referred to as Tone 301, Tone 305 and Tone 310 respectively and "Tone" collectively. The strings of soft sites (hashed spheres in Figure 4-1) 'going out' from a node are termed node arms.

Of the two types of systems modeled, the first was fully connected (i.e. no dangling or lose ends). This system type was built by placing nodes on a diamond lattice and cross-linking the nodes with freely jointed hard-sphere sites using ECCB type moves. The lattice structure was modified so that each node was trifunctional, as opposed to the usual diamond structure with four neighbors. The sites had a fixed bond length, but no restriction on bond angels. All cross-links were the same length and contained the same fraction of hard and soft sites. The cross-link length depended both on Tone molecular weight and hard segment content. Figure 4-2 shows how cross-link length varies with varying hard segment content.

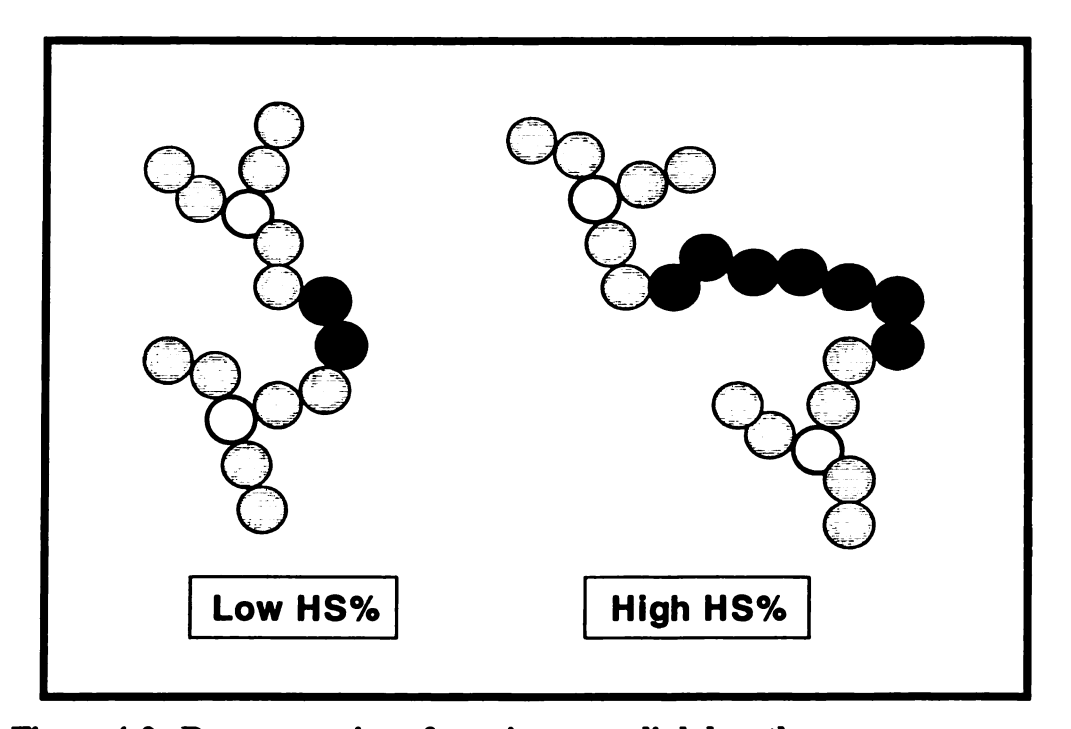


Figure 4-2. Representation of varying cross-link length.

In Figure 4-2 the nodes are represented by white spheres, hard sites by black spheres and soft node arm sites by hashed spheres. As the hard segment content changes, the number of hashed spheres remains constant and the count of black spheres increases. This corresponds to the experimental situation of constant tone size with varying hard segment content. Varying the Tone size on the other hand in the model is equivalent to keeping the number of black spheres constant and varying the number of shaded spheres in each node arm. The building process insured that both this type of system was fully connected (i.e. not dangling ends) and that all nodes were trifunctional. Figure 4-3 shows a view of a fully extended fully cross-linked system from one side of the simulation box.

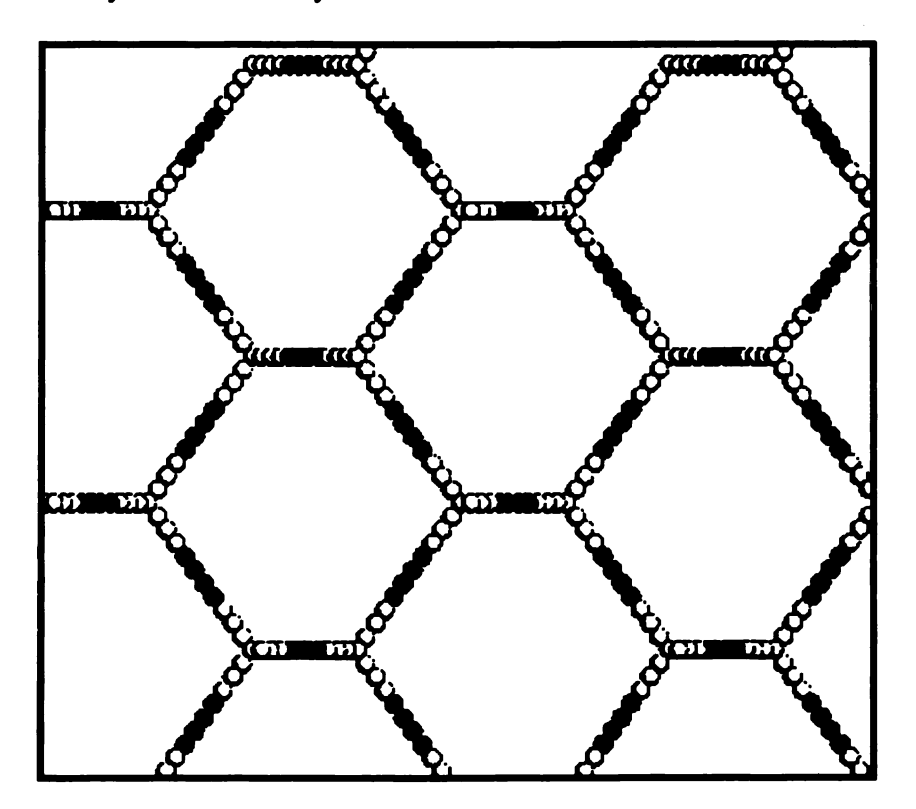


Figure 4-3. Fully extended fully cross-linked system.

The clear spheres correspond to soft sites, the black spheres to hard sites in the crosslinks. The diamond lattice structure is apparent in Figure 4-3. Once the structure was built, all sites (including nodes) were free to move, as long as bonding constraints (i.e. constant bond length) were respected. The system was not restricted by a fixed lattice structure.

TABLE 4-1 FULLY CROSS-LINKED SYSTEM SPECIFICATIONS

Tone 301	Tone 305	Tone 310
	17 % Hard Segment Cont.	13 % Hard Segment Cont.
	1836 Sites in System	2484 Sites in System
		37 % Hard Segment Cont.
		1024 Sites in System
50 % Hard Segment Cont.	50 % Hard Segment Cont.	50 % Hard Segment Cont.
1836 Sites in System	928 Sites in System	1312 Sites in System
65 % Hard Segment Cont.	63% Hard Segment Cont.	
2484 Sites in System	1216 Sites in System	·

Table 4-1 shows the details of the fully cross-linked systems modeled in this work. The system parameters where chosen to allow comparison with samples prepared in the work by Agrawal & Drzal (1995a, 1995b, 1996). In all cases in Table 4-1 the ratio of soft to hard energy well depth ($\varepsilon_{ss}/\varepsilon_{hh}$) was 0.1. The choice of this system also allowed the effect of increasing hard segment content and tone size (cross-link length) to be investigated. Further system statistics can be found in Appendix B.

Special cases of fully cross-linked systems were used to investigate the effect of varying the energy-well depth ratio. The Tone 310, 50% hard segment content system was modified, so that the $\varepsilon_{ss}/\varepsilon_{hh}$ -ratio was 1 and 10. These two systems were then compared with the original case shown in Table 4-1.

The second type of system modeled was partially connected. This system type was created by placing nodes randomly in a simulation box, placing soft sites to create node arms and randomly linking the arms with hard sites. The building process insured that at least one hard site was contained in each cross-link. This type of system contained dangling ends and a distribution of cross-linked and dangling end lengths.

TABLE 4-2 PARTIALLY CROSS-LINKED SYSTEM PARAMETERS

Tone Type	Hard Segment Content (%)	Average number of sites in cross-links	Average number of sites in lose ends	Total number sites in system
0305	50	5.5	7.2	989
0310	38	7.5	6.6	1066
0310	50	7.4	9.8	1071

Table 4-2 shows statistics for the partially connected systems, also termed modified systems. The system parameters where chosen to allow a comparison with similar cases among the fully cross-linked systems (see Table 4-1). Further statistics on the modified systems can be found in Appendix B.

In all systems Isothermal-isobaric (NPT) Monte Carlo (MC) simulations were conducted using periodic boundary conditions to simulate bulk behavior. As afore mentioned, 'slab' and ECCB moves developed by Escobedo and de Pablo (1995a, 1995b) were used to equilibrate the system mechanically and thermally.

The NPT simulations were run at 373 K and 1 atm, corresponding to polyurethane curing conditions in experiments conducted by Agrawal & Drzal (1995a). Detailed calculations of reduced parameters are found in Appendix C.

Modeling was conducted with the square-well energy function as defined in Eq. (4):

$$U(r) = \infty \qquad \sigma < r$$

$$= -\varepsilon \qquad \sigma \le r \le \lambda \sigma \qquad (4)$$

$$= 0 \qquad \lambda \sigma < r$$

In Eq. (4), r is the distance between site centers, σ the site diameter, ε the energy well depth and (λ -1) the width of the well. The hard-hard interaction $\varepsilon_{hh} = 1.0$ corresponds to the ε calculated in Appendix C. The soft-soft interaction ε_{ss} has a value 1/10th of that of ε_{hh} , i.e. $\varepsilon_{ss} = 0.1$. The hard-soft interaction ε_{hs} is defined by the Lorentz-Berthehold rule, which states that $\varepsilon_{hs}^2 = \varepsilon_{hh}\varepsilon_{ss}$.

All systems were initially equilibrated with a ratio of ECCB to volume moves of 1:1. As packing fraction and system energy curves showed a significant decrease in slope the ratio of ECCB moves to volume moves was switched to 2,500:1 or 10,000:1 for more efficient sampling.

4.2 RADIAL DISTRIBUTION FUNCTIONS

Phase segregation of hard and soft segments was investigated with radial distribution functions (RDF). The RDF is a subset of pair correlation functions in which molecular interactions are described by spherical potentials. The RDF is obtained by Eq. (5),

$$g(r) = \frac{H(r)V_{BOX}}{H_{SUM} \frac{4}{3}\pi(R_{out}^3 - R_{in}^3)N_{rdf}}$$
(5)

where H(r) is the number of pairs in a shell with a central radius r, V_{BOX} the volume of the simulation box, H_{SUM} the total number of pairs, and N_{rdf} the number of times the RDF is measured during the run. The shell for which H(r) is counted is described by R_{out} and R_{in} , the outer and inner radius respectively. These values are defined as $r + -0.05\sigma$. In

the case of polymers the RDF does not include nearest bonded neighbors in its calculations. These neared bonded neighbors are always at the same distance from a given site, and thus their inclusion in the RDF would both not provide any new information and possibly obstruct noteworthy results.

The RDF is a measure of the correlation between molecule pairs and the resulting structure of the fluid. In a physical sense, the RDF represents the likelihood relative to the bulk number density of finding a second molecule at a given distance r from the center of a molecule. Values of the radial distribution function g(r)=1 indicate no correlation between the molecules. This indicates that the bulk density and local number density are identical and hence the presence of one molecule does not affect the position of another molecule. If $g(r)\neq 1$, then the first molecule affects the likelihood of finding the second molecule in the area. Specifically if g(r)>1, then the probability is enhanced with regards to the average density that a site lies at that distance. Conversely if g(r)<1 there is a decreased probability.

4.2.1 DETERMINATION OF PHASE SEGREGATION

Thermodynamics teaches that the mixing process is a function of both energy and entropy. These factors are considered in Monte Carlo simulations where the number of possible ensembles affects the configurations sampled and the energetic interactions contribute to the acceptance criteria. From an energetic viewpoint phase segregation occurs when interactions between like-copolymers become larger then between unlike copolymers and an 'un-mixing' or phase segregation occurs. The RDF graph reflects this phenomenon of phase segregation when both the soft-soft and hard-hard curves have greater magnitude than the hard-soft curve.

4.2.2 CALCULATED RDF CURVES

Systems are evaluated using three types of radial distribution functions: soft-soft, hard-hard, and hard-soft. In the soft-soft case the variable H(r) of Eq. (5) only counts pairs of soft sites. The other two RDFs only count pairs consisting of the site types indicated by the curve name.

Four additional RDF types, listed in Appendix A, are used in certain cases to clarify the relative contribution of sites on the same node or segment vs. sites on different nodes or segments. In this case the variable H(r) of Eq. (5) only counts pairs of:

- 1) soft sites on the same node (i.e. nodal site and node arms)
- 2) hard sites on the same segment
- 3) soft sites on different nodes
- 4) hard sites on different segments

The H_{SUM} of points 1 and 3 is the total number of all soft pairs, *NOT* the number of soft pairs on different nodes or on the same node. The same applies to the hard site measurements.

5. RESULTS & DISCUSSION

5.1 GENERAL OBSERVATIONS

5.1.1 LENGTH OF RUNS

Table 5-1 on the following page shows a summary of the systems simulated and corresponding number of ECCB and volume moves. In all cases the partially linked systems require a smaller number of volume moves compared to the fully cross-linked systems to calculate an equilibrated system. In two cases this also applies to the ECCB moves. The exception is the Tone 305 – 50% hard content system. In this case more ECCB moves were necessary. One must consider though that volume moves are computationally more expensive. It follows that the partially linked system presents a model that allows a more efficient calculation of the equilibrated structure.

TABLE 5-1 SUMMARY OF LENGTH OF RUNS

	ARI OF DENGIN								
Tone	Hard Segment Content (%)	Number of Volume Moves	Number of ECCB Moves	Number of Sites in System					
Fully Cross-									
Linked Systems									
301	50	3.08E+05	1.76E+08	1836					
301	65	2.03E+05	4.52E+07	2484					
305	17	2.63E+05	1.74E+07	1836					
305	50	6.01E+05	7.30E+07	928					
305	63	3.36E+05	1.11E+08	1216					
310	13	1.89E+05	1.53E+08	2848					
310	37	5.07E+05	2.26E+08	1024					
310	50	4.18E+05	2.92E+08	1312					
Partially Cross-									
Linked Systems									
305	50	3.13E+05	1.65E+08	989					
310	38	3.19E+05	9.53E+07	1066					
310	50	2.61E+05	1.83E+08	1071					

5.1.2 RDF BEHAVIOR DUE TO SQUARE-WELL MODEL

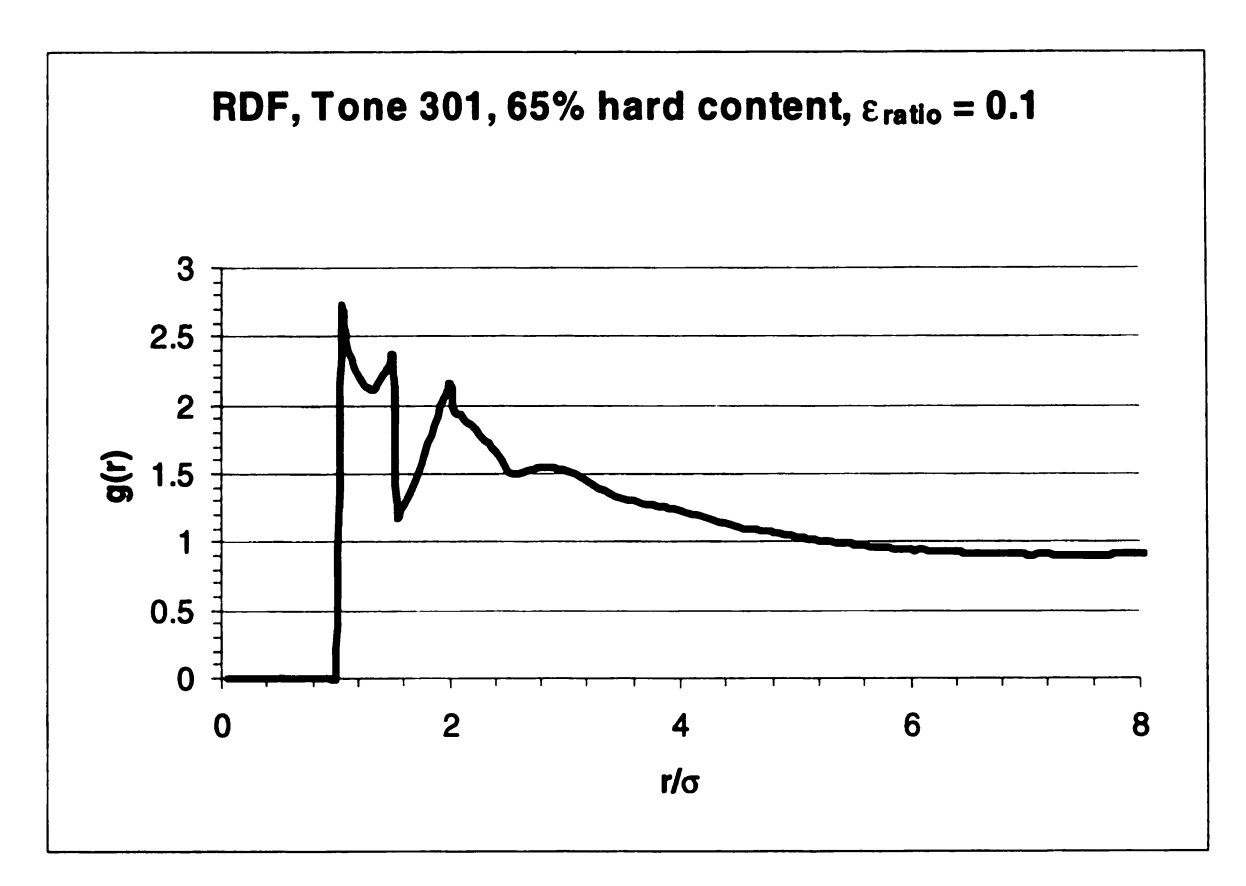


Figure 5-1. General RDF, Tone 305, 17% hard content, ε -ratio = 0.1

Figure 5-4 shows a general RDF of a given system (e.g. Tone 305, 17% hard content) and serves as illustration for the following discussion. The general curve correlates all sites, without respect for hard or soft sites. All RDF curves show a g(r)=0 for σ -values below 1.0 σ . Most of the RDF curves show a peak at 1.0 σ and a local maximum followed by a local minimum at 1.5 σ . This behavior is a result of the energy model chosen for the simulations: the square-well potential model. At values smaller than 1.0 σ the hard spheres cannot overlap and have an infinite repulsion. The energy well with a depth of ε between 1.0 σ and 1.5 σ leads to energetically favorable interactions of site pairs within this radius and normally larger g(r) values. Sites within this well form a cluster around

the site, creating what is commonly referred to as a first coordination shell. This cluster of sites physically prevent other sites from occupying space near the coordination shell, leading to the local minimum around 1.5 σ . The curve falls off after the 1.0 σ peak, but peaks around 1.5 σ , right before falling to the local minimum. This is explained by the sites in the region preferentially falling' into the energy well if possible. In the case of fluids these local structures, and associated short-range correlations, determine the uniqueness of the thermodynamic properties.

Whereas the RDF behavior to the left of $1.5 \,\sigma$ is explained by the potential model, the behavior to the right of $1.5 \,\sigma$ is a result of the composition and structure of each individual run. The discussion of each of these runs in detail follows. In the following discussion soft sites are identified as being associated with nodes. Hard sites are identified as being associated with segments, the segment referring to the central section of the cross-link that they occupy.

In the following discussion, the term "short-range" will refer to distances less than 1.5 σ , and "long-range" to distances larger than 1.5 σ .

5.2 Effect of Hard Segment Content

5.2.1 TONE 301, 50% HARD SEGMENT CONTENT

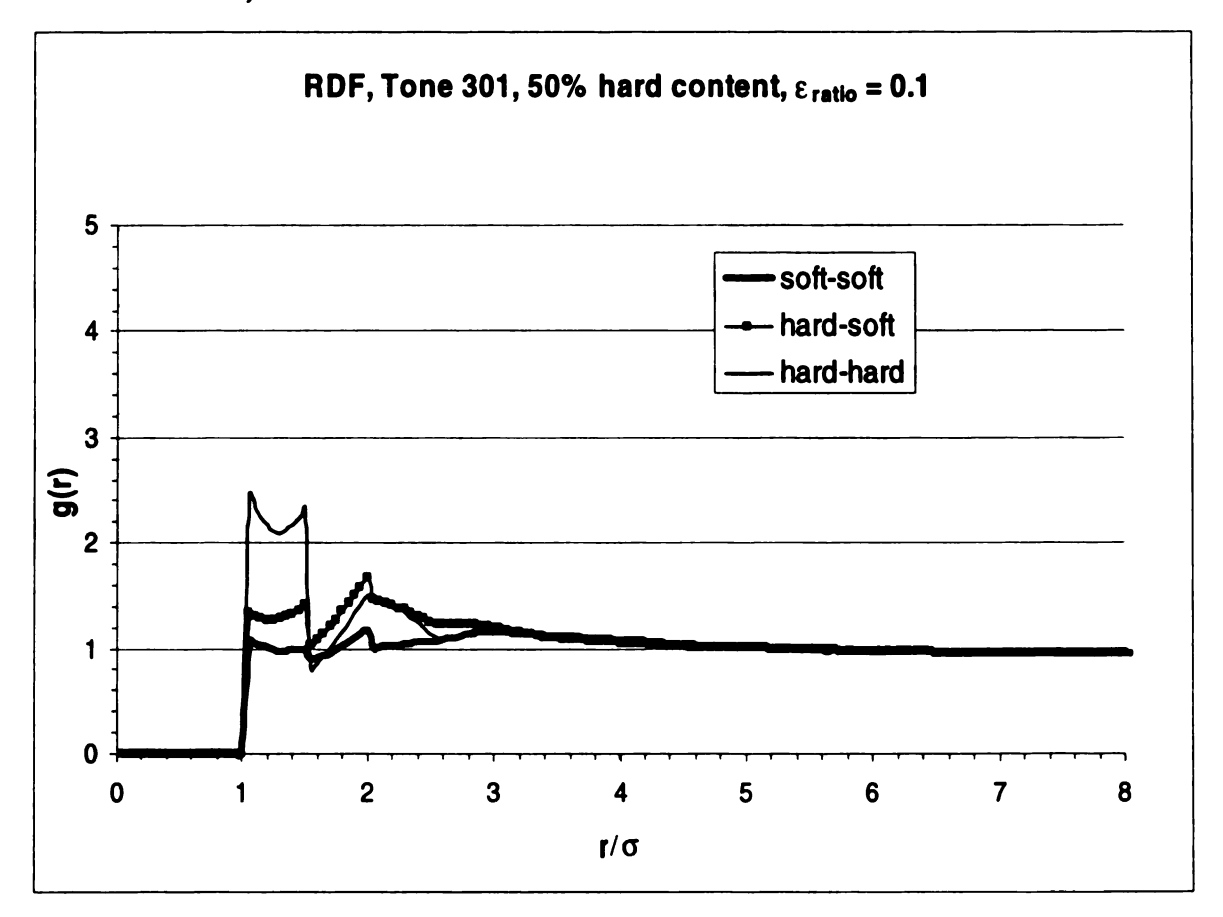


Figure 5-2. RDF, Tone 301, 50% hard content, ε -ratio = 0.1

In this system the soft sites on a given node are no further then 2 σ from each other, hence the sharp drop after 2 σ signifies the transition from intra-nodal to inter-nodal correlation. The weak correlation at long range corresponds to the distance of soft sites on different node arms. This follows from the hard segment length of three sites. The weak short-range behavior stands in contrast to Figure A-2, which indicates that the majority of sites on a given node arm lie at short-range distance. This is explained by the

fact that for Tone 301 the nodes lie at most 2 σ from each other. The correlation in Figure A-2 is a result of the bonded nature of the system, not energetic interactions. The greater correlation of the hard-hard curve, compared to the soft-soft curve, is due to the stronger hard-hard interaction. The absence of a sudden drop after 2 σ in the hard-hard curve represents correlation beyond the 2 σ range between different hard segments, since hard sites on the same segment are at most 2 σ apart. Figures A-1 and A-2 indicate that a substantial amount of interaction in the square-well range is due to sites from different segments. As the hard segments align with each other they position the nodes on average 3 σ to 4 σ from each other. This fact is indicated by the soft-soft curve behavior within this range.

The hard-soft curve in Figure 5-2 does not indicate phase segregation. Though the hard sites appear to interact strongly with each other, the system as a whole does not phase segregate.

5.2.2 TONE 301, 65% HARD SEGMENT CONTENT

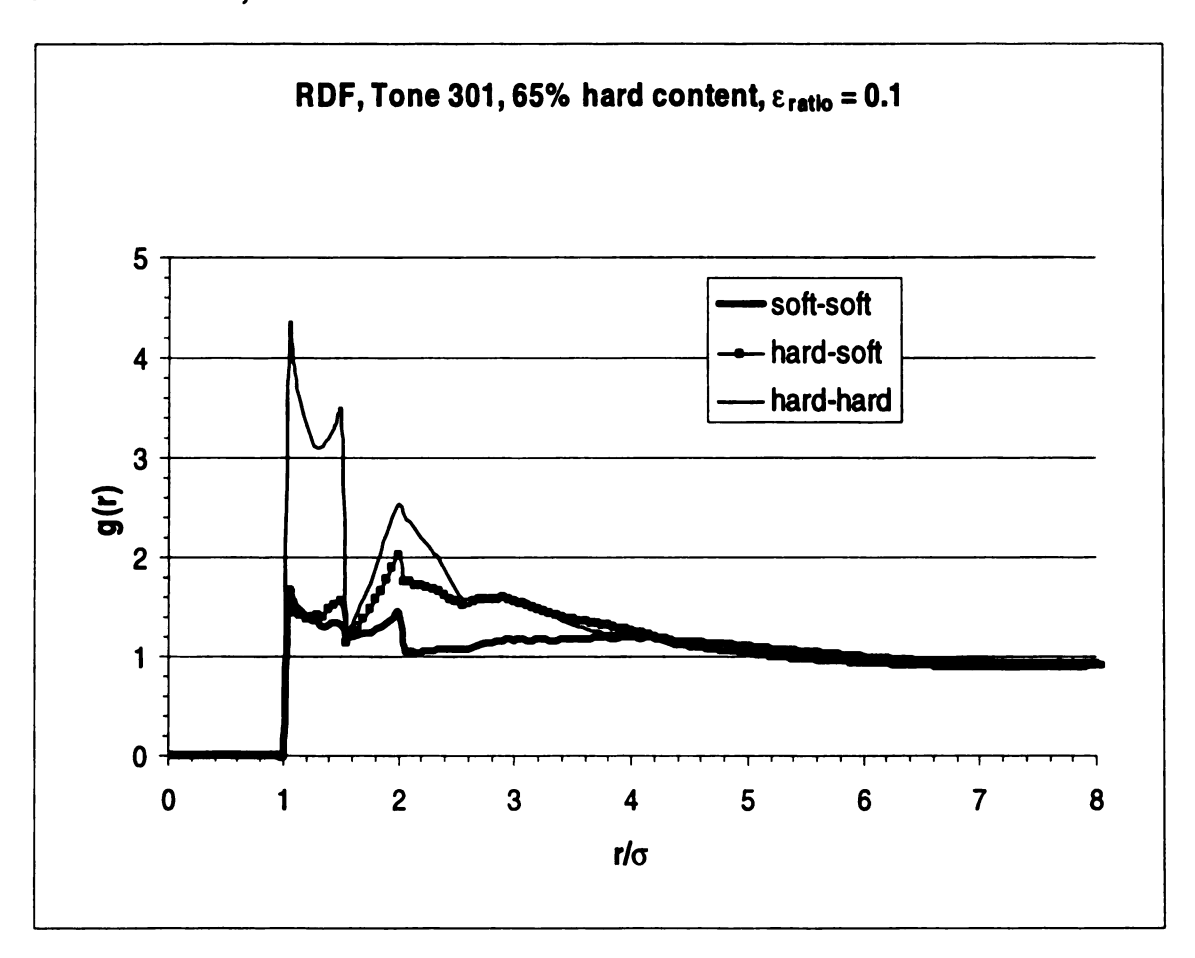


Figure 5-3. RDF, Tone 301, 65% hard content, ε -ratio = 0.1

The soft-soft peak at 1 σ is shown in Figure A-3 and A-4 to result mostly from node arms on the same node moving within this range to each other. The peak of the same curve at 2 σ is the result of sites on the same node being no further than 2 σ from each other. The 3 σ to 5 σ range curve behavior shows the physical limitation imposed on nodal movement by a hard segment of 5 sites.

Figures A-3 and A-4 show the hard-hard short-range behavior to be more strongly influenced by hard sites on the same hard segment when compared with the Tone 301, 50% hard segment case. This is due to the greater number of hard sites, three vs. five, in

each segment. A major contribution to the curve at this short range still comes from hard sites on different segments, so that here too the hard segments align with each other. Figure A-4 also shows that there is no hard site correlation between sites on the same segment beyond 3 σ . The hard segment appears to have contracted substantially. The longer-range correlation in this case is again due to different segments interacting with each other.

The relation of the curves to each other here also shows no phase segregation.

5.2.3 TONE 301 CONCLUSION

In both cases the stronger interaction between the hard segments leads to the hard segments folding on themselves and their alignment with each other. This behavior determines the placement of the nodes in relationship to each other. As the cross-link increases in number of sites, the node arms on the same node show more freedom to move together. In both cases no phase segregation was observed.

5.2.4 Tone 305, 17% hard segment content

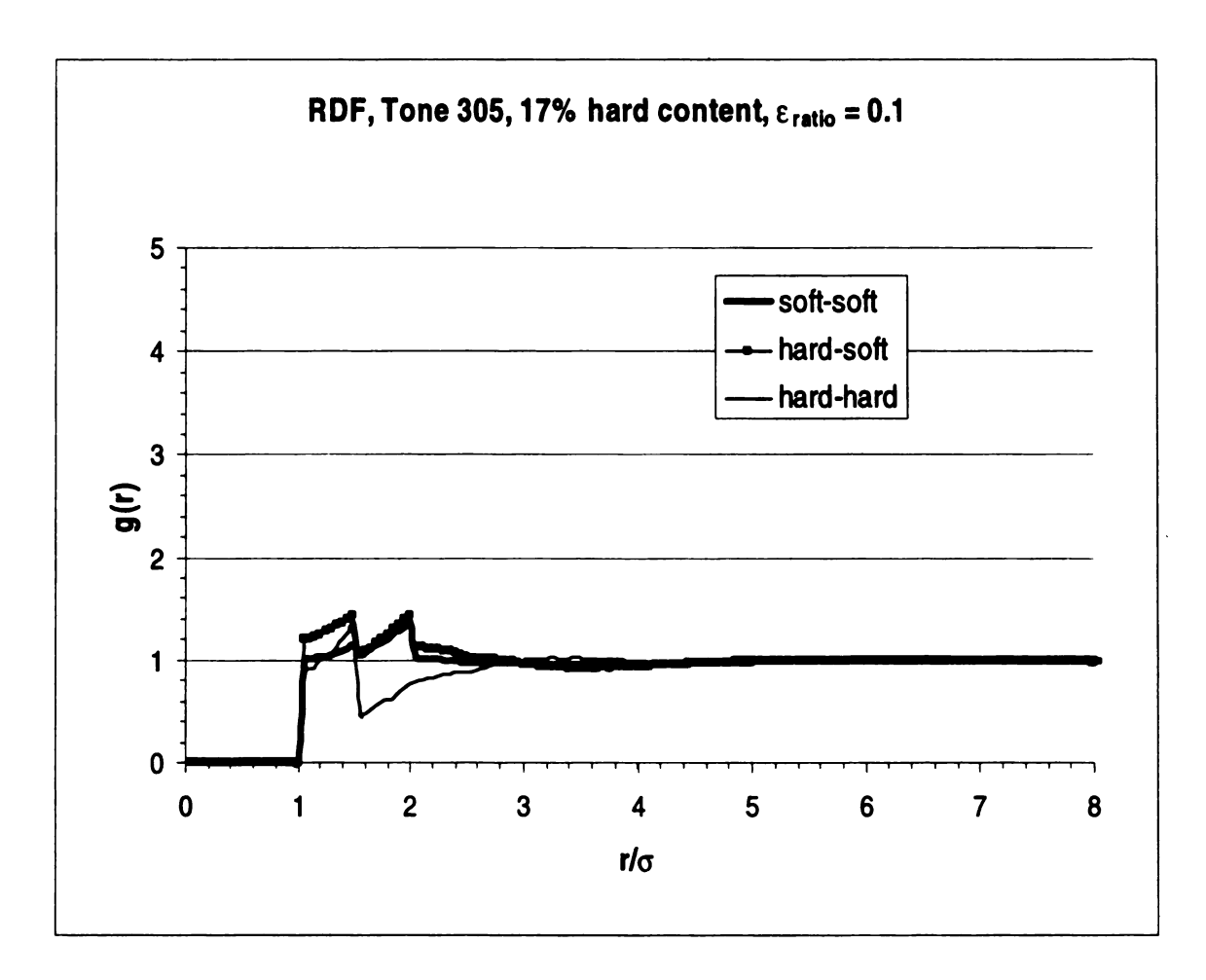


Figure 5-4. RDF, Tone 305, 17% hard content, ε -ratio = 0.1

Figure A-6 shows that soft sites on both the same node and different nodes contribute equally to the 1.5σ soft-soft peak in Figure 5-4. The 2σ peak though is dominated by contributions from sites on different nodes. This shows that the node arms have not folded on themselves to an appreciable extent. Had the arms folded on themselves the soft curve in Figure A-6 would fall to 0 sooner than at the 3σ observed.

The hard segment in this case consists of one hard site, so that the 1.5 σ peak is due exclusively to hard sites from different cross-links. This shows that where hard sites

came within range of the energy-well during the simulation, the interaction energy is sufficiently strong to keep the hard sites at this range. This interaction is sufficiently strong to overcome the large number of soft sites that could prevent interaction through stearic hindrance.

This case is not phase segregated.

5.2.5 TONE 305, 50% HARD SEGMENT CONTENT

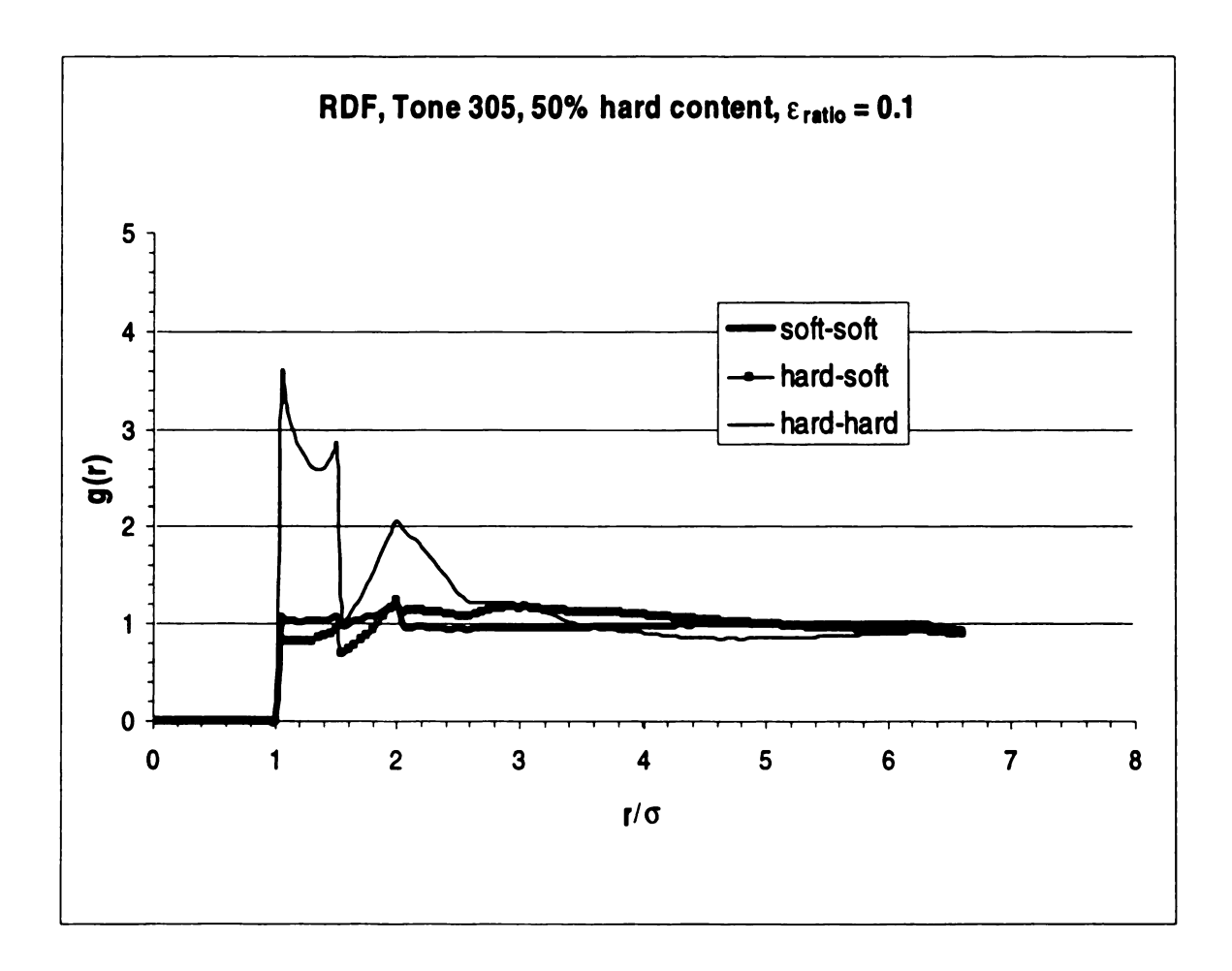


Figure 5-5. RDF, Tone 305, 50% hard content, ε -ratio = 0.1

Figure 5-5, in correlation with Figures A-7 and A-8, shows that the only appreciable soft-soft correlation is between soft sites on different nodes.

The hard segment in this case consists of five sites. The absence of correlation around 4 σ and strong correlation at shorter ranges indicate that the hard segments have folded on themselves. Figures A-7 and A-8 confirm this. The appendix figures do show that the hard sites from different segments contribute the most to the overall hard RDF curve. The g(r) < 1 values around 5 σ are due solely to a lack of interactions between sites from

different segments. This is a result of hard segments folding on themselves and aligning themselves, thus interacting overall at short range.

Phase segregation is shown to have occurred.

5.2.6 TONE 305, 63% HARD SEGMENT CONTENT

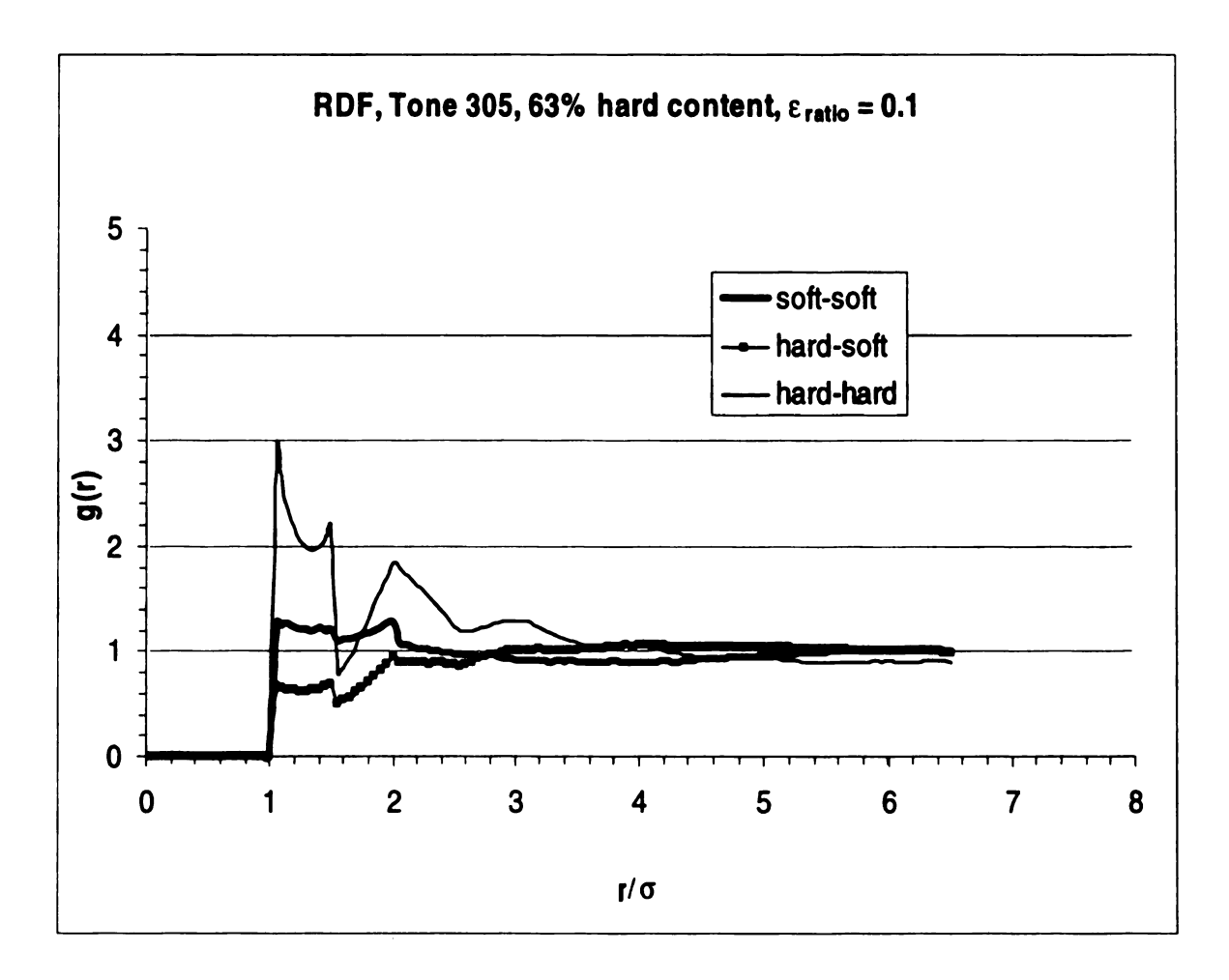


Figure 5-6. RDF, Tone 305, 63% hard content, ε -ratio = 0.1

The soft-soft short-range behavior is shown by Figures A-9 and A-10 to be contributed to in approximately equal proportions by sites on the same and different nodes. The sites on different nodes contribute more strongly to the soft-soft correlation in this case than in the Tone 305, 50% hard segment content case. This indicates that the nodes have a greater degree of freedom in this case.

The hard-hard curve only showing correlation up to a range of 4 σ indicates a segment that has folded on itself. This follows from a hard segment length of 8 sites. This is

substantiated by figure A-10. Figure A-9 shows that the segments have aligned with each other. The below-1.0 values at longer range are due to the hard segments aligning and interacting at short range.

Phase segregation is indicated in this case.

5.2.7 TONE 305 CONCLUSION

The low hard segment content case shows the strength of the hard site interaction compared to the soft site interaction. In cases of larger hard segments the stronger interaction between the hard segments leads to contraction of the hard segments and their alignment with each other. As the cross-link increases the Tone 305 node arms on the same node also show, compared to the Tone 301 node arms, a greater degree of freedom. In the low hard segment content case the fraction of hard sites is so low as to not allow phase segregation. The other two Tone 305 cases show increased phase segregation as hard segment content increases.

5.2.8 TONE 310, 13% HARD SEGMENT CONTENT

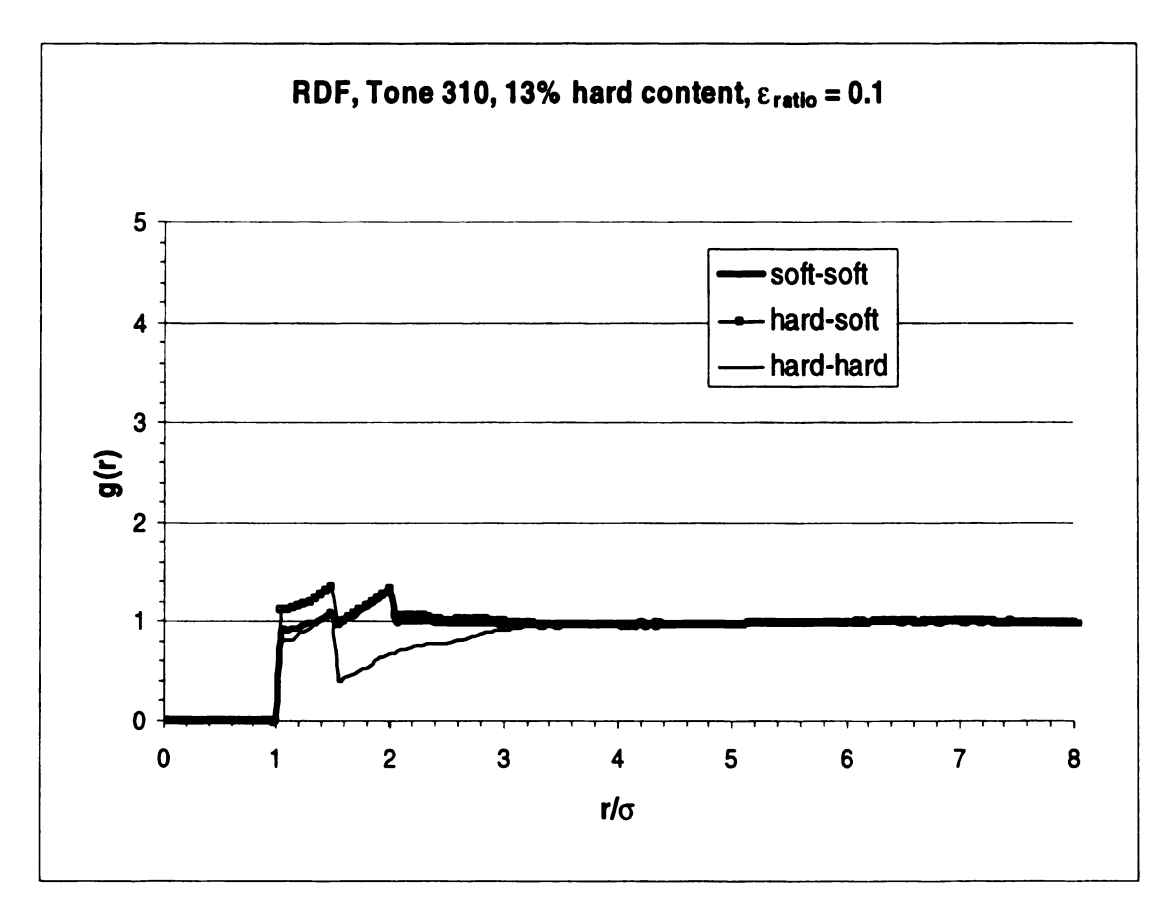


Figure 5-7. RDF, Tone 310, 13% hard content, ε -ratio = 0.1

The soft-soft curve behavior is comparable to the Tone 305, 17% case in Figure 5-3. The soft curves in Figures A-6 and A-12 are also comparable. As mentioned with the Tone 305, 17% hard segment case the node arms here also do not appear to fold on themselves to an appreciable extent.

This system is another case of the cross-link containing one hard site out of a total of seven. Here, as in the Tone 305 - 17 % hard segment case, hard sites that manage to come within the range of the square-well potential during the simulation are retained at

this range through the strong hard-hard interaction potential. The interaction energy is sufficient to overcome the relatively number of soft-soft interactions.

The hard-soft curve indicates that not phase segregation has occurred. The hard-soft and soft-soft curves are identical after $1.5 \, \sigma$ due to the fact that any interaction beyond the $1.5 \, \sigma$ range is soft-soft and hence this contribution dominates the hard-soft curve. The Figure 5-4 hard-soft curve shows similar behavior. The effect is more pronounced in the Tone 310 case due to higher ratio of soft sites in the cross-link. The Tone 305 case has 4 soft sites out of a total of 5, the Tone 310 case has 6 soft sites out of a total of 7.

5.2.9 TONE 310, 37% HARD SEGMENT CONTENT

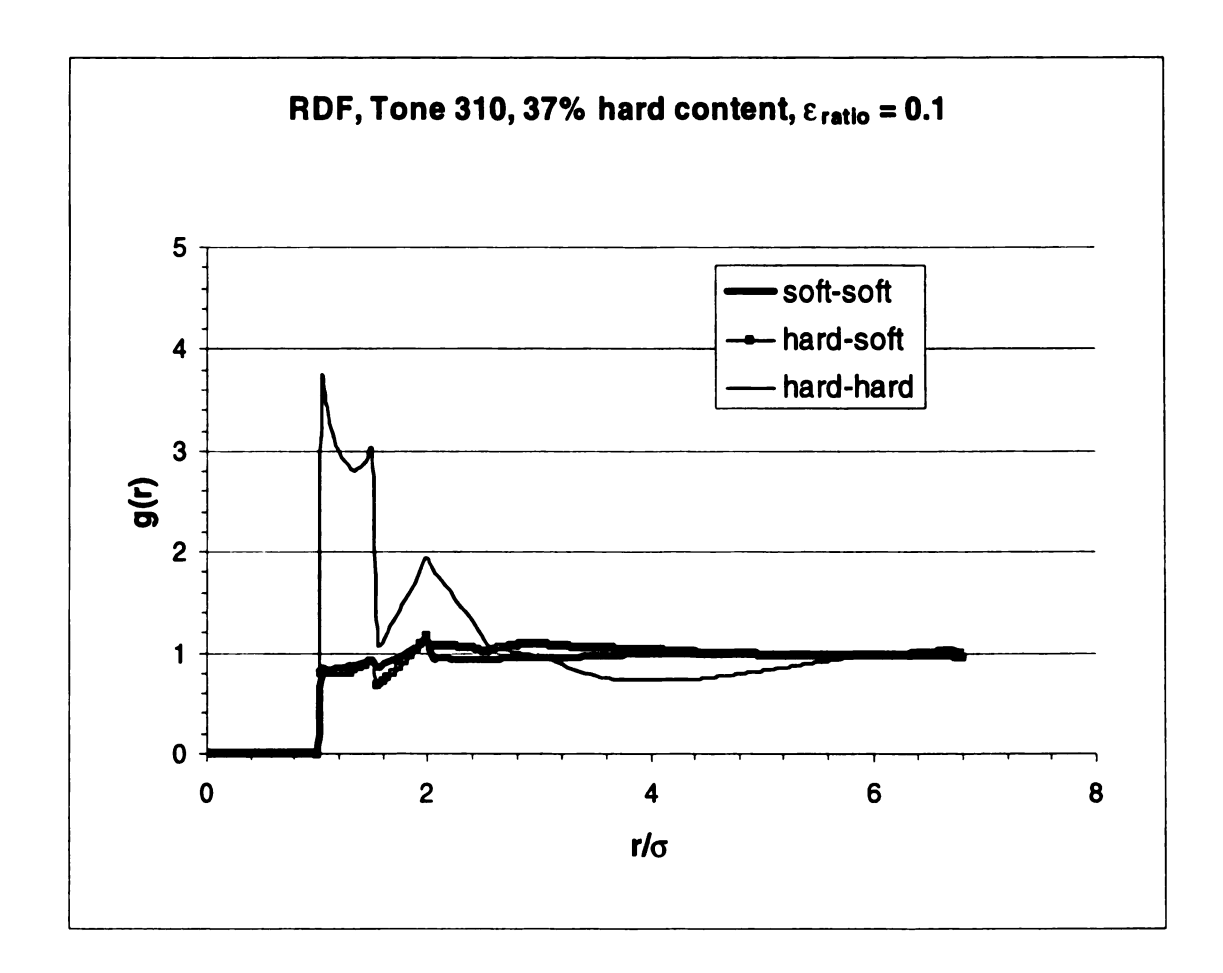


Figure 5-8. RDF, Tone 310, 37% hard content, ε -ratio = 0.1

The soft sites do not interact to an appreciable extent. The small peak at 2σ appears to be a result of the soft sites that neighbor the node being within this range due to connectivity constraints.

The hard-hard curve in Figure A-14 shows that most segments have folded on themselves. This follows from the hard segment in this system consisting of 4 sites.

Some segments still have sites interacting at ranges larger then 2 σ compared with the

largest range possible of 3 σ at full extension. Comparing hard curves in Figures A-13 and A-14 with each other shows that hard sites on different segments mostly contribute to the peaks in Figure 5-7. This shows that in addition to folding on themselves the hard segment of different cross-links align. The majority of the hard sites interact at short range leading to an absence of correlation at longer range. The curve drop below 1.0 at larger σ -values supports this observation.

The hard-soft curve indicates that phase segregation may have occurred in some regions and not in other areas.

5.2.10 TONE 310, 50% HARD SEGMENT CONTENT

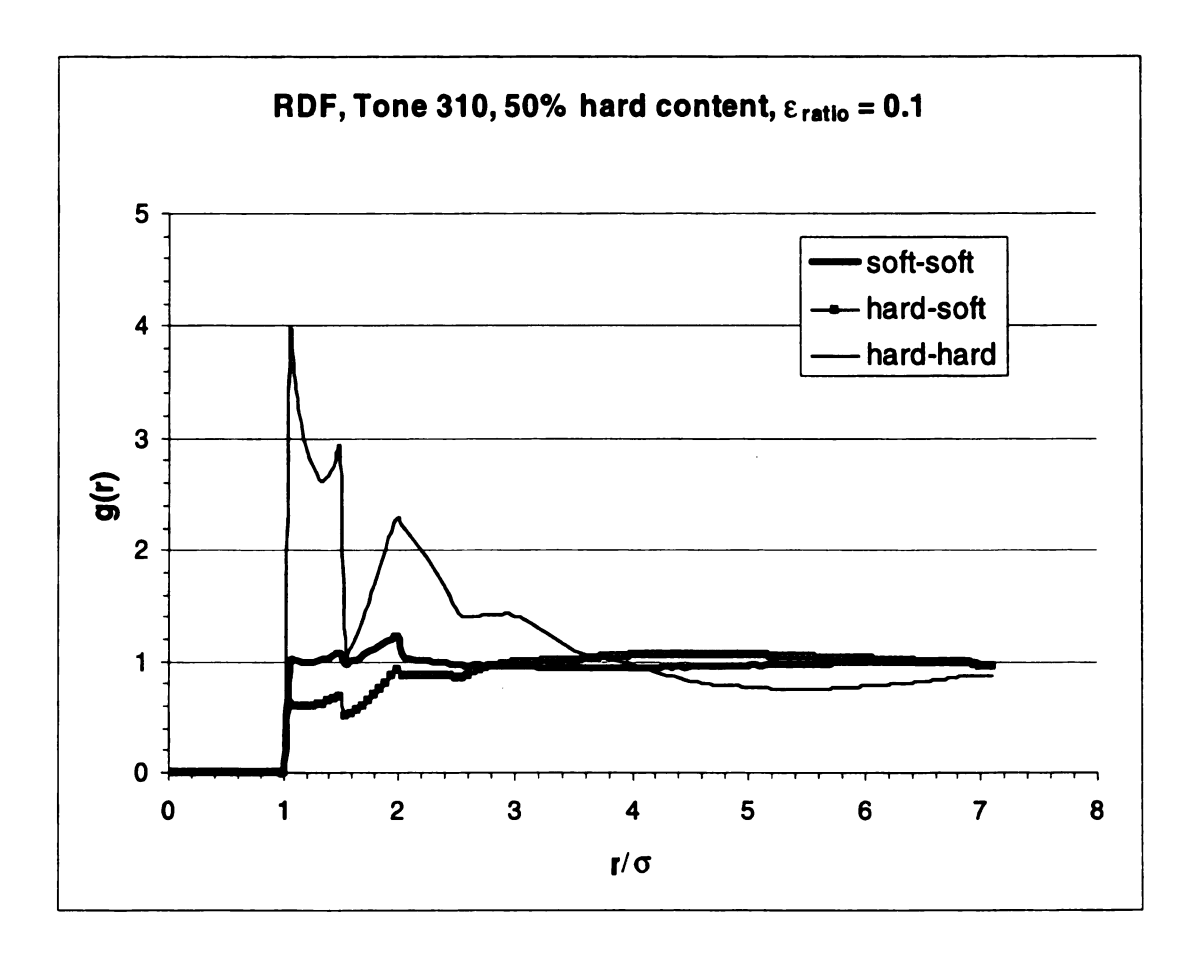


Figure 5-9. RDF, Tone 310, 50% hard content, ε -ratio = 0.1

The soft-soft behavior in Figure 5-9 is comparable to the soft curve results in the two previously discussed Tone 310 systems. Here also the soft sites do not interact or correlate to a noticeable extent.

Figure A-16 shows that the fraction of hard-hard interactions contributed to by sites on the same segments are larger than in the Tone 310, 37% hard segment case. This indicates that the segments have folded on themselves to a greater extent than in lower hard segment systems. Figure A-15 shows that the hard-hard interactions of hard sites on

different segments still dominate the overall correlation, thus indicating that segments of different cross-links align. The drop of the Figure 5-8 hard curve below 1.0 at longer range is once again a result of the majority of hard sites on different segments interacting at short range. This is substantiated by the hard curve behavior in Figure A-15.

The hard-soft curve shows that phase segregation has occurred.

5.2.11 TONE 310 CONCLUSION

Here also the low hard segment content case shows the capability of the strong hard site interaction potential to overcome the steric hindrance of a larger number of soft sites. In spite of this strong interaction the system's hard fraction is to small to lead to phase segregation.

In the case of higher hard segment content hard segments fold on themselves and align with other hard segments, thus creating regions with relatively high concentrations of hard sites. In all three Tone 310 cases the soft curve RDFs alone did not indicate that increasing cross-link length increased the node's degree of freedom. This is in contrast to Tone 301 and Tone 305, where an increase in the degree of freedom was observed.

Tone 310 showed a marked dependence of phase segregation on hard segment content.

The degree of phase segregation increased as hard site fraction increased.

5.3 EFFECT OF TONE SIZE

5.3.1 Low Hard Fraction

The Tone 305 - 17 % hard segment content and Tone 310 - 13% hard segment content systems show very similar behavior. Phase segregation did not occur in either case. The only noticeable effect of the tone size is the extent to which the soft-soft sites dominate the overall soft-hard correlation. At larger tone molecular weight the soft and hard-soft curve overlap sooner (see Figure 5-4 and Figure 5-7).

5.3.2 50% HARD FRACTION

In all 50% hard segment content cases the soft-soft behavior remains similar. The hard-hard correlation increases as Tone size increases. The degree of phase segregation also increases as Tone size increases. This indicates that the hard-hard interaction plays an important role in bringing about phase segregation. The added degree of freedom of longer cross-links also appears to be a contributing factor.

5.3.3 HIGH HARD FRACTION

At high hard fraction increasing Tone molecular weight contributes to a greater degree of phase segregation.

5.4 EFFECT OF CROSS-LINKING

5.4.1 TONE 305, 50% HARD FRACTION, INCOMPLETE CROSS-LINKING

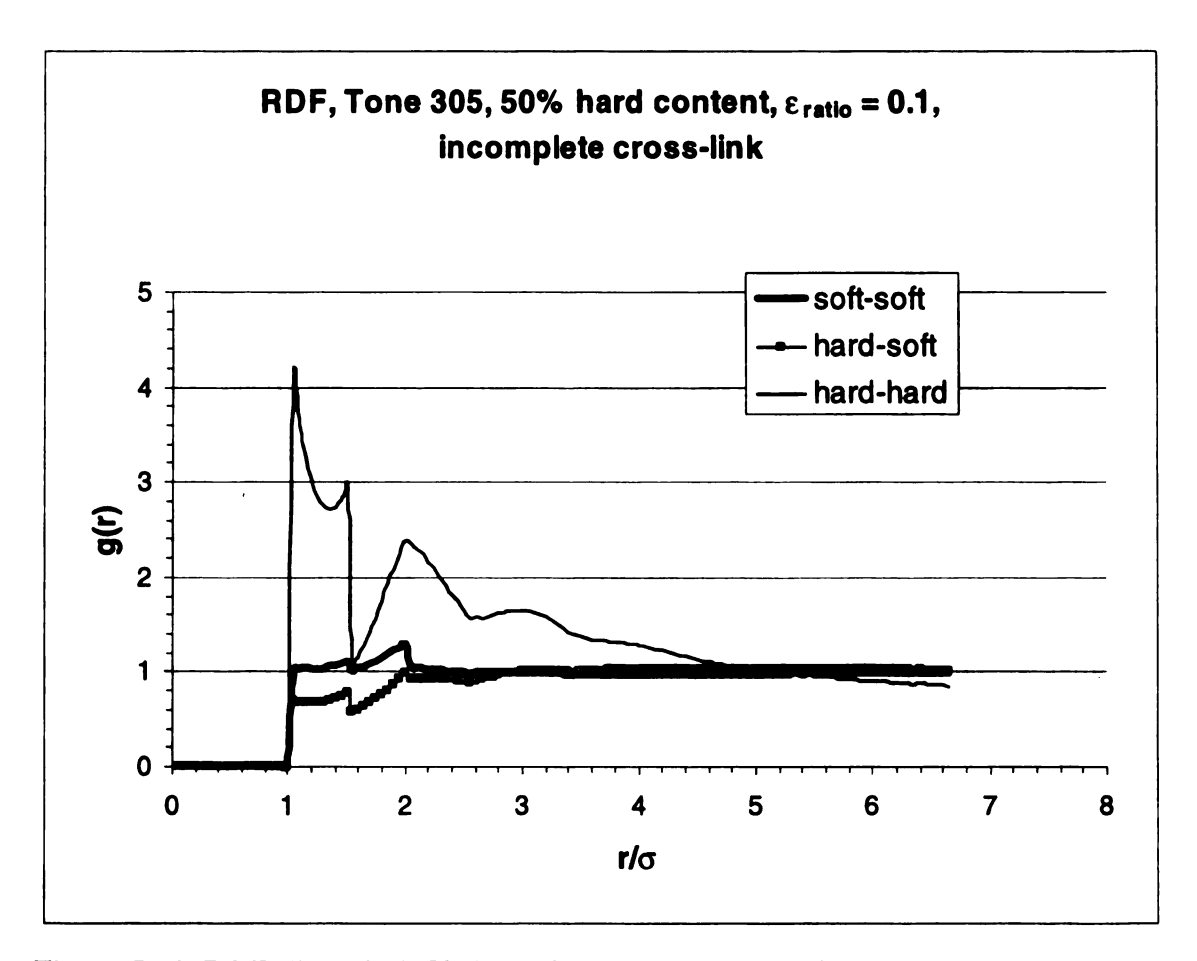


Figure 5-10. RDF, Tone 305, 50% hard content, ϵ -ratio = 0.1, incomplete cross-linking

The two Tone 305 - 50% hard fraction systems, fully cross-linked and partially cross-linked, are comparable. The fully linked system contains 928 sites, including 448 soft sites and 480 hard sites. The partially linked system has 469 soft sites and 520 hard sites, totaling 989 sites.

The soft curves in both cases are similar, though the partially linked system shows stronger correlation at 2 σ . Comparisons of the soft-soft curves indicate a greater degree of freedom in the partially linked system.

The hard-soft curve in Figure 5-10 indicates that phase segregation occurs to a greater extent in the partially cross-linked system than in the fully cross-linked system (see Figure 5-5).

Figures A-7, A-8, A-17 and A-18 show comparable soft site behavior. The hard sites on the same chain show weaker interaction, those on different chains stronger interaction in the partially cross-linked system than in the fully linked system. The chains in the fully linked system appear to fold upon themselves to a greater degree compared with the partially linked system. On the other hand the partially linked system shows a greater degree of alignment between different chains than does the fully connected system. These observations indicate a greater range of possible configurations in the partially cross-linked system. Two factors contribute to this situation. First, the smaller degree of cross-linking presents fewer constraints due to bonding for the remaining sites.

Secondly, the dangling ends have a greater range of space to be placed in during a move. Overall this leads to a more efficient relaxation of the system (see Table 5-1).

5.4.2 Tone 310, 38% Hard Fraction, Incomplete Cross-Linking

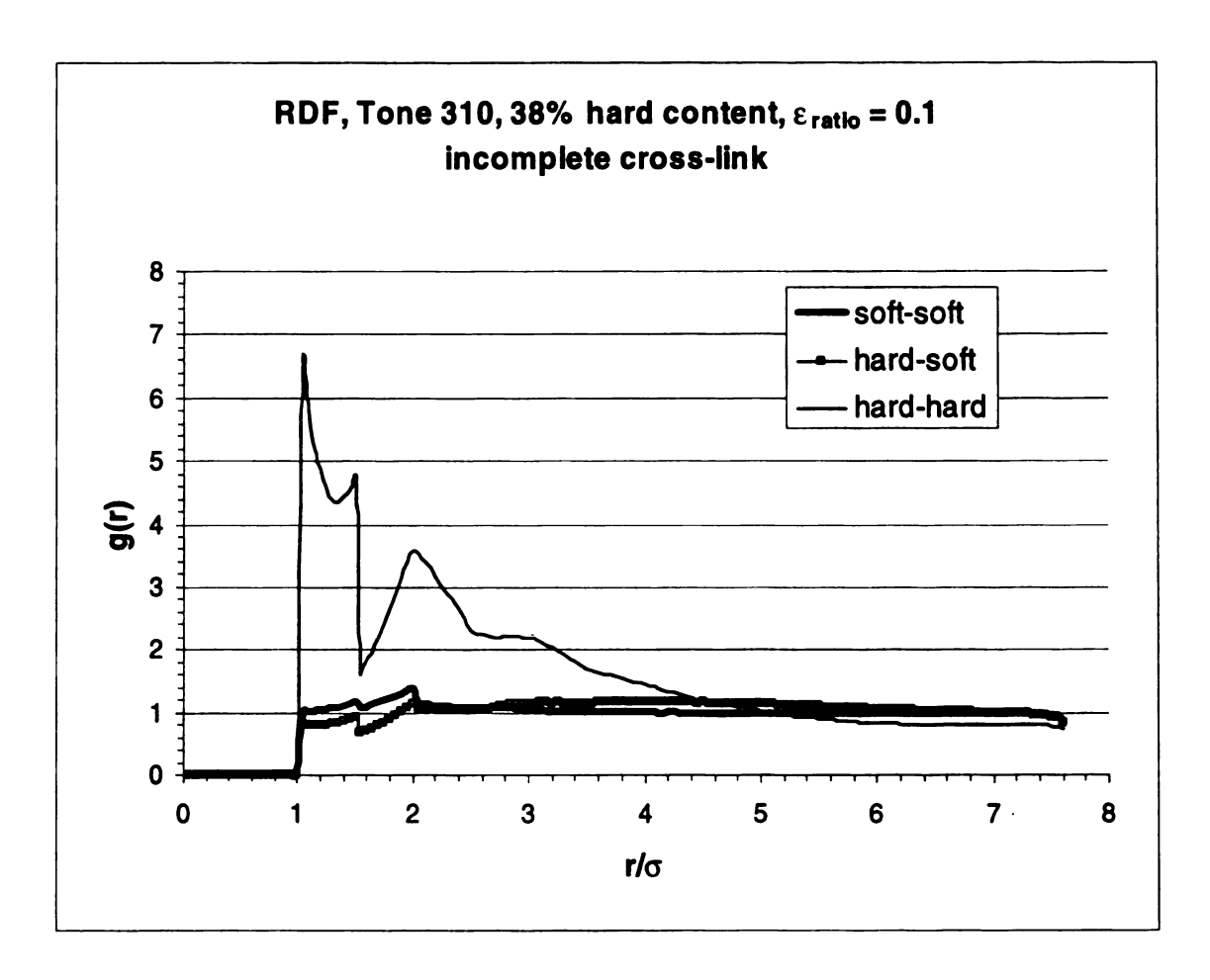


Figure 5-11. RDF, Tone 310, 38% hard content, ϵ -ratio = 0.1, incomplete cross-linking

The fully cross-linked Tone 310 - 37% hard content and partially linked Tone 310 - 38% hard content system also show similar system size and hard site content. The fully linked system has 640 soft sites and 384 hard sites, totaling 1024 sites. The partially linked, or modified, system contains 1066 sites, with 660 soft and 406 hard sites.

The soft-soft and hard-hard curve in Figure 5-11 show greater correlation than the soft-soft and hard-hard curve in Figure 5-8. The modified system's hard curve also shows correlation over a greater range than does the unmodified system.

The hard-soft curve's position relative to the other curves in the fully linked system does not show a conclusive proof for phase segregation. In the partially linked system the hard-soft curve definitely indicates phase segregation.

Figures A-13, A-14, A-19 and A-20 show comparable soft site behavior. The hard site behavior is comparable to the Tone 305 system discussed above. The partially linked system in this case also shows a lesser degree of hard segments folding on themselves and a greater degree of alignment between different chains.

Here also the partially cross-linked system has a greater sampling space. This allows this system to accomplish equilibrium more efficiently (see Table 5-1). In all three systems another factor may also have some effect. In the fully cross-linked system the nearest bonded neighbors, which are not counted in the radial distribution function, prevent other sites from coming near a given site. In the partially linked system the dangling ends allow sites from other chains to move into interactions at locations that are occupied by neighbors in the fully linked system. The lack of this form of steric hindrance may contribute to the greater hard curve values observed.

5.4.3 Tone 310, 50% Hard Fraction, Incomplete Cross-Linking

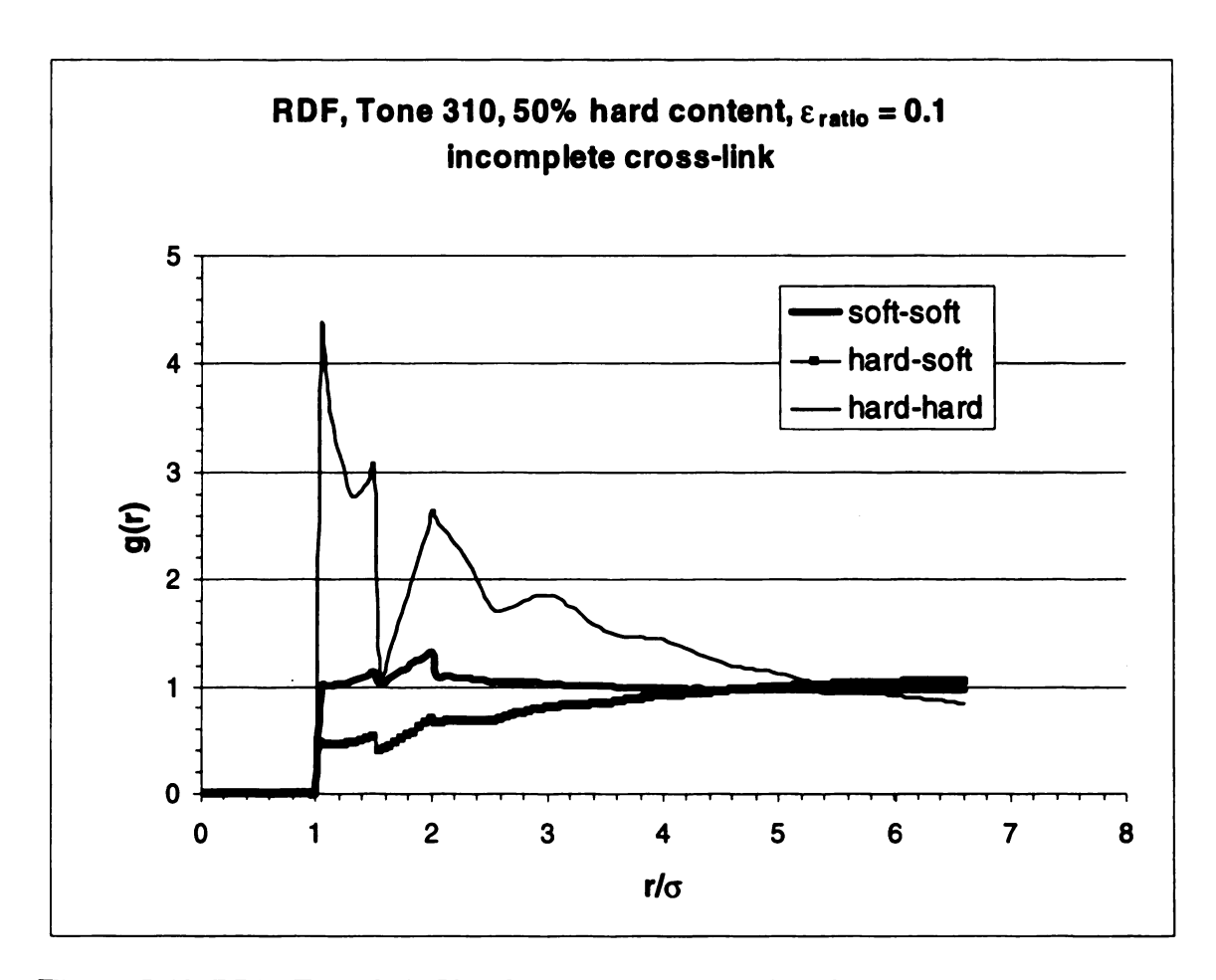


Figure 5-12. RDF, Tone 310, 50% hard content, ϵ -ratio = 0.1, incomplete cross-linking

The partially lined Tone 310 - 50% hard content system consists of a total of 1071 site, including 510 soft sites and 561 hard sites. The fully linked system with the same hard site content has 640 soft site and 672 hard sites, totaling 1312 sites. The size difference between fully cross-linked and modified system is the greatest in this case.

The soft curves in Figures 5-12 and Figure 5-9 show similar soft site behavior. The hard curve in Figure 5-12 on the other hand indicates a greater degree of correlation over a greater range than in Figure 5-9.

As in the previous two case descriptions the hard-soft curve indicates a greater extent of phase segregation in the partially linked system than in the fully linked system.

Figure A-15 and A-21 also indicate that the chains of the partially linked system fold on themselves to a lesser degree than in the fully linked system. The modified system does show a greater degree of alignment between the different chains.

As discussed before the partially cross-linked system exhibits a larger space in which to place displaced sites. This is also indicated by a more efficient calculation of the equilibrated system (see Table 5-1).

5.5 EFFECT OF ε-RATIOS

5.5.1 ε-RATIO OF 1

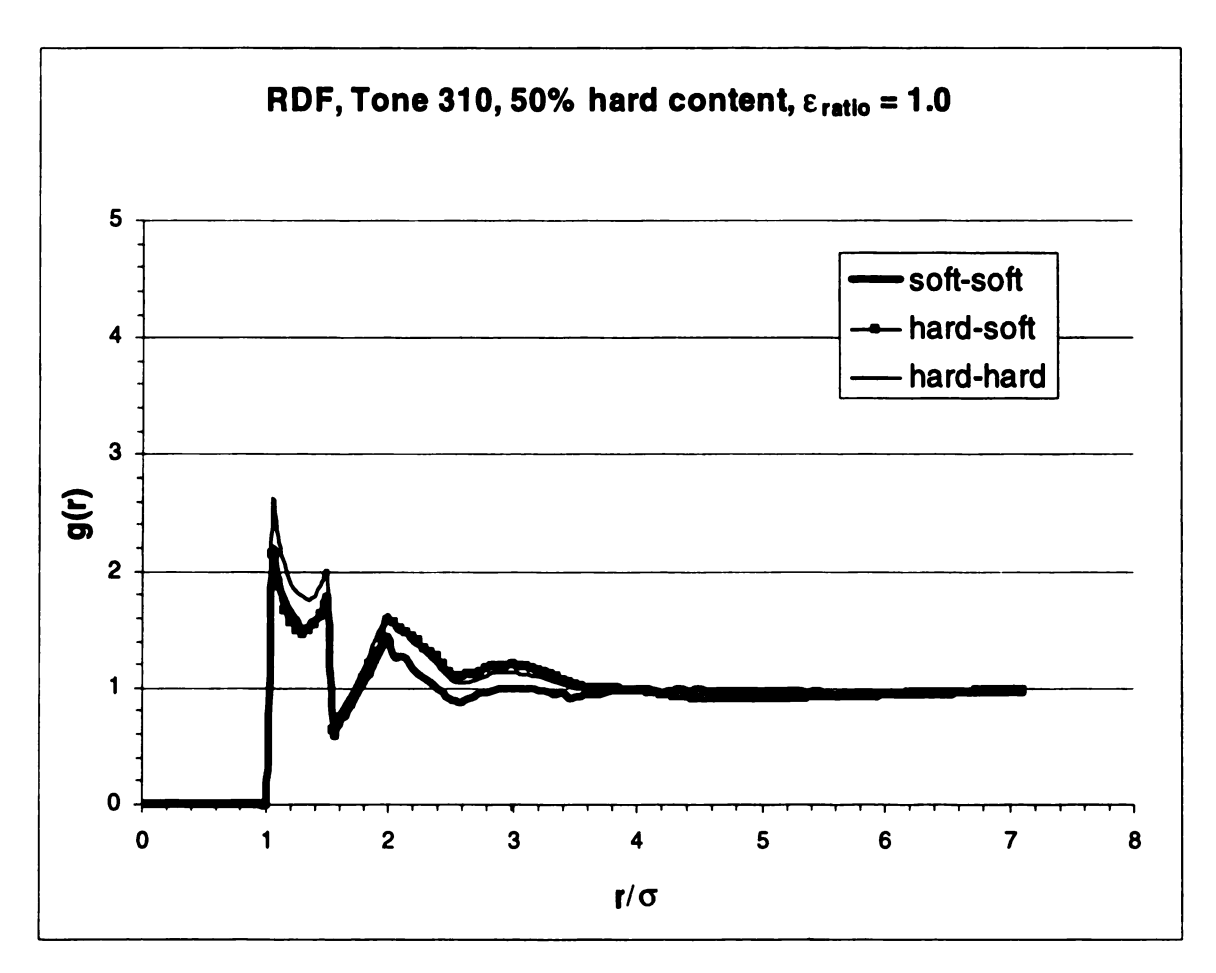


Figure 5-13. RDF, Tone 310, 50% hard content, ε -ratio = 1

The RDF in Figure 5-13 shows a system in which the energy well depth of all sites is equal. In essence this system represents a homopolymer. The hard-hard and soft-soft sites are identified in name only and the location of the sites in the cross-link: the soft sites in the node and node arms, the hard sites in the connecting segments between the nodes. No phase segregation is apparent. The hard segments appear to have a slightly higher structural correlation. This can be ascribed to a slightly greater degree of freedom

of the cross-link center segments than the nodes. The segments only have two points of attachment, the nodes three points. This somewhat greater degree of freedom is expressed in the higher correlation. This system indicated that the phenomenon of phase segregation is largely due to the difference in energetic interactions between hard and soft sites. Structural effects are negligible.

5.5.2 ε-RATIO OF 10

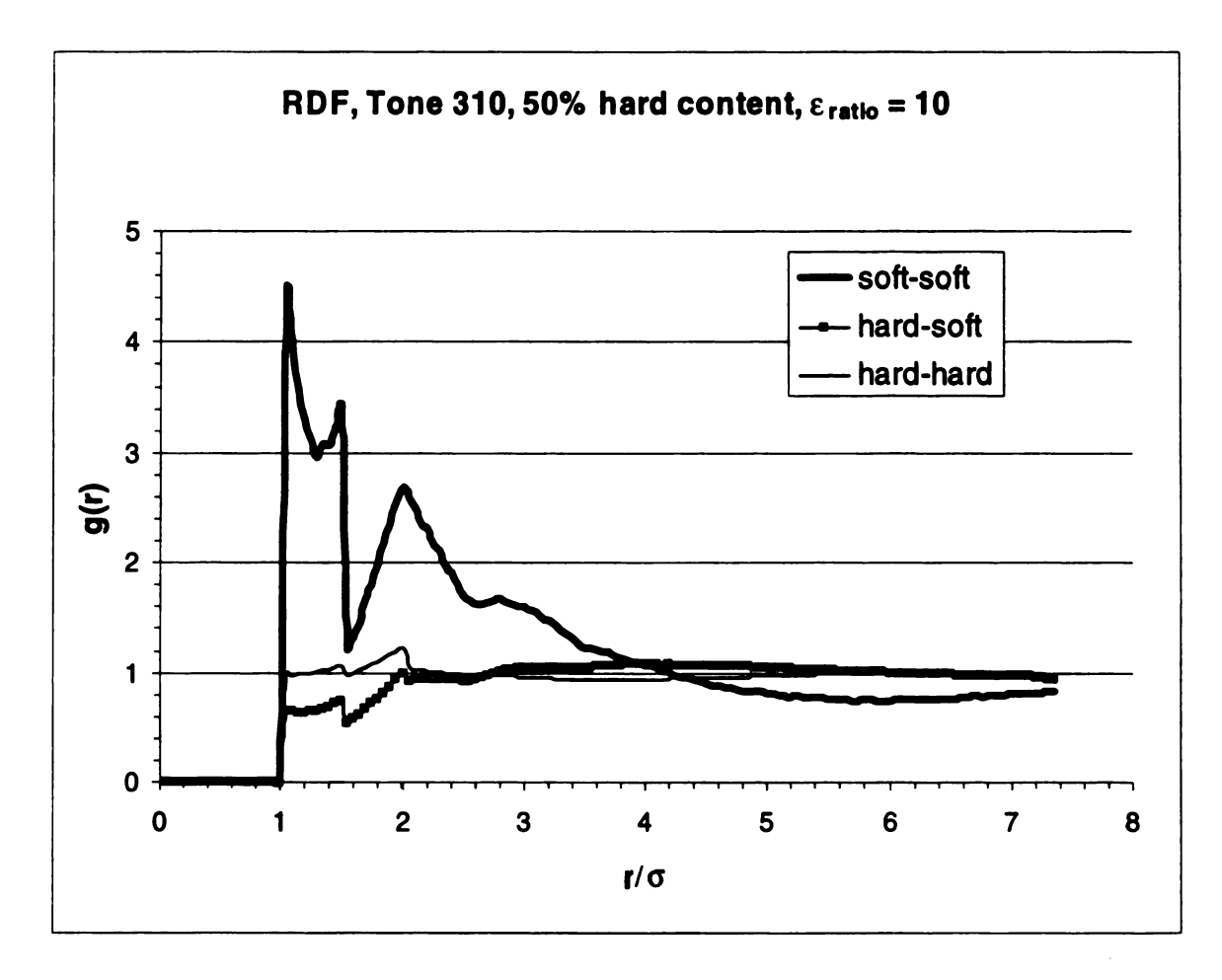


Figure 5-14. RDF, Tone 310, 50% hard content, ε -ratio = 10

In this system the node sites have an energy well-depth ten times that of the segment sites. The soft sites have the higher attractive energy and this is reflected in the larger correlation in the radial distribution function. The segment sites show a lower degree of correlation reflecting the lower energy potential.

Figure 5-14 clearly indicates that phase segregation has occurred. This is partly expected due to the difference in energetic interaction between the different sites and partly due to the cross-link length.

5.5.3 Node-Node Distribution for varying ϵ -ratios

Figures 5-9, 5-13 and 5-14 compare a system with the same cross-link length, but differing energetic interactions. Figure 5-9 and 5-14 appear to be similar since in both cases phase segregation occurs, though the curve magnitudes differ. Figure 5-15 shows an important structural difference.

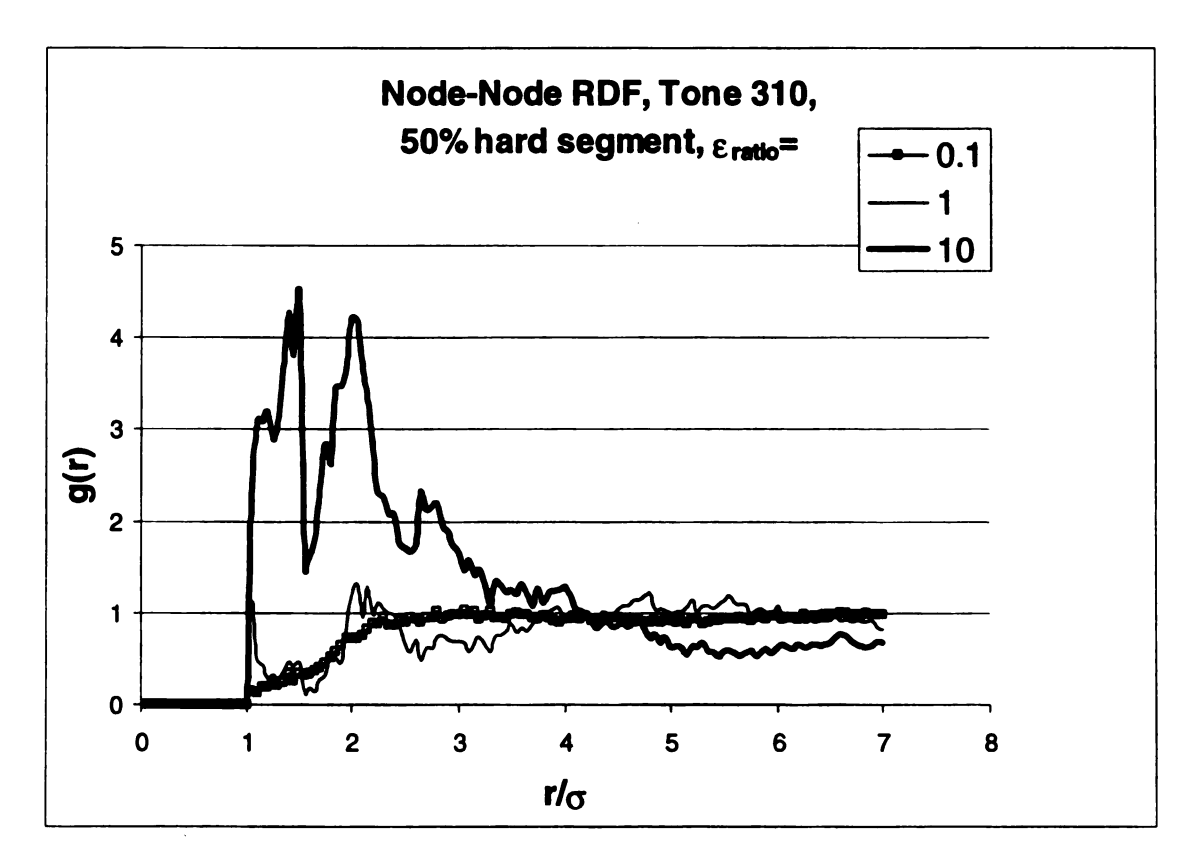


Figure 5-15. Node-Node RDF, Tone 310, 50% hard segment with varying ϵ -ratios

Figure 5-15 shows the radial distribution function for the nodes in each of the three Tone 310, 50% hard segment systems. The curves show that as the ε -ratio becomes greater the average distance between the nodes decreases. An increase in the ε -ratio means that the soft-soft attraction increases in comparison to the hard-hard interaction. Figure 5-15

indicates that in Figure 5-9 the nodes are spread apart, whereas in the case of Figure 5-14 the nodes are clustered.

5.7 Comment on Qualitative Analysis

Another possible method to determine phase segregation is the evaluation of snapshots taken of the simulations box. Figures 5-16 and 5-17 were taken using visualization software (IRIS Explorer 4.0) on a SGI workstation.

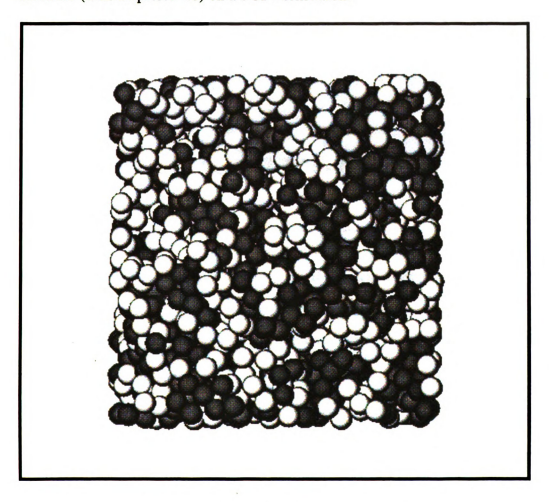


Figure 5-16. Snapshot: Tone 301, 50% hard segment content



Figure 5-17. Snapshot: Tone 301, 65% hard segment content

In these snapshots the light spheres represent nodes and node arms, the dark sphere represent the hard segments of the cross-links.

Comparing Figures 5-16 and 5-17 shows that determination of phase segregation based on snapshots is mostly a subjective exercise. Figure 5-17 for example may appear phase segregated, when in fact the system is not phase segregated. Hence an objective method, such as radial distribution functions, is needed and applied in this work. Further snap shots can be found in Appendix E.

5.8 Summary of Results

TABLE 5-2 SUMMARY OF PHASE SEGREGATION OBSERVED

Tone	Experimental	Modeling	Experiment	Flory	Modeling
	Hard Fract. (%)	Hard Fract. (%)		Theory	5
310	23	13	No	No	No
310	38	37	No	Yes	Maybe
310	48	\bigvee	Maybe	Yes	$>\!\!<$
310	52	50	Yes	Yes	Yes
310	67	\bigvee	Yes	Yes	$>\!\!<$
305	33	17	No	No	No
305	44	\bigvee	No	Yes	$>\!\!<$
305	57	50	Yes	Yes	Yes
305	65	63	Yes	Yes	Yes
301	43	>	No	No	$>\!\!<$
301	57	50	No	No	No
301	64	65	No	No	No

Table 5-1 compares the observations of this work with experimental results and Flory Theory predictions taken from the work of Agrwal and Drzal (1995a, 1995b, 1996). In general the results agree and indicate that configurational-bias Monte Carlo simulations can successfully predict physical behavior of networked block-copolymers. Thus this method shows a number of possible applications, such as the validation of obtained results, or the investigation of contributing factors to various physical behaviors.

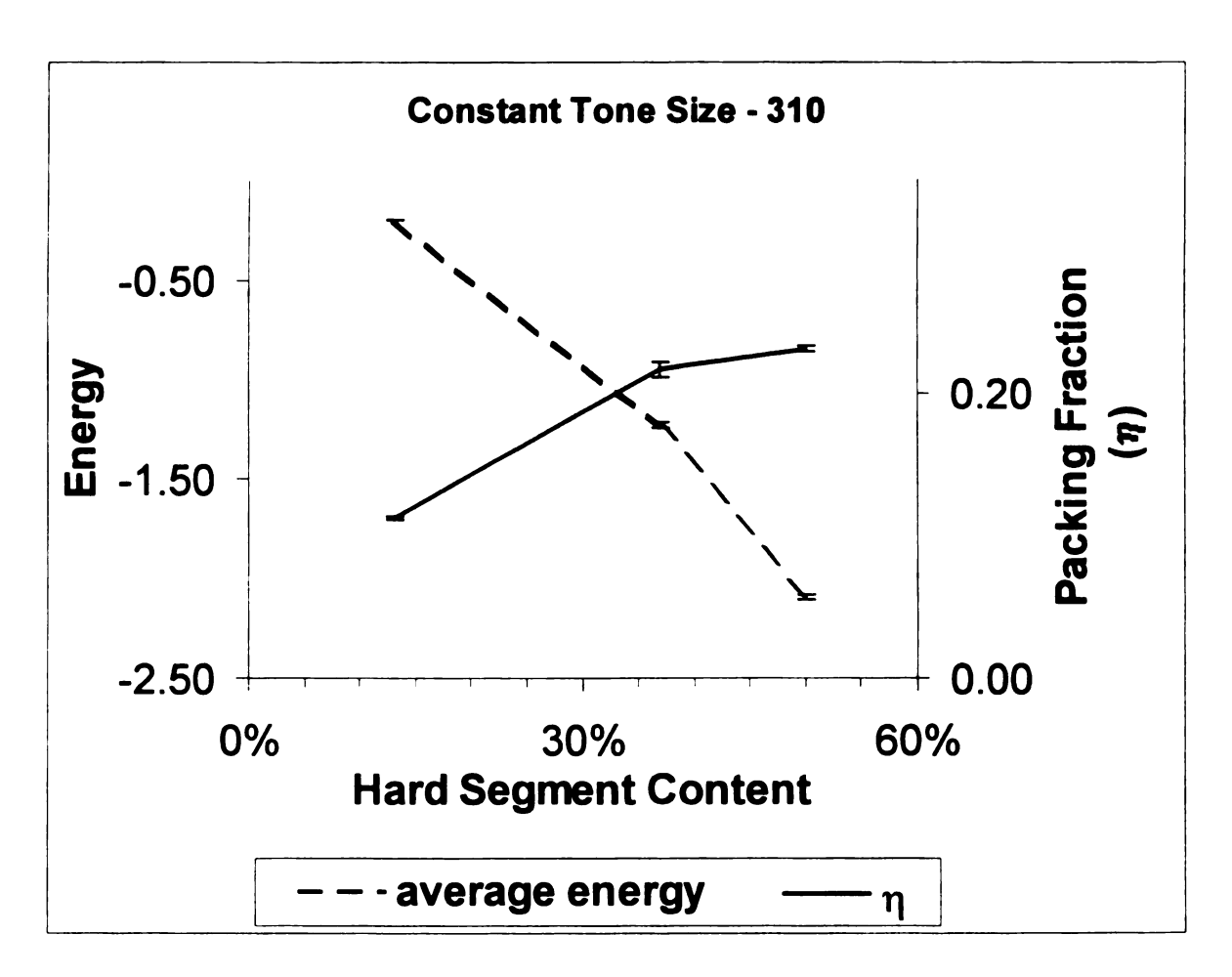


Figure 5-18. Effect of Constant Tone Size for Tone 310

Figure 5-18 shows a the effect of constant tone size on packing fraction and average energy per site (denoted 'energy' in Figure 5-18) in the case of the Tone 310 system. The average energy per site is obtained by dividing the system's total energy by the number of sites. The figure shows that as hard segment content increases the average energy increases in magnitude. This is a result of the higher number of hard sites, which have higher energetic interaction.

The packing fraction is obtained by summing the volume of all sites and dividing the total by the simulation box volume. The packing fraction in the Tone 310 case also increases as hard segment fraction increases. This observation correlates with

the higher average energy. As the average attractive energy increases between sites, the chains are pulled closer together, thus increasing packing fraction.

Figure 5-19 shows the same trends for the case where the tone size is kept constant with the Tone 305 system.

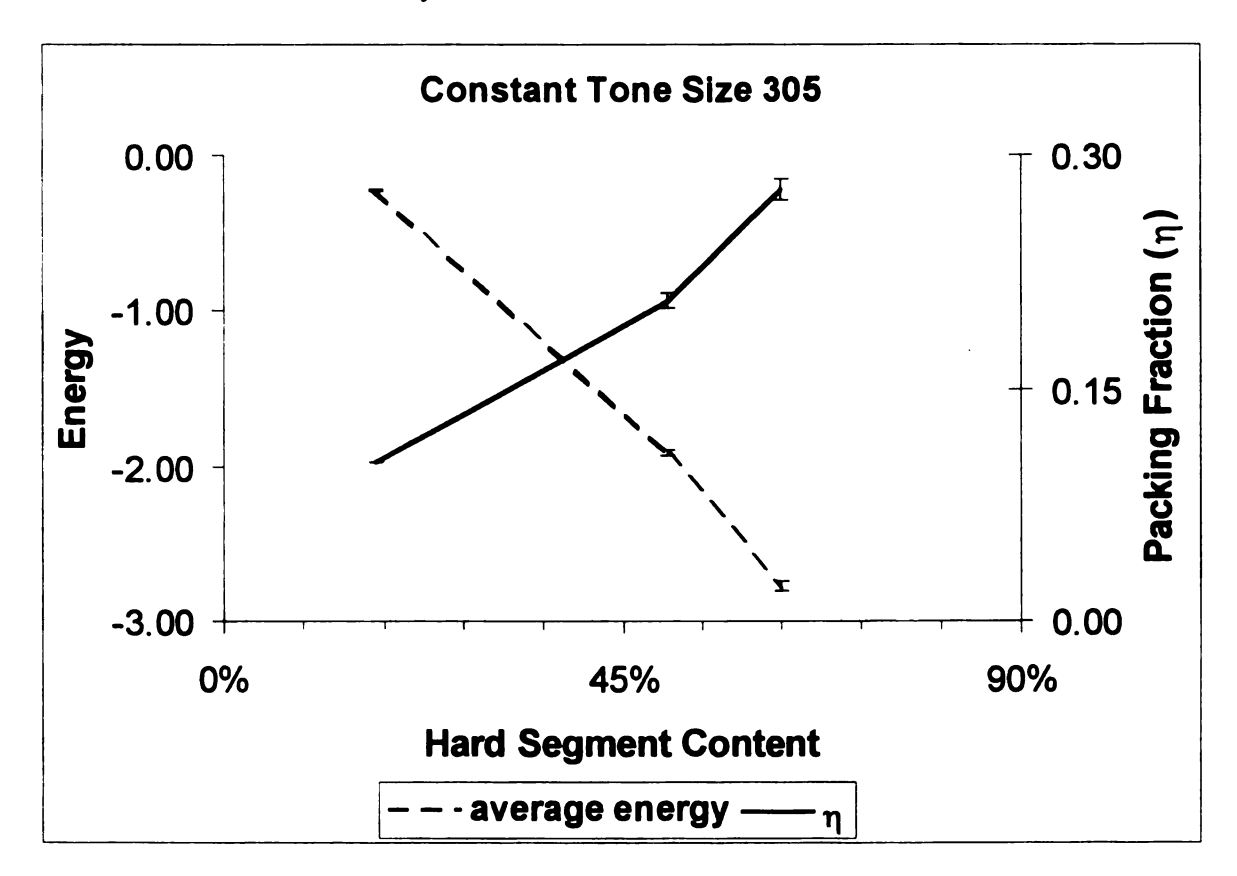


Figure 5-19. Effect of Constant Tone Size for Tone 305

	i
	í
	1
	1
	1
	i
	1
	İ
	1
	1
	1
	ł
	1
	1
	1
	١
	1
	1
	1
	1
	1
	ı
	1
	1
	1
	-
	1
	1
	ı
	ı
	1
	1
	ı
	1
	ı
	1
	1
	1
	ı
	ł
	1
	1
	1
	1
	1
	1

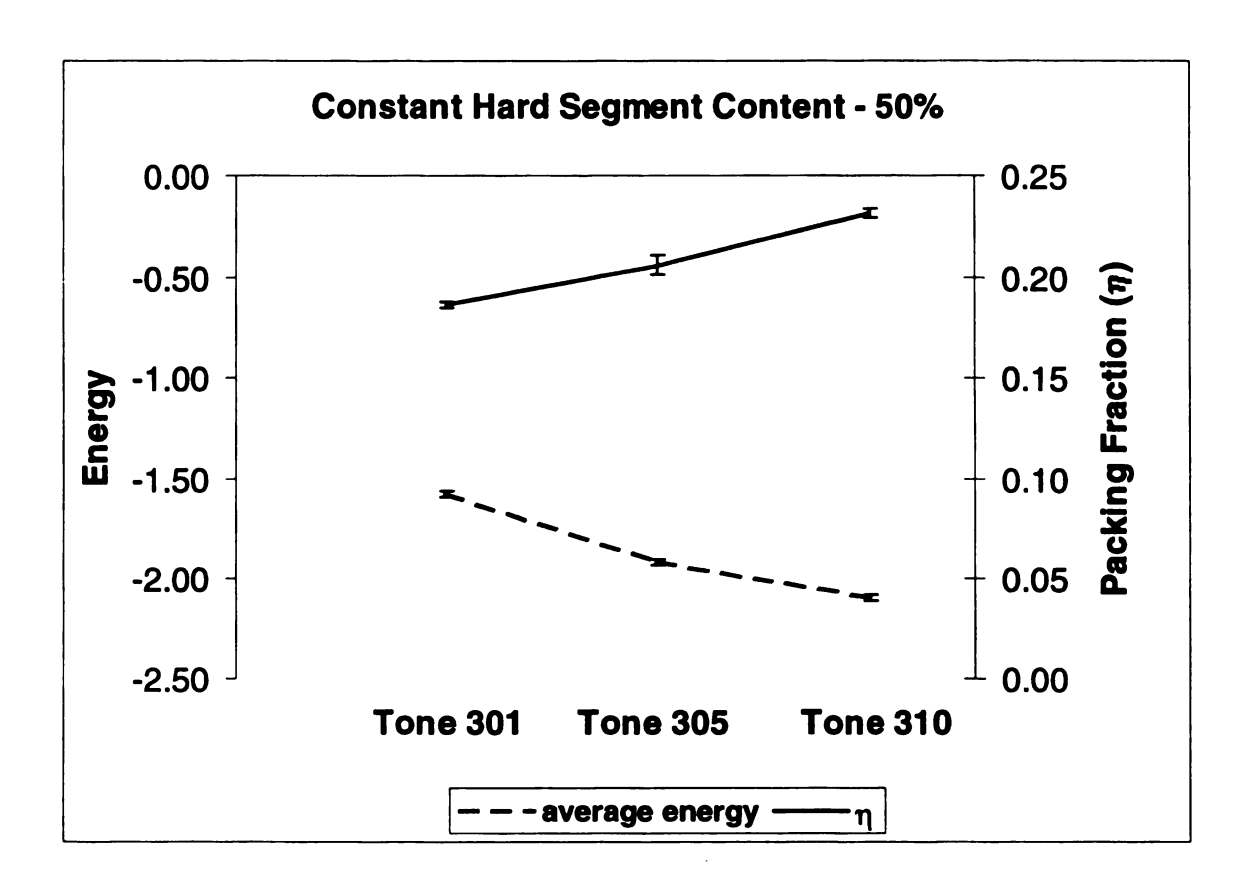


Figure 5-20. Effect of Constant Hard Segment Content - 50%

For the case that hard segment content is held constant and tone size varied Figure 5-20 shows that the average energy increases in magnitude as the Tone size increases. This is explained by the higher number of hard sites per cross-link that can interact with each other. A part of the increase is also due to the greater number of hard-soft interactions. The packing fraction is also shown to increases with larger tone size.

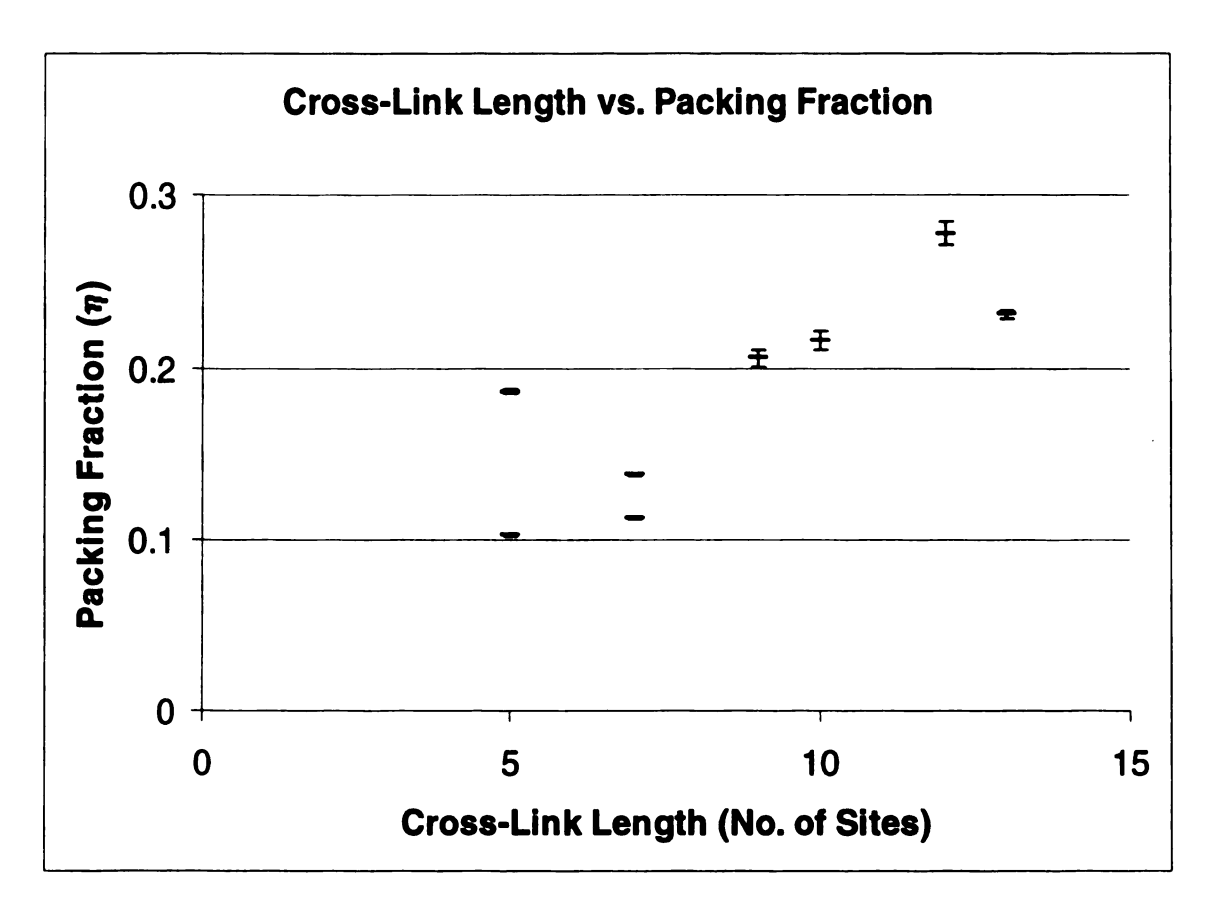


Figure 5-21. Correlation of Cross-Link Length with Packing Fraction

Figure 5-21 shows comparable packing fractions for given cross-link lengths. The values are taken from all systems investigated in this study. The exception to this general trend is a Tone 301 case. The Tone 301 – 50% hard segment content and Tone 305 – 50% hard segment content systems both have a cross-link length of 5 sites. The Tone 301 case though shows a packing fraction nearly double that of the Tone 305 case. This is explained by the higher number of hard sites per cross-link in the Tone 301 case. This higher number leads to a stronger interaction between sites and hard segments, thus increasing the packing fraction. In the Tone 305 case the cross-link only has one hard site. Tabulated values for Figures 5-18 through 5-21 can be found in Appendix D.

6. CONCLUSIONS

Block copolymer phase segregation is favored by three main factors: (1) longer cross-link length (i.e. larger Tone size), (2) higher hard segment content and (3) greater ratio of interaction energies. The modeling of this work shows agreement with trends observed in previous theoretical (Flory Theory) and experimental work by Agrawal and Drzal. Phase segregation was also shown to be largely controlled by energetic interaction, though some negligible structural effect is observed.

Partially cross-linked systems show similar behavior to the fully cross-linked counterparts. Greater mobility and larger degrees of phase segregation are observed in the modified systems. Here also larger tone sizes and greater hard segment content increases the degree of phase segregation. The partially cross-linked system's equilibrated structure was calculated in a more efficient manner than the fully cross-linked system, while obtaining similar results.

This work obtained results comparable to those of experimental work, thus indicating that modeling provides a method of predicting macroscopic behavior of block copolymers while investigating contributing factors at the molecular level.

7. RECOMMENDATIONS FOR FUTURE WORK

Previous work by Agrawal and Drzal showed an interphase region between the matrix and glass surface. This work investigated the bulk phase of the polyurethane matrix. A future line of work may be the investigation of the interphase region. This would entail the simulation of systems studied in this work next to a hard continuos surface. The nature of the future work would be of a heterogeneous nature, compared with the homogeneous nature of this study.

The equilibrated structure of the partially cross-linked systems was shown to be more efficiently calculated than the fully cross-linked system, while displaying similar results to the fully cross-linked system. The partially linked system also had a greater resemblance to the physical cases investigated in previous works. Future work may include investigating a larger number of partially cross-linked systems.

APPENDICES

APPENDIX A

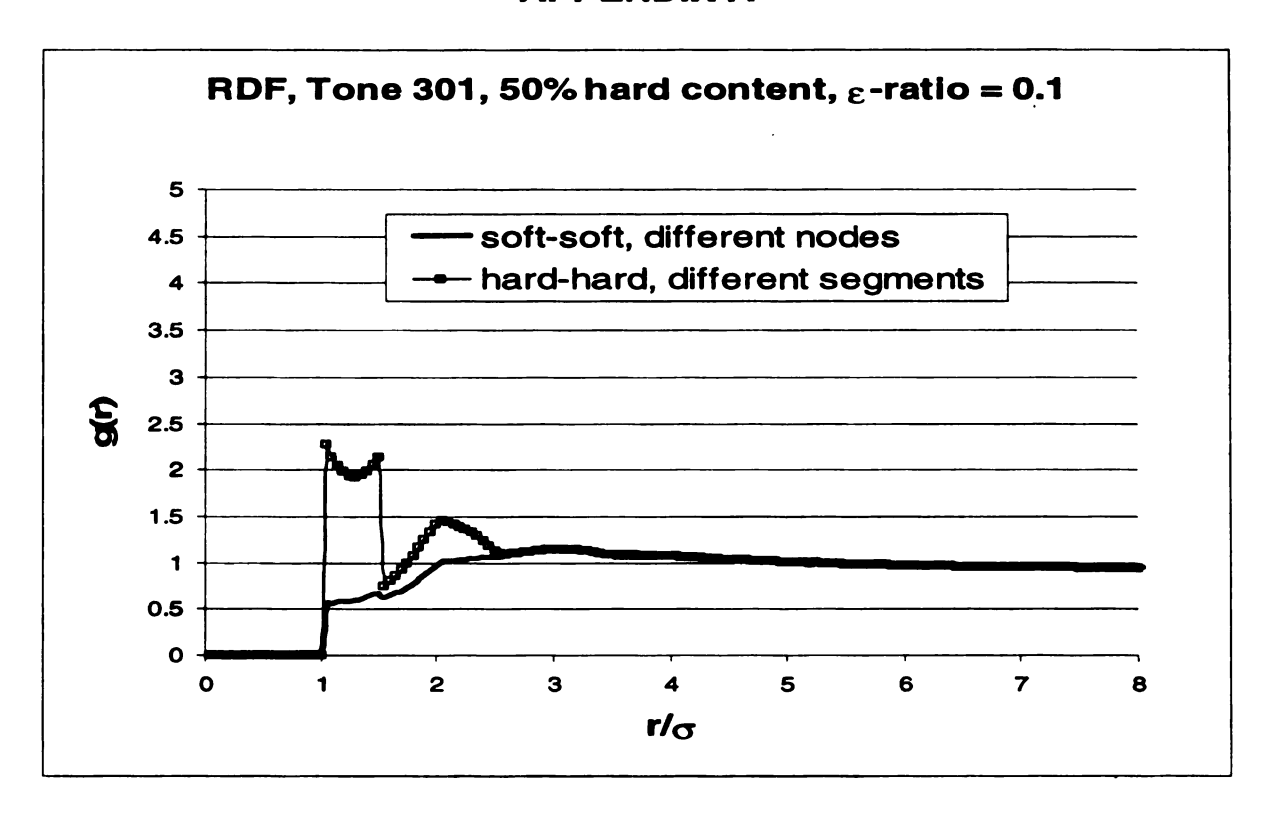


Figure A-1. RDF, Tone 301, 50% hard content, ϵ -ratio = 0.1, different chains

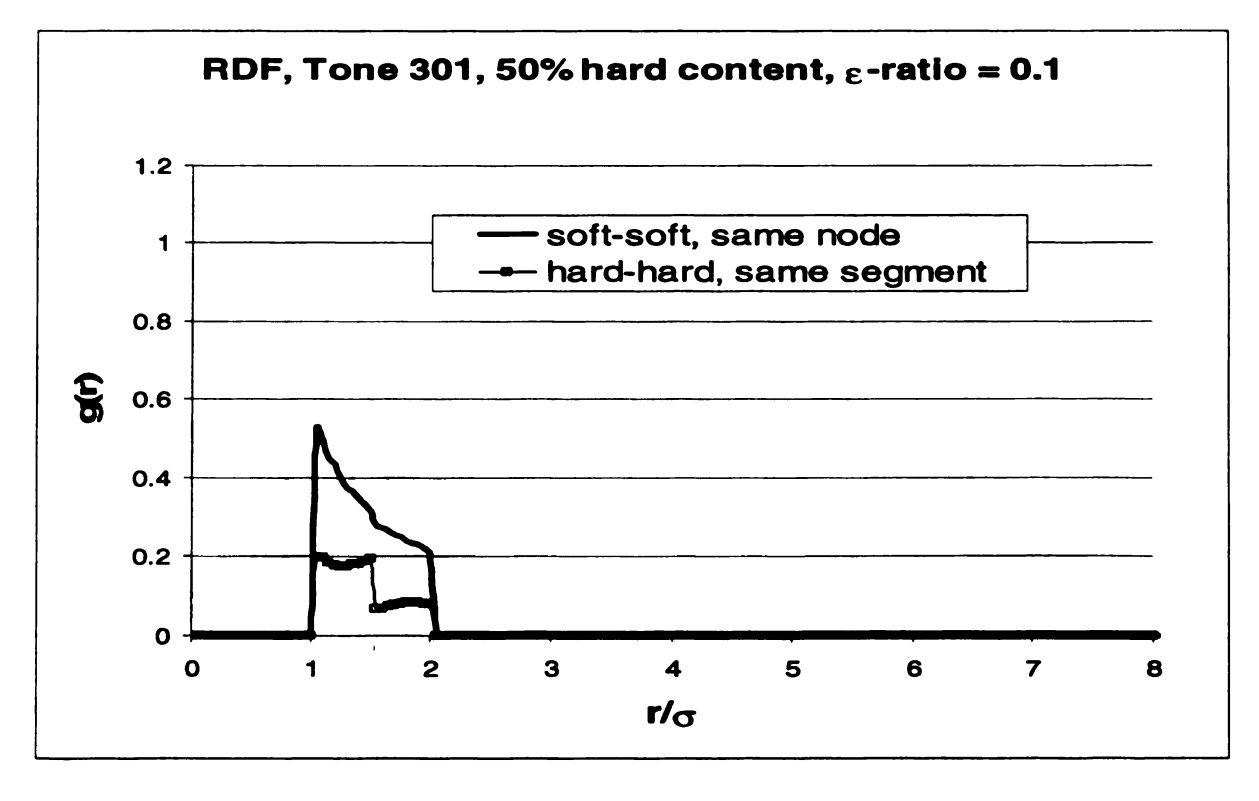


Figure A-2. RDF, Tone 301, 50% hard content, ε -ratio = 0.1, same chains

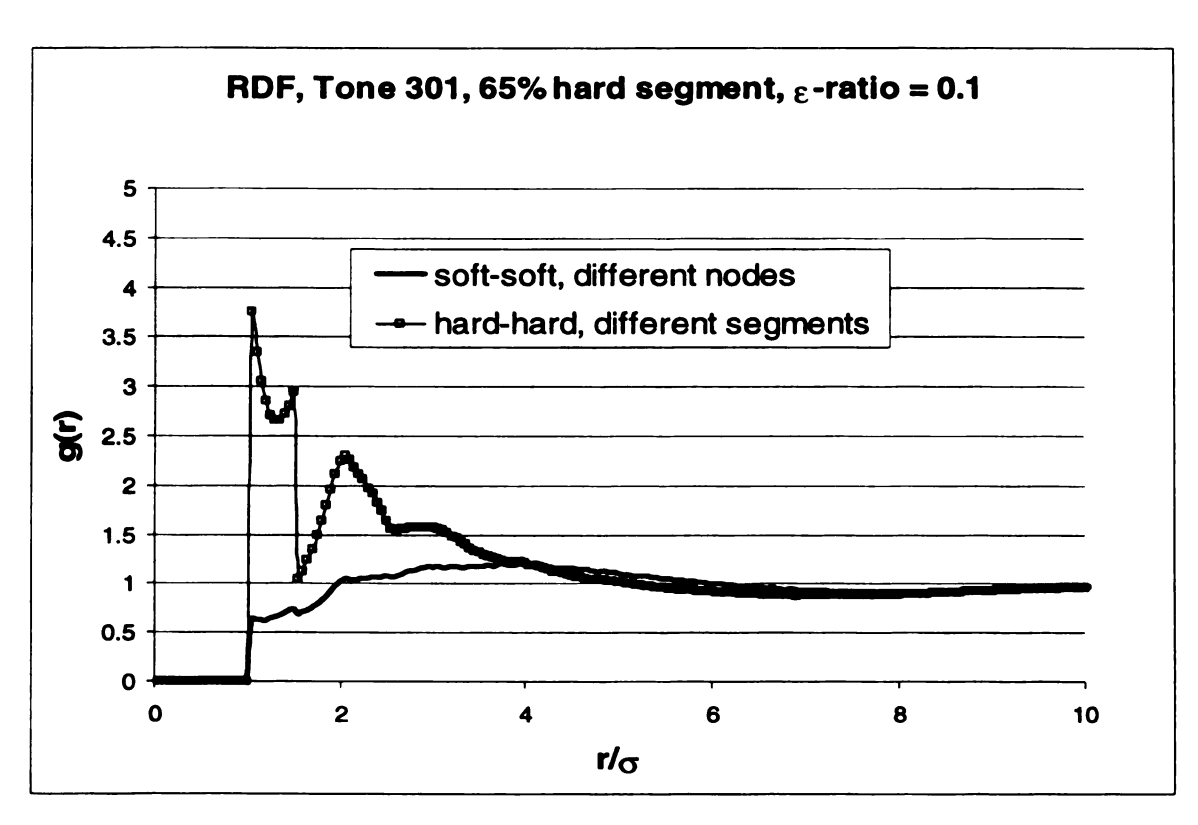


Figure A-3. RDF, Tone 301, 65% hard content, ϵ -ratio = 0.1, different chains

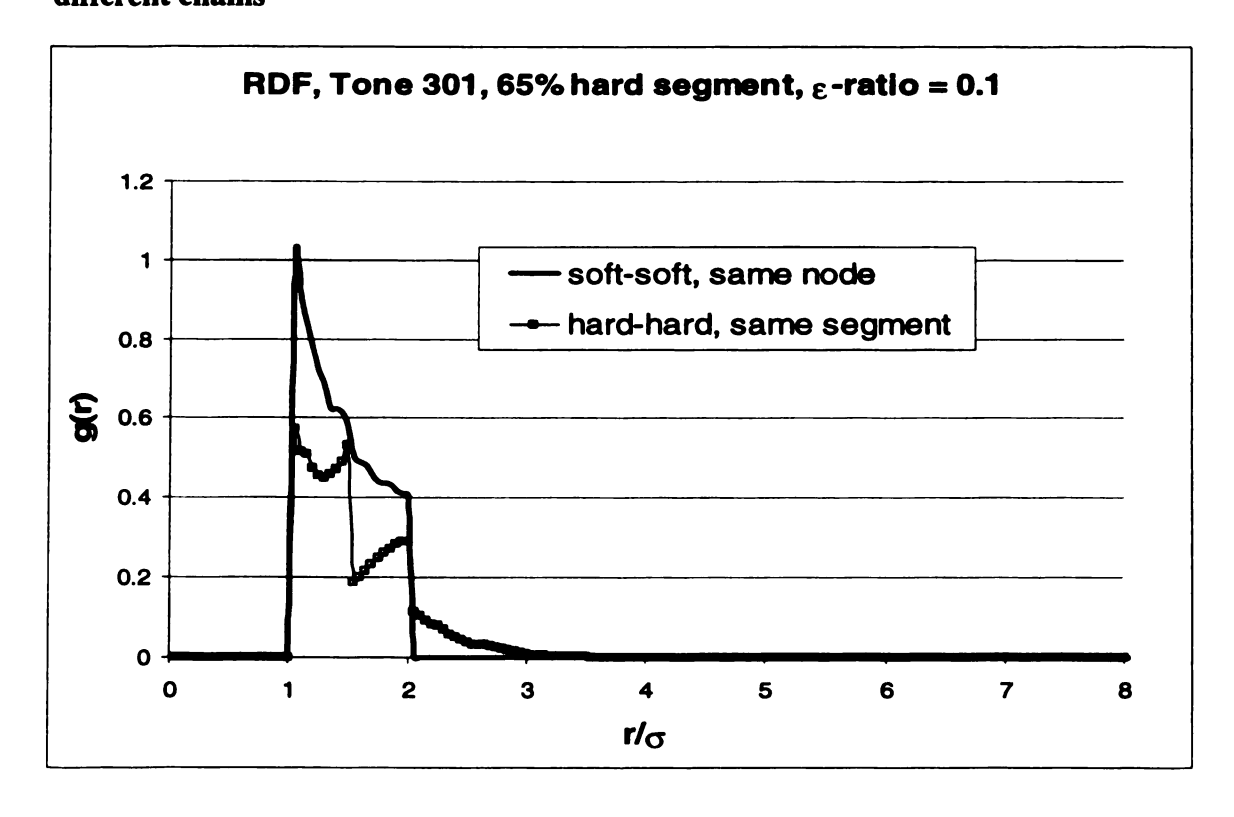


Figure A-4. RDF, Tone 301, 65% hard content, ε -ratio = 0.1, same chains

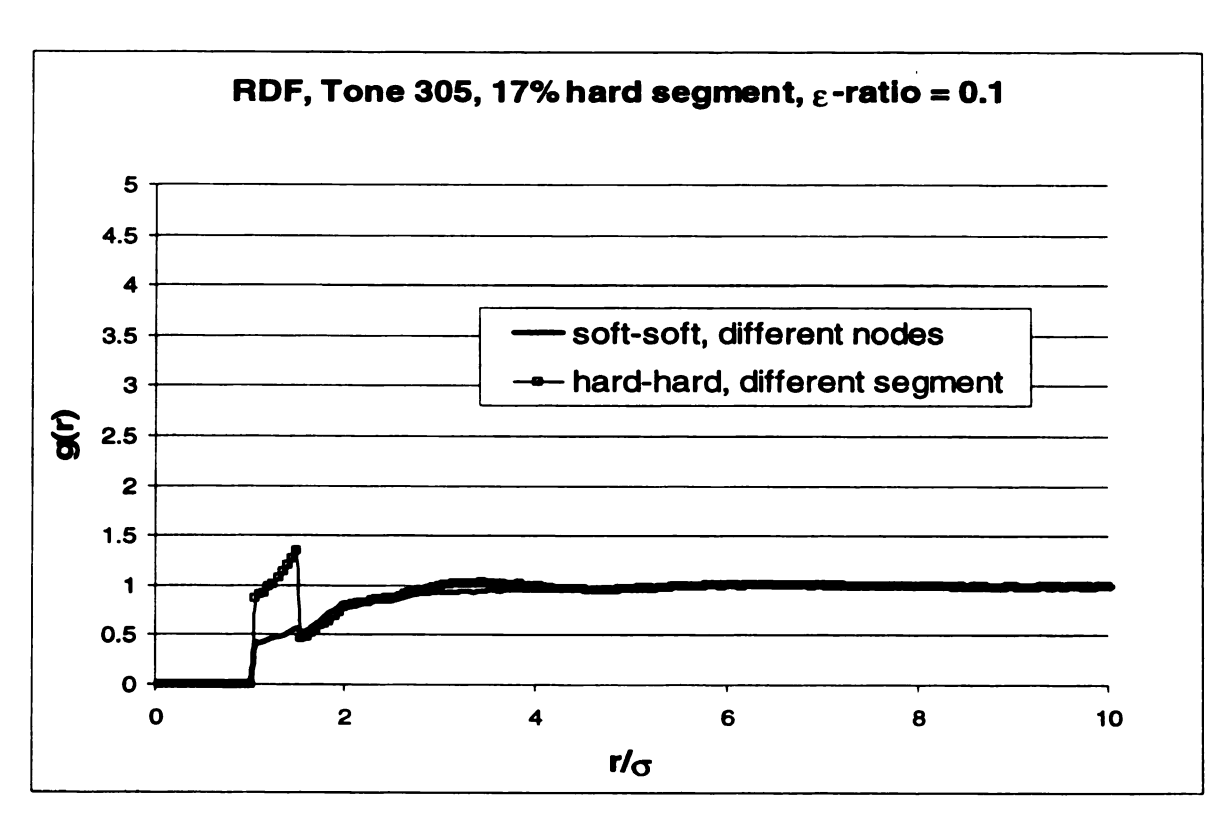


Figure A-5. RDF, Tone 305, 17% hard content, ϵ -ratio = 0.1, different chains

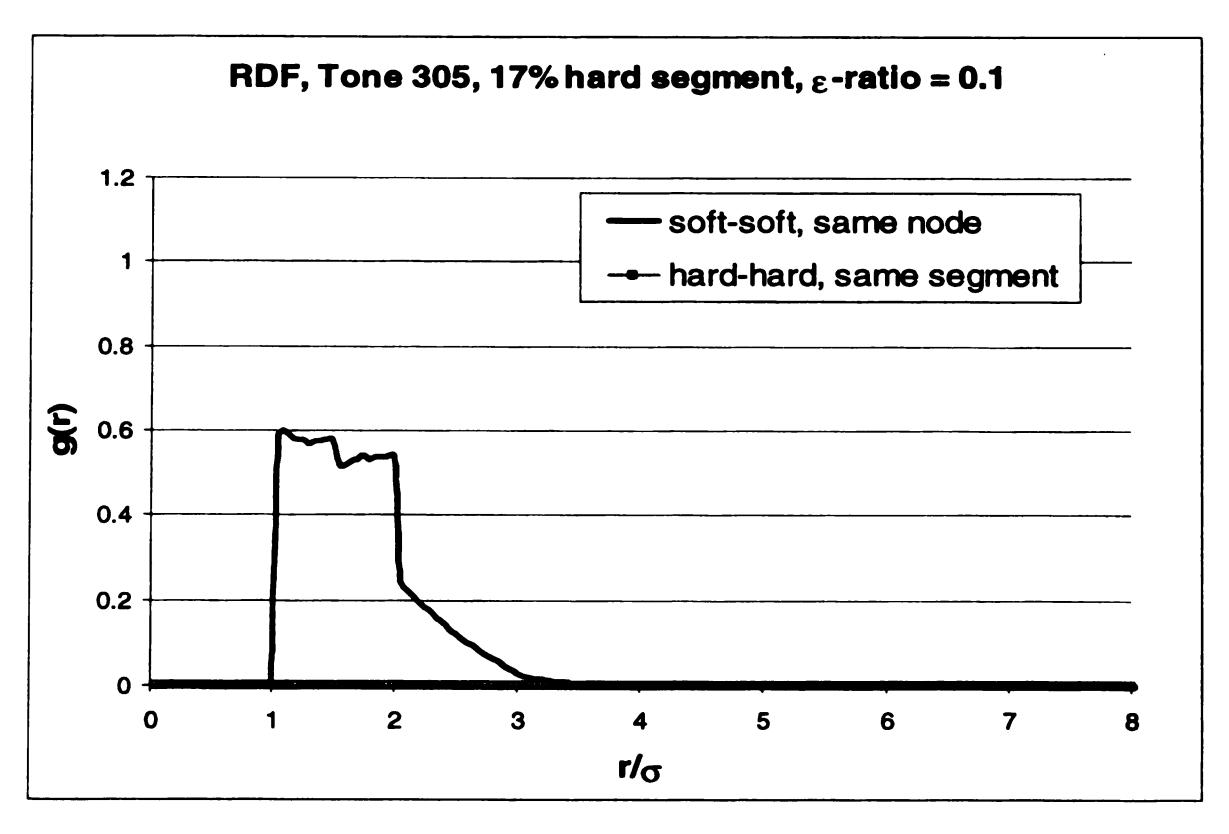


Figure A-6. RDF, Tone 305, 17% hard content, ε -ratio = 0.1, same chains

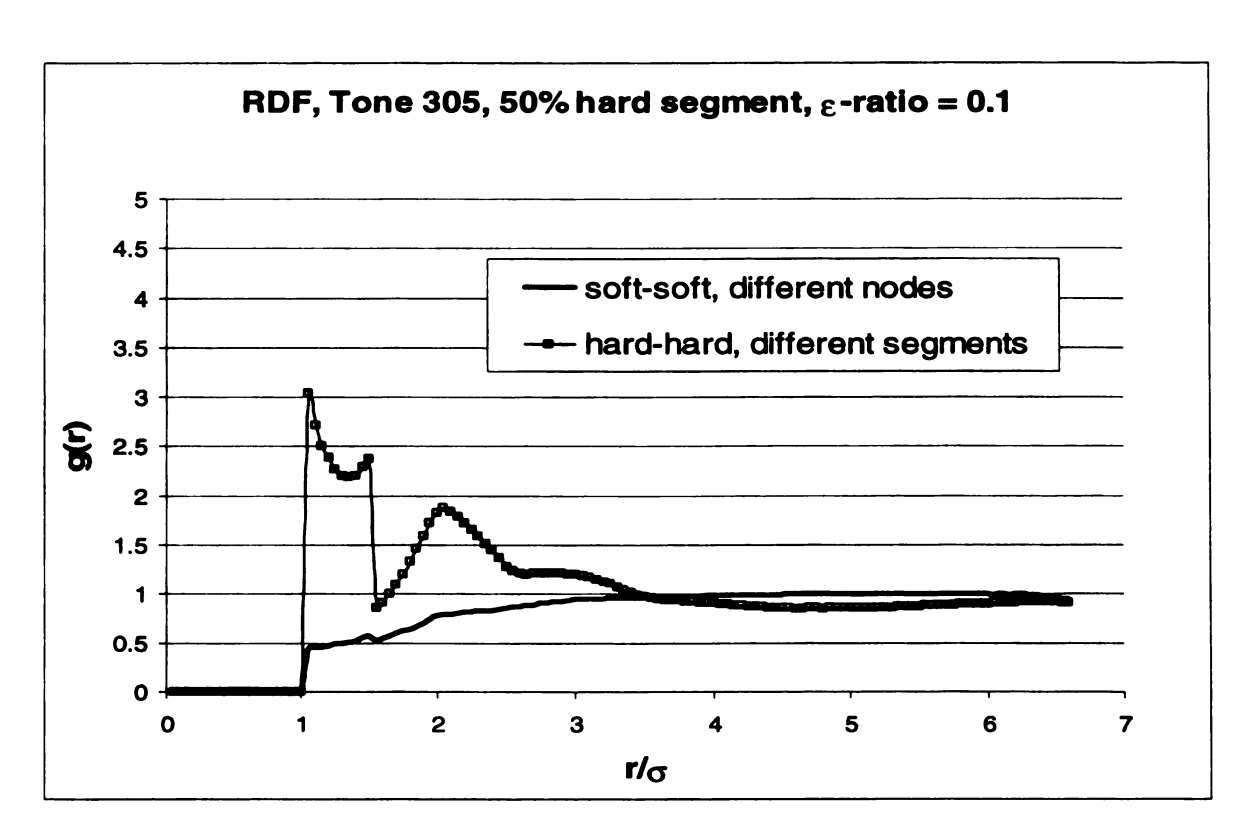


Figure A-7. RDF, Tone 305, 50% hard content, ϵ -ratio = 0.1, different chains

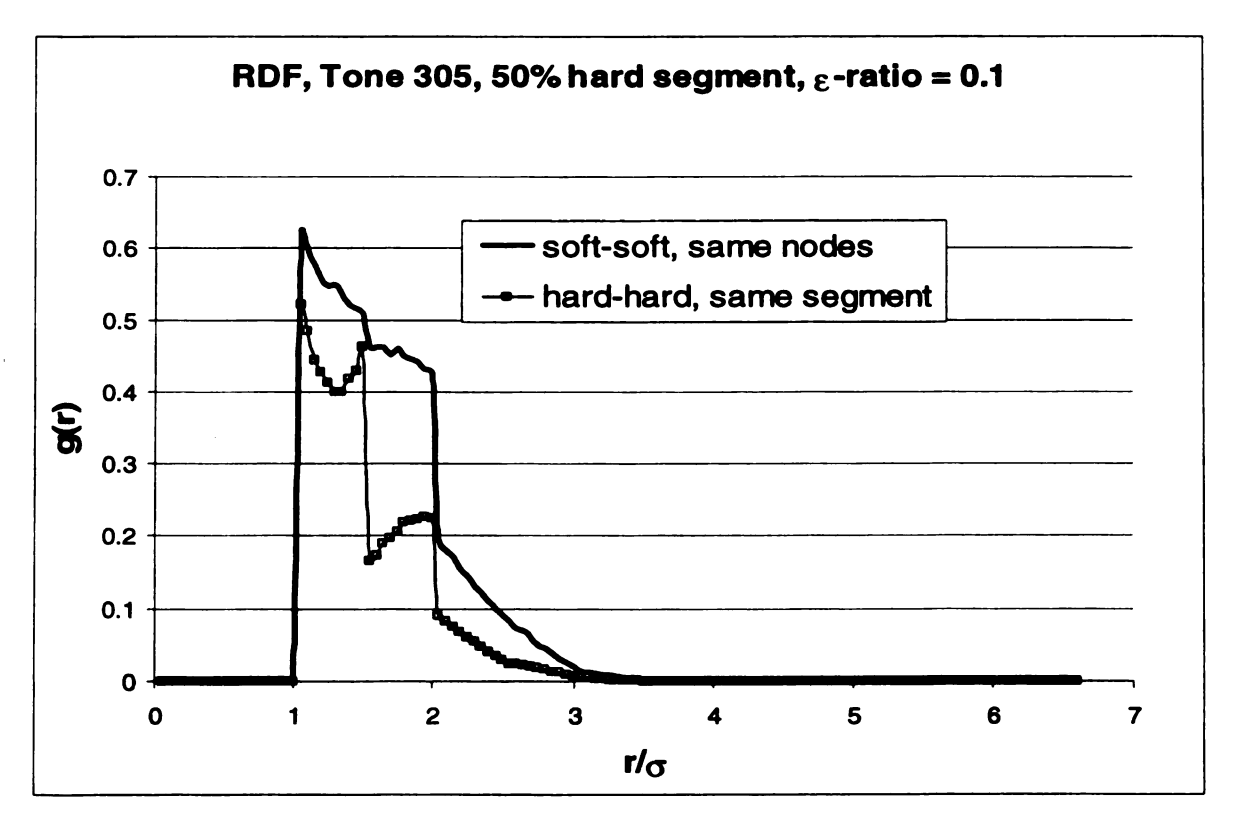


Figure A-8. RDF, Tone 305, 50% hard content, ϵ -ratio = 0.1, same chains

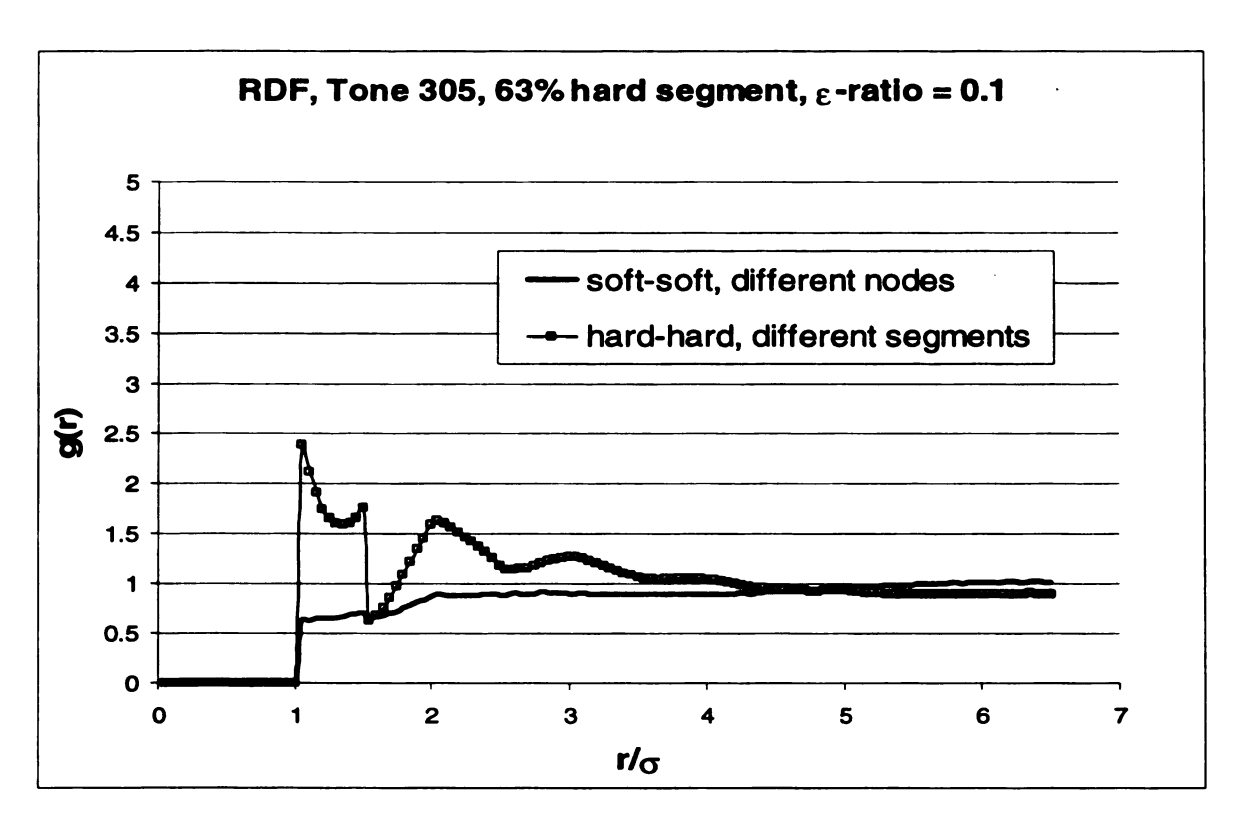


Figure A-9. RDF, Tone 305, 63% hard content, ϵ -ratio = 0.1, different chains

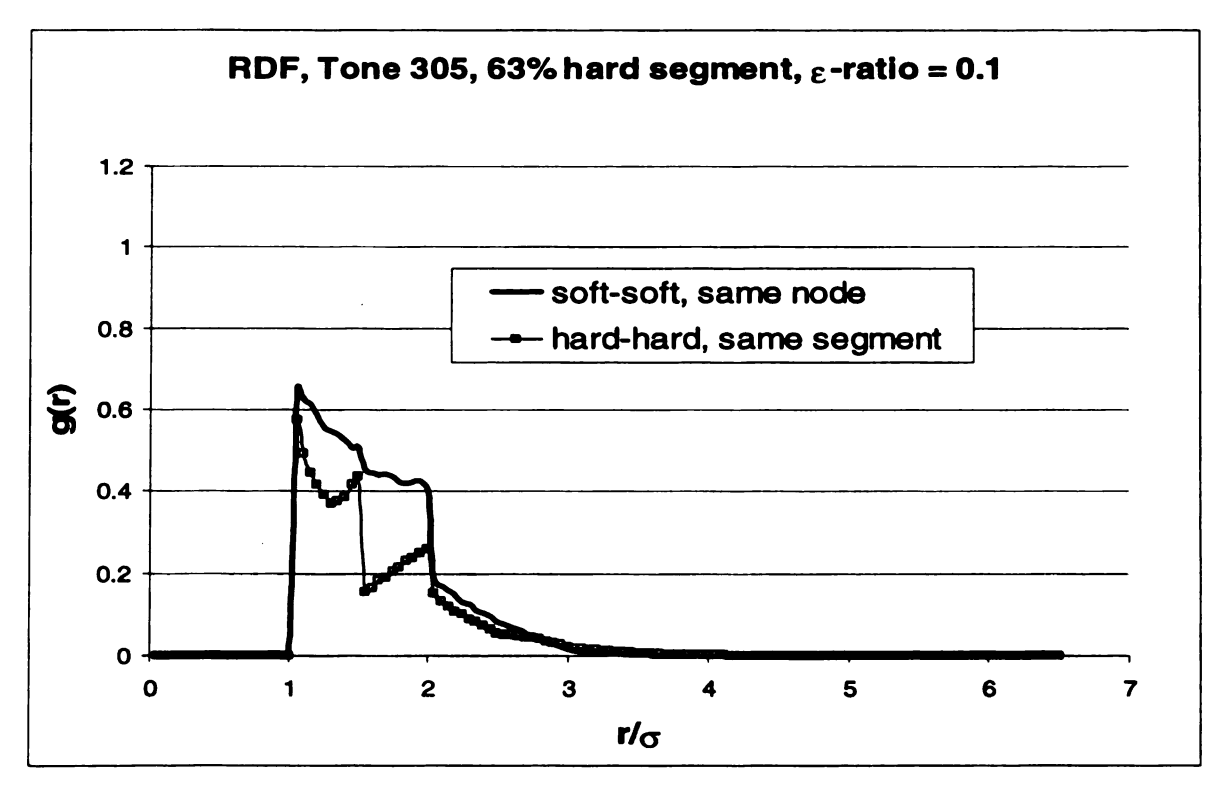


Figure A-10. RDF, Tone 305, 63% hard content, ε -ratio = 0.1, same chains

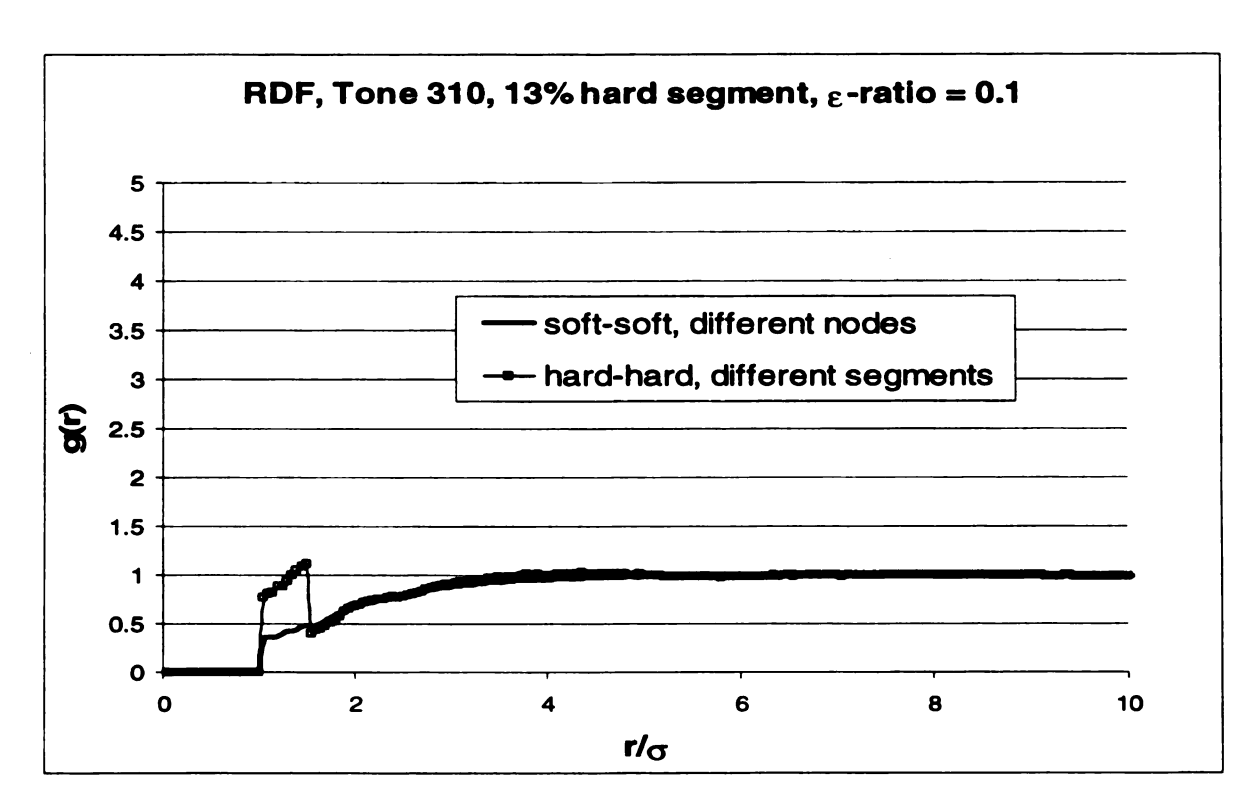


Figure A-11. RDF, Tone 310, 13% hard content, ϵ -ratio = 0.1, different chains

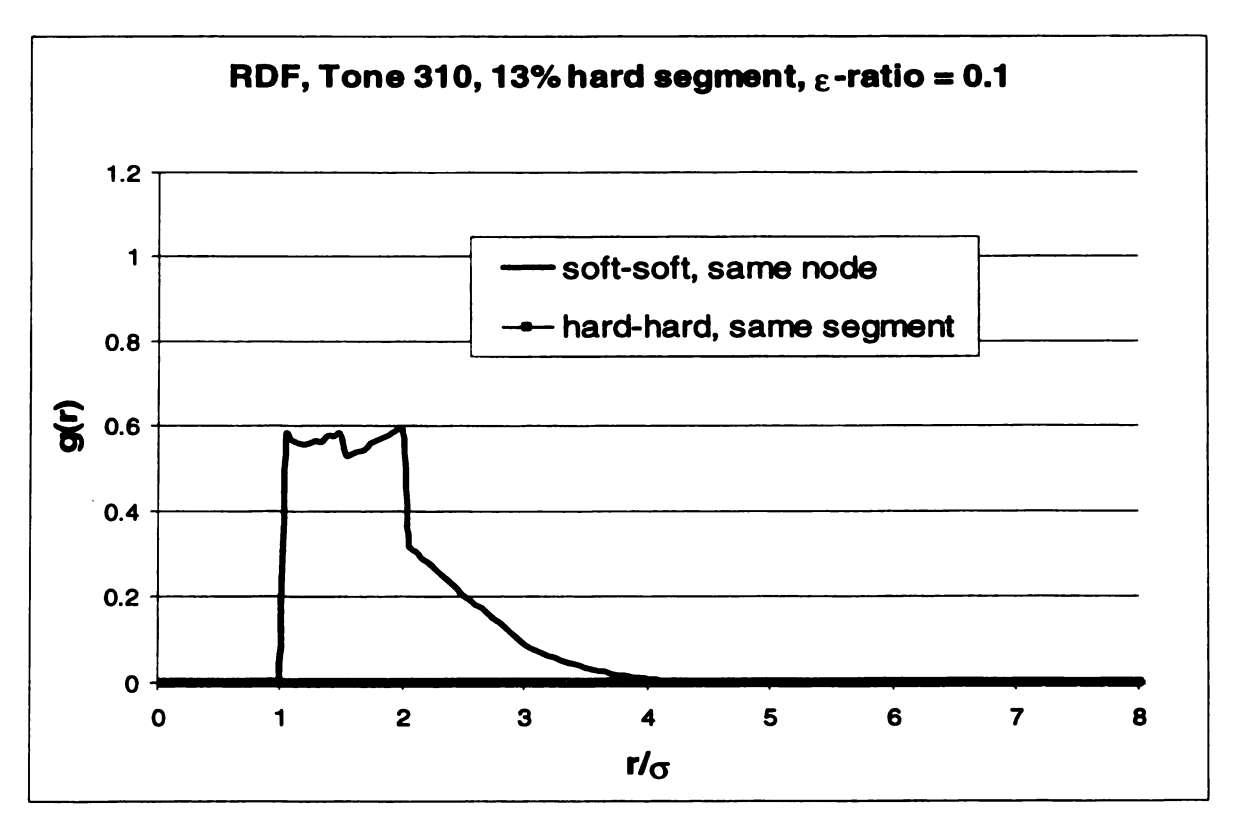


Figure A-12. RDF, Tone 310, 13% hard content, ε -ratio = 0.1, same chains

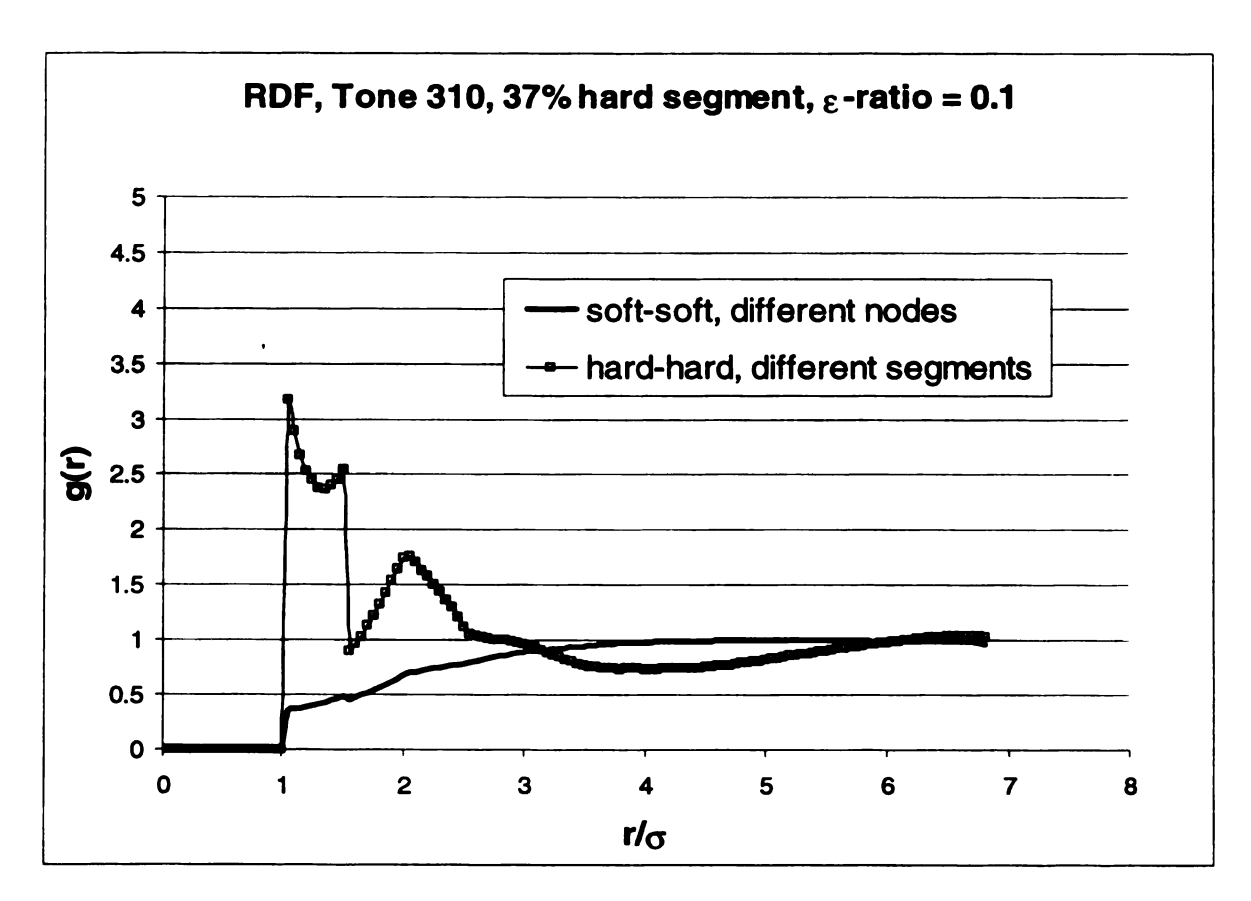


Figure A-13. RDF, Tone 310, 37% hard content, ϵ -ratio = 0.1, different chains

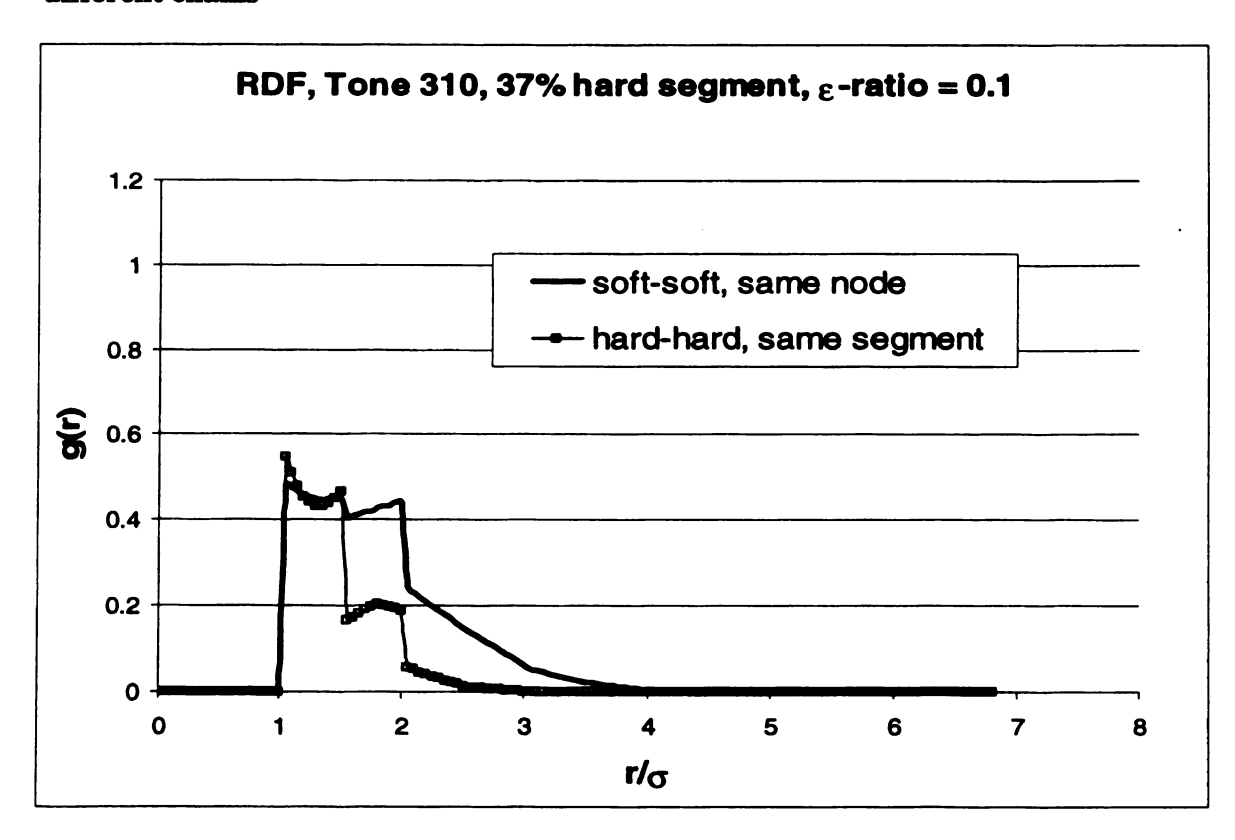


Figure A-14. RDF, Tone 310, 37% hard content, ε -ratio = 0.1, same chains

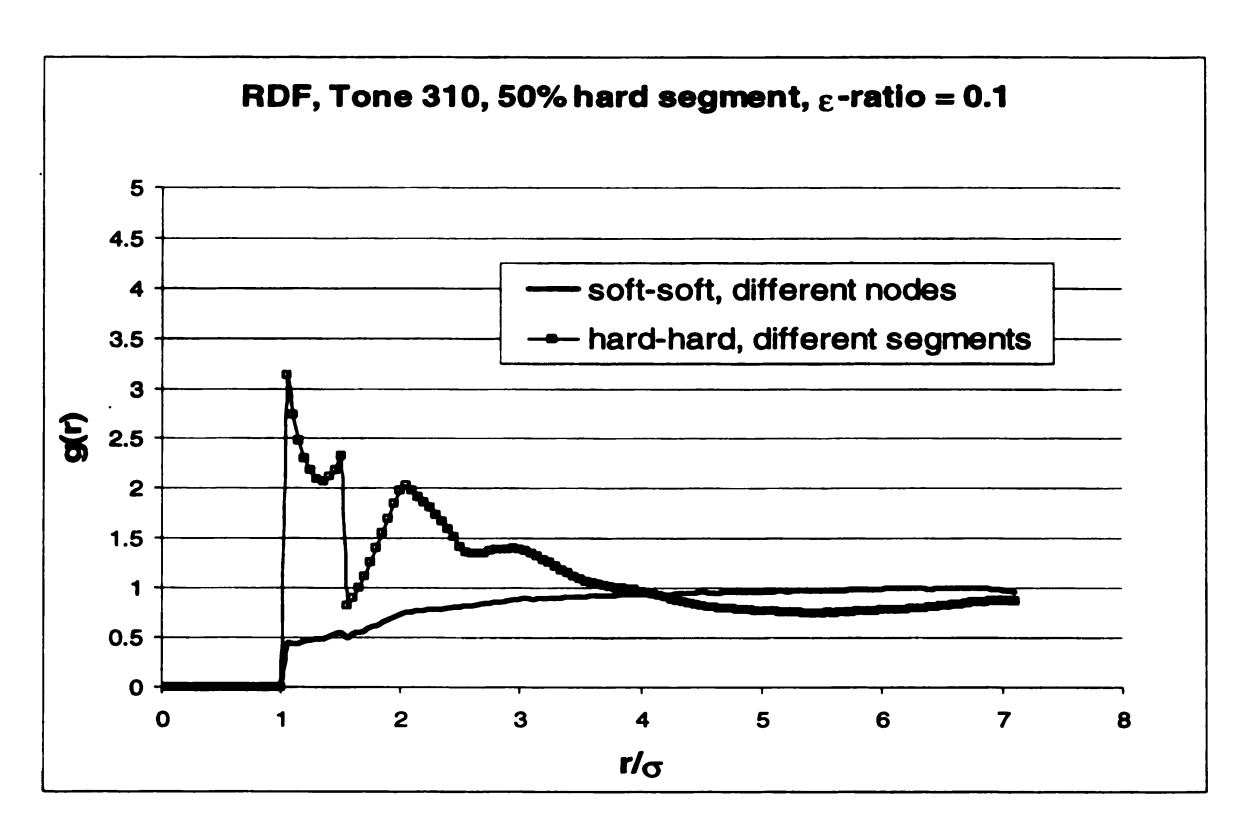


Figure A-15. RDF, Tone 310, 50% hard content, ϵ -ratio = 0.1, different chains

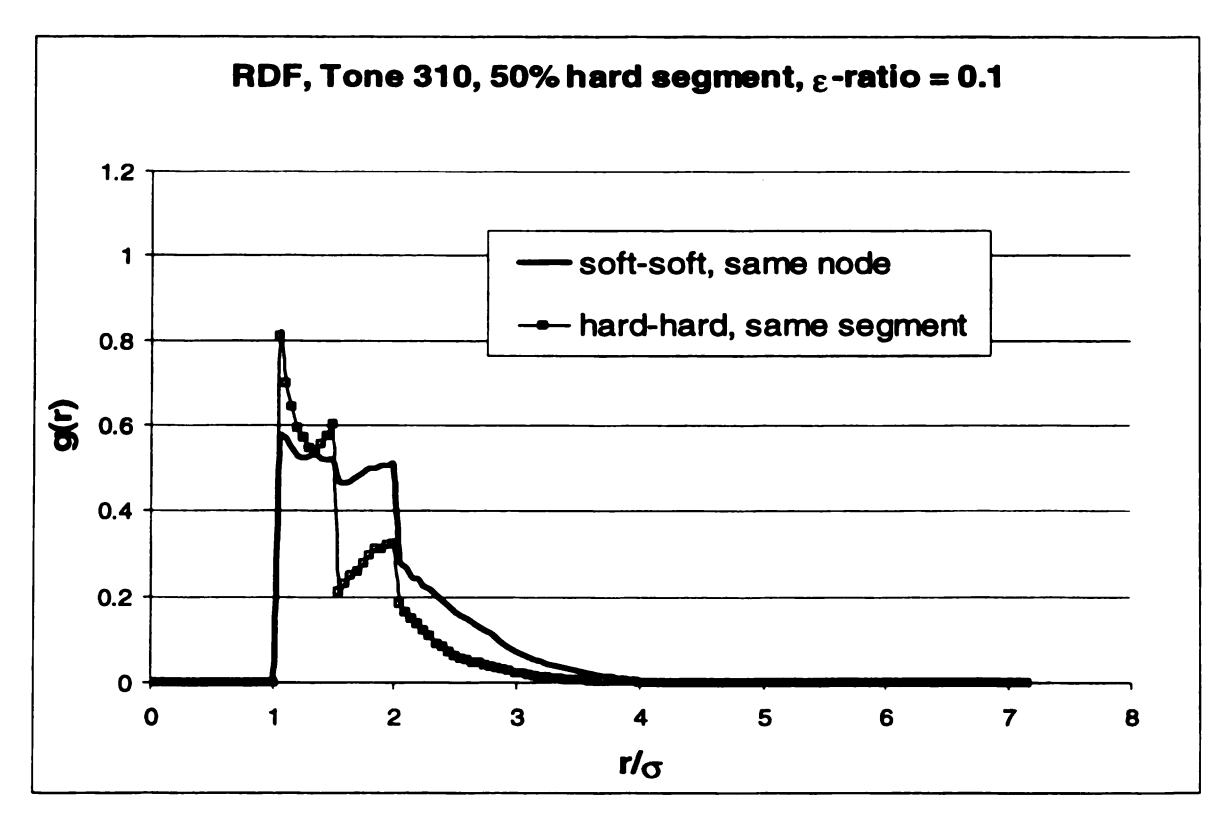


Figure A-16. RDF, Tone 310, 50% hard content, ε -ratio = 0.1, same chains

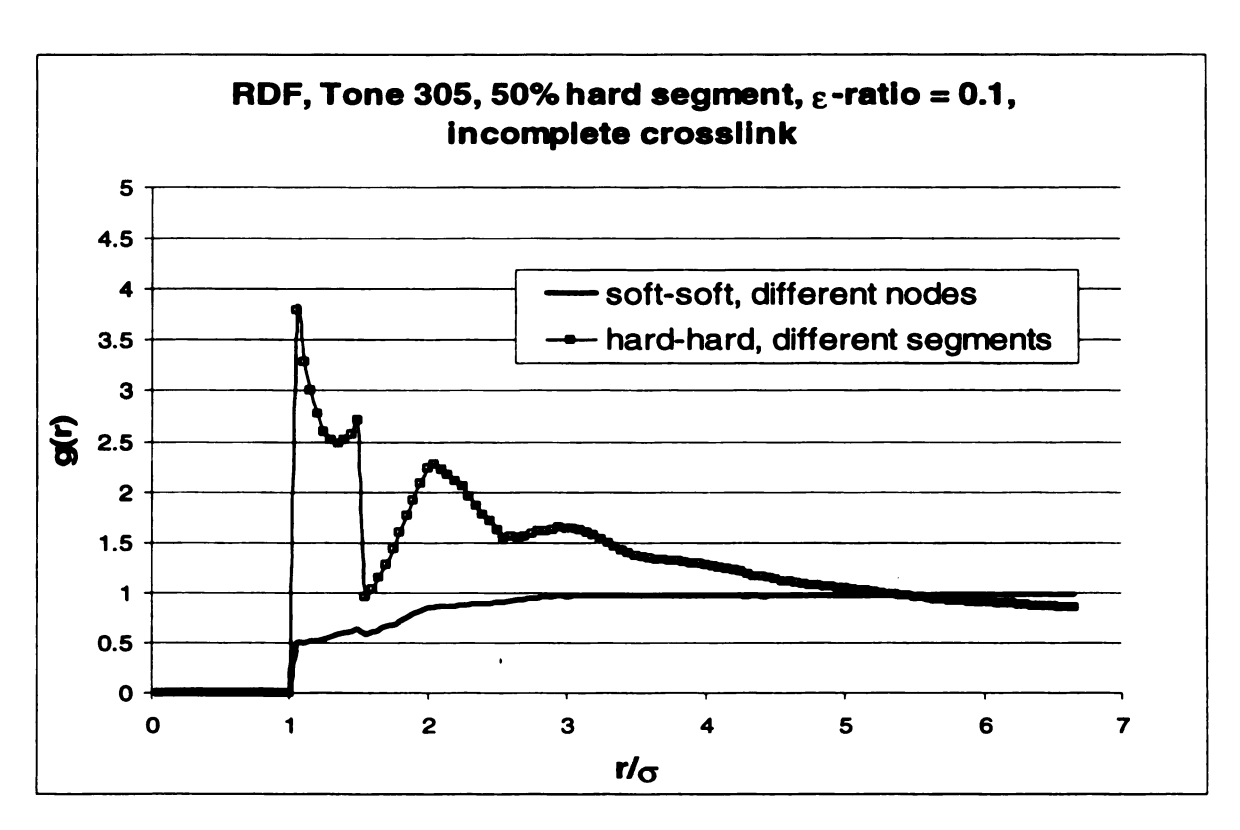


Figure A-17. RDF, Tone 305, 50% hard content, ϵ -ratio = 0.1, incomplete crosslink, different chains

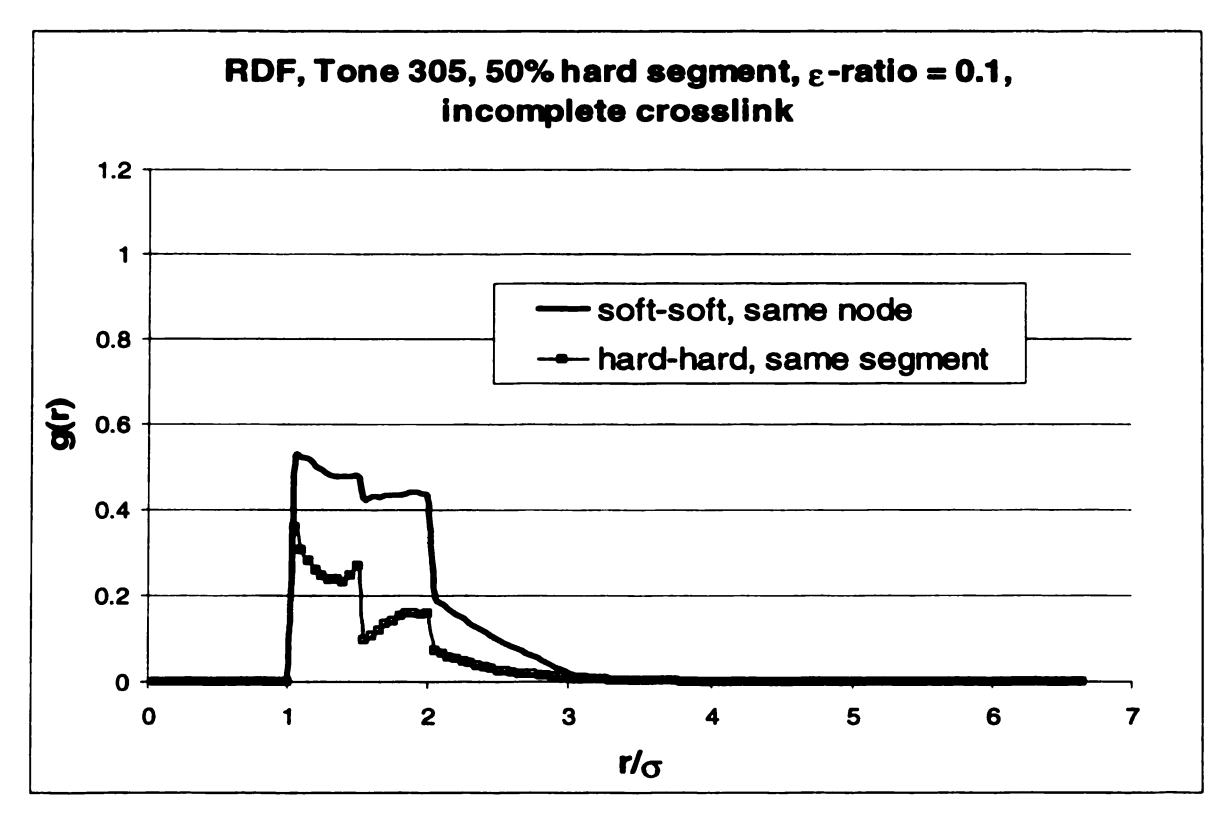


Figure A-18. RDF, Tone 305, 50% hard content, ϵ -ratio = 0.1, incomplete crosslink, same chains

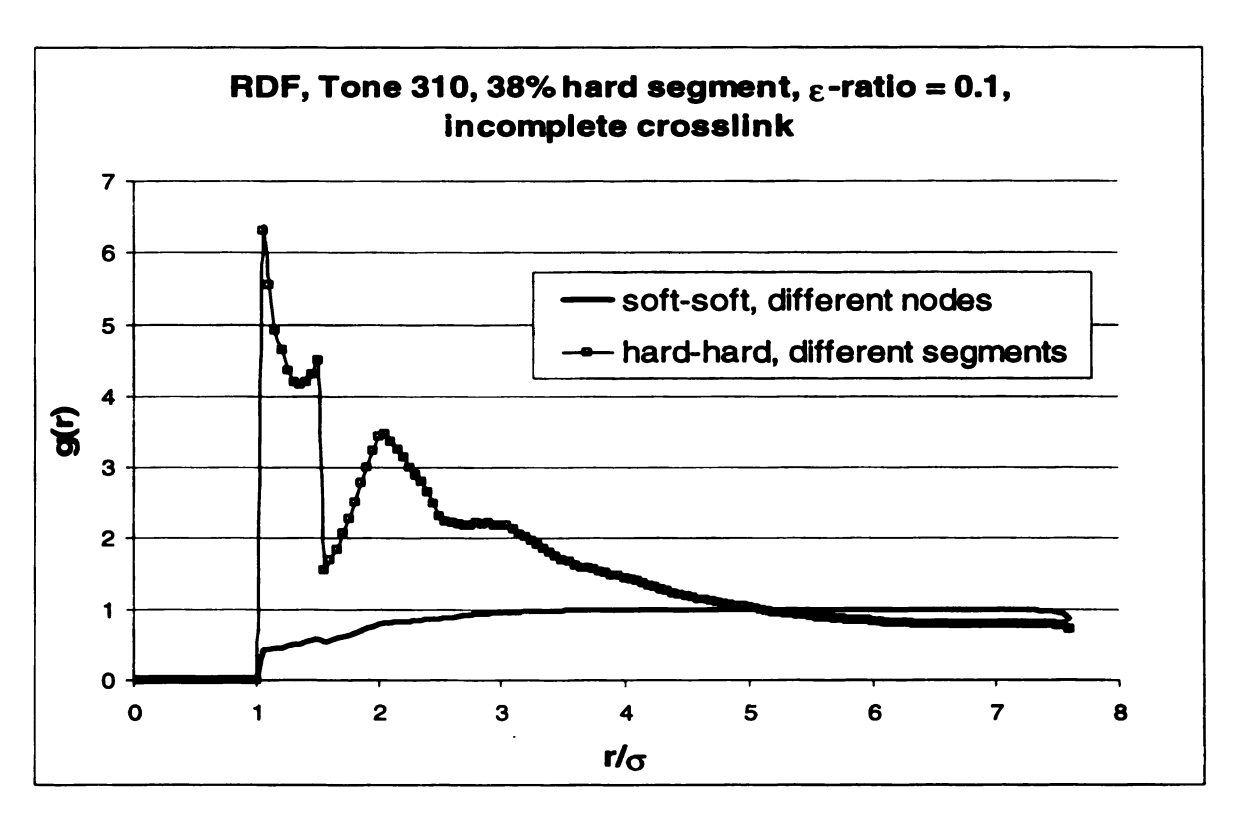


Figure A-19. RDF, Tone 310, 38% hard content, ϵ -ratio = 0.1, incomplete crosslink, different chains

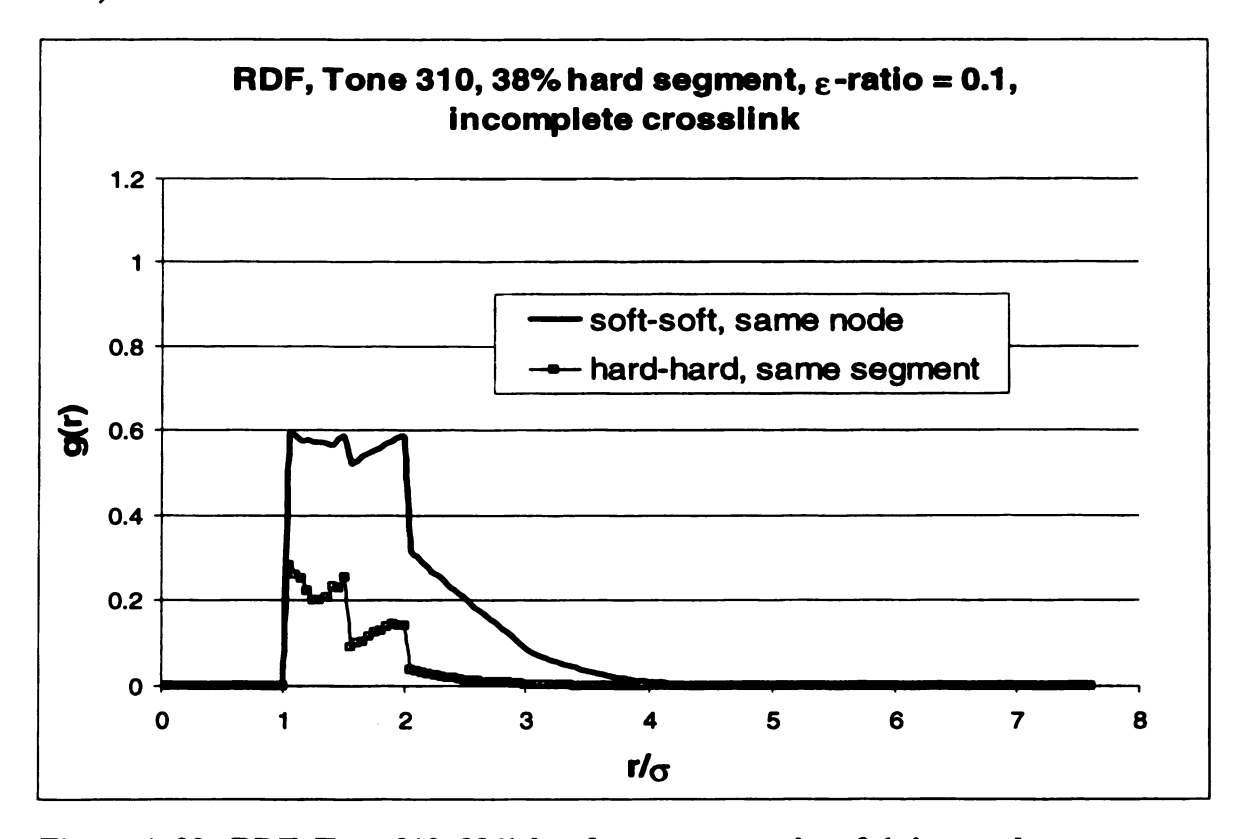


Figure A-20. RDF, Tone 310, 38% hard content, ϵ -ratio = 0.1, incomplete crosslink, same chains

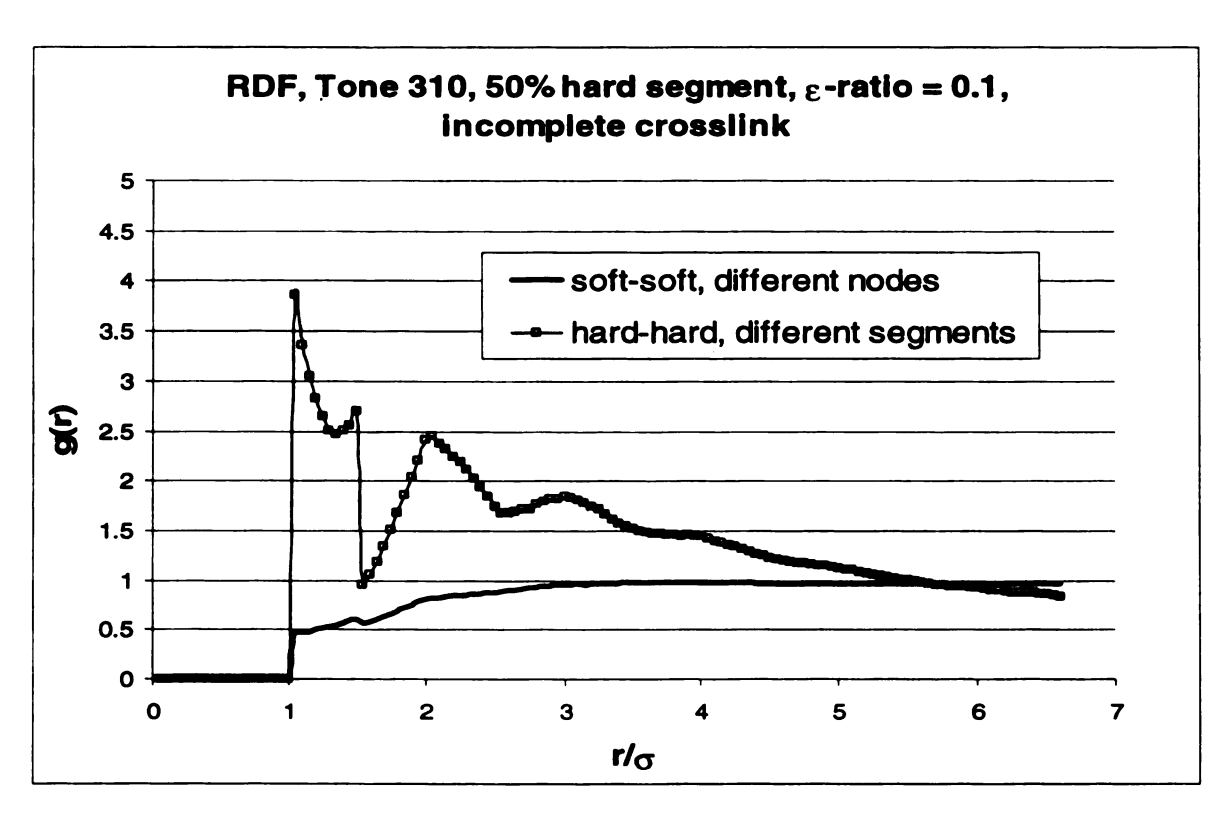


Figure A-21. RDF, Tone 310, 50% hard content, ϵ -ratio = 0.1, incomplete crosslink, different chains

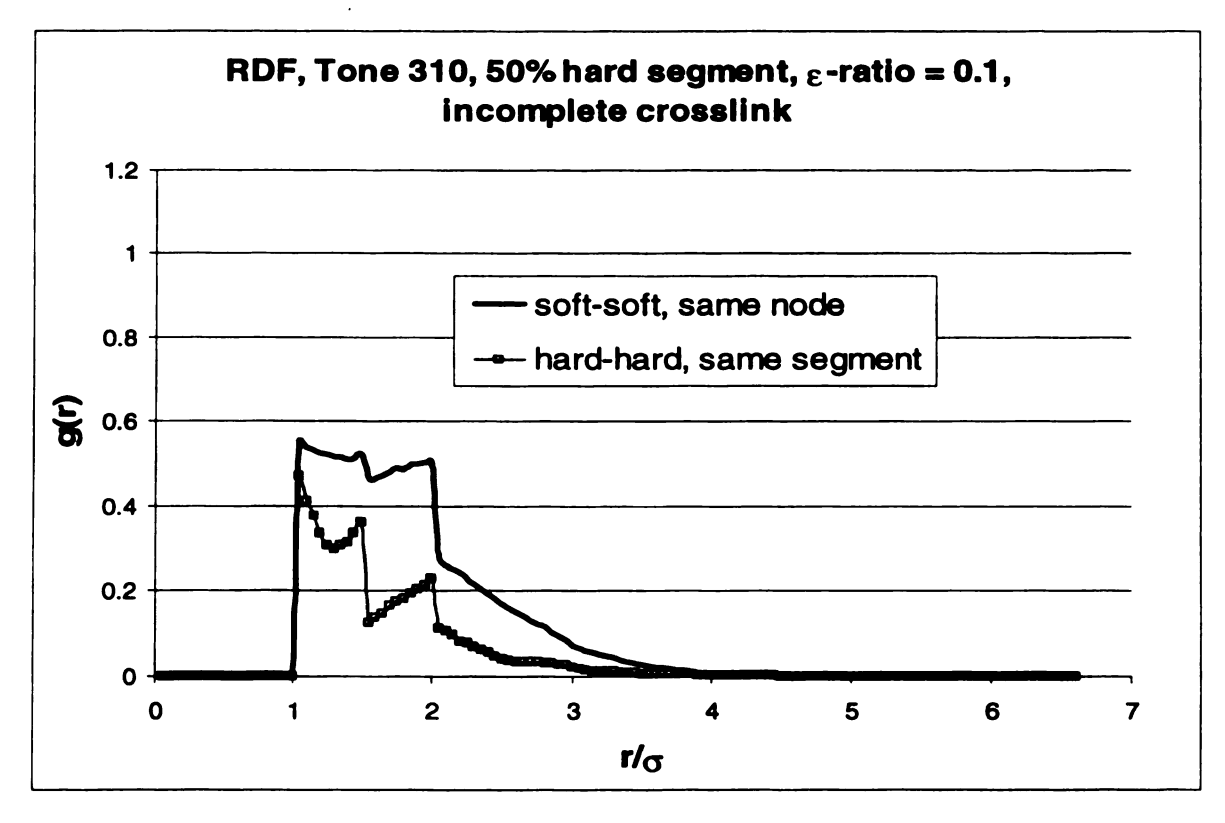


Figure A-22. RDF, Tone 310, 50% hard content, ϵ -ratio = 0.1, incomplete crosslink, same chains

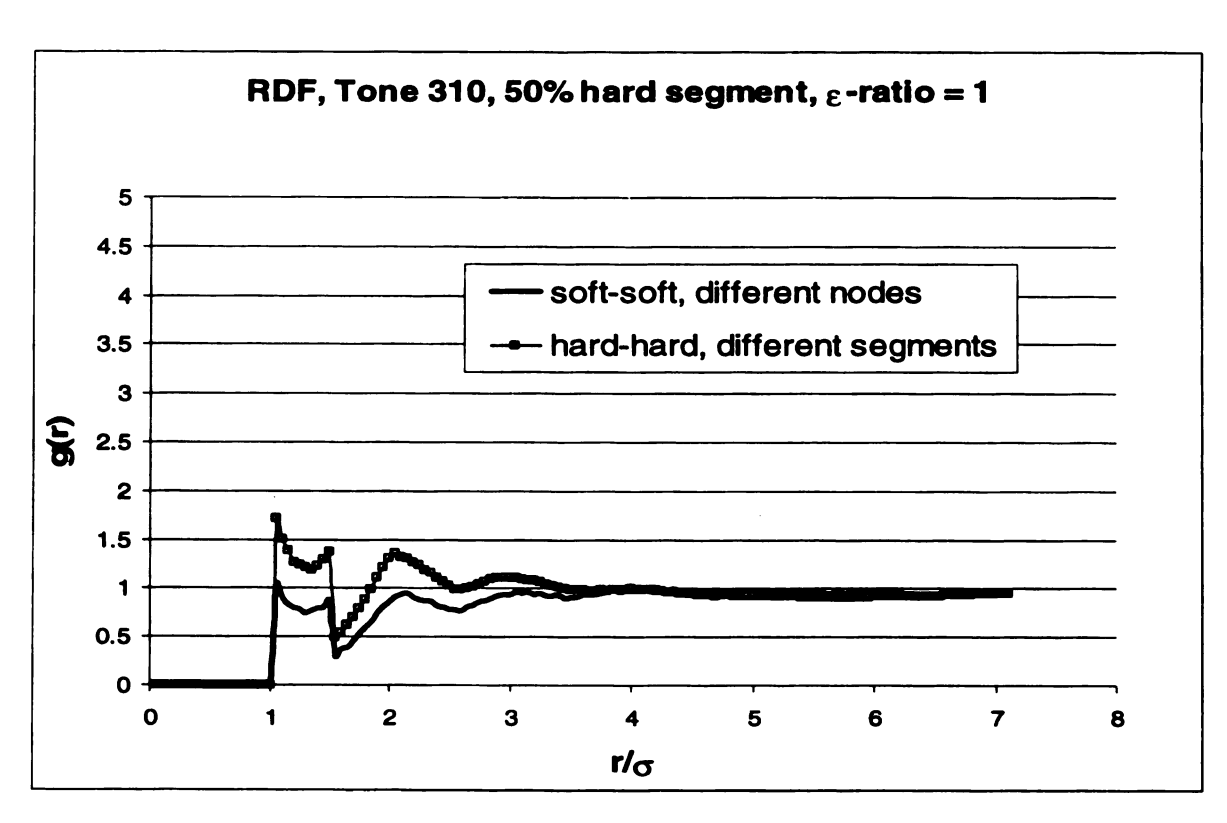


Figure A-23. RDF, Tone 310, 50% hard content, ϵ -ratio = 1, different chains

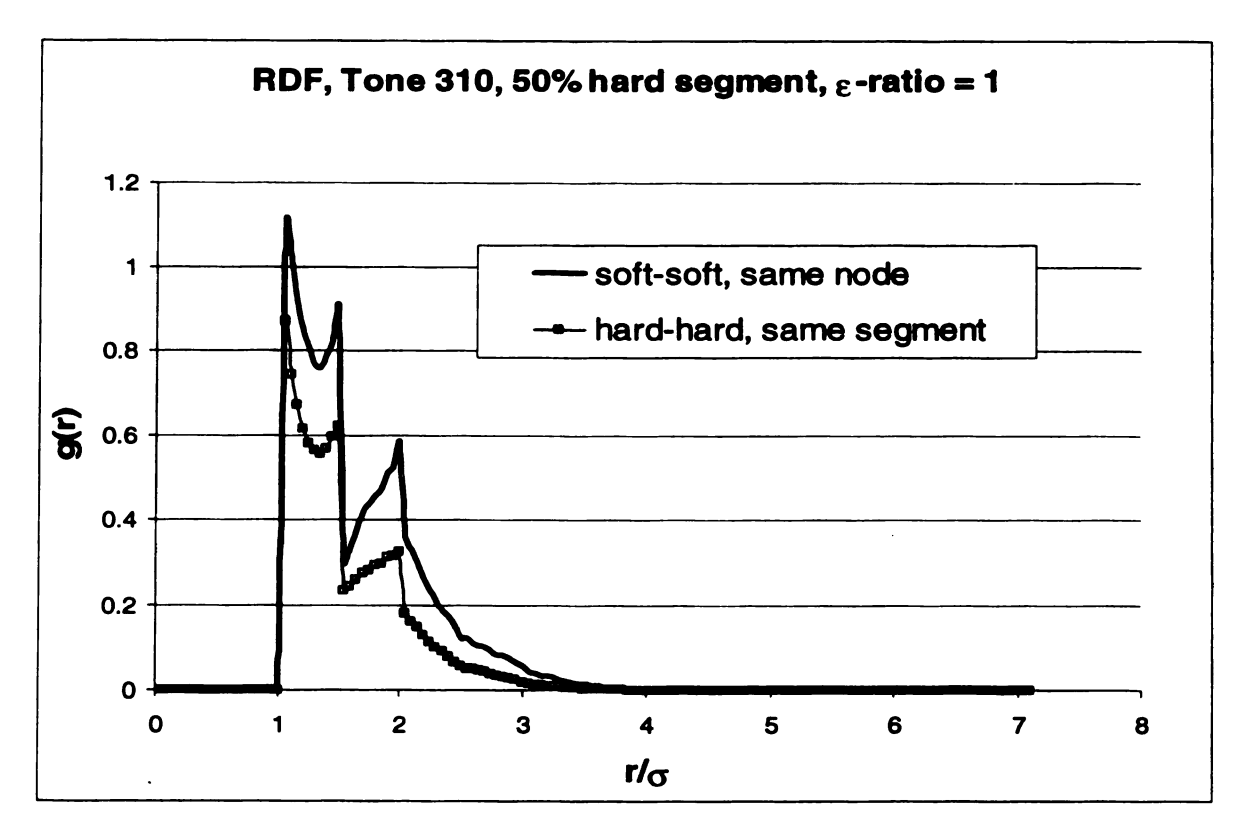


Figure A-24. RDF, Tone 310, 50% hard content, ε -ratio = 1, same chains

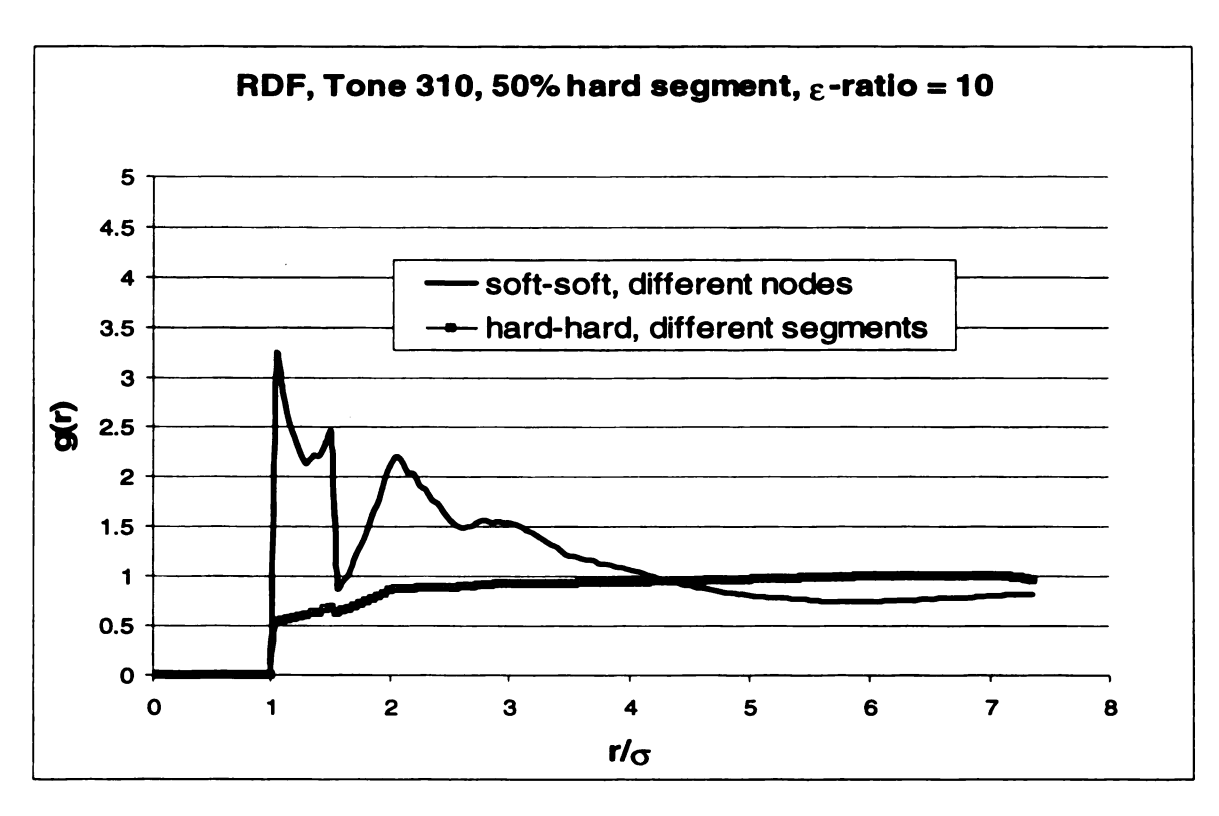


Figure A-25. RDF, Tone 310, 50% hard content, ϵ -ratio = 10, different chains

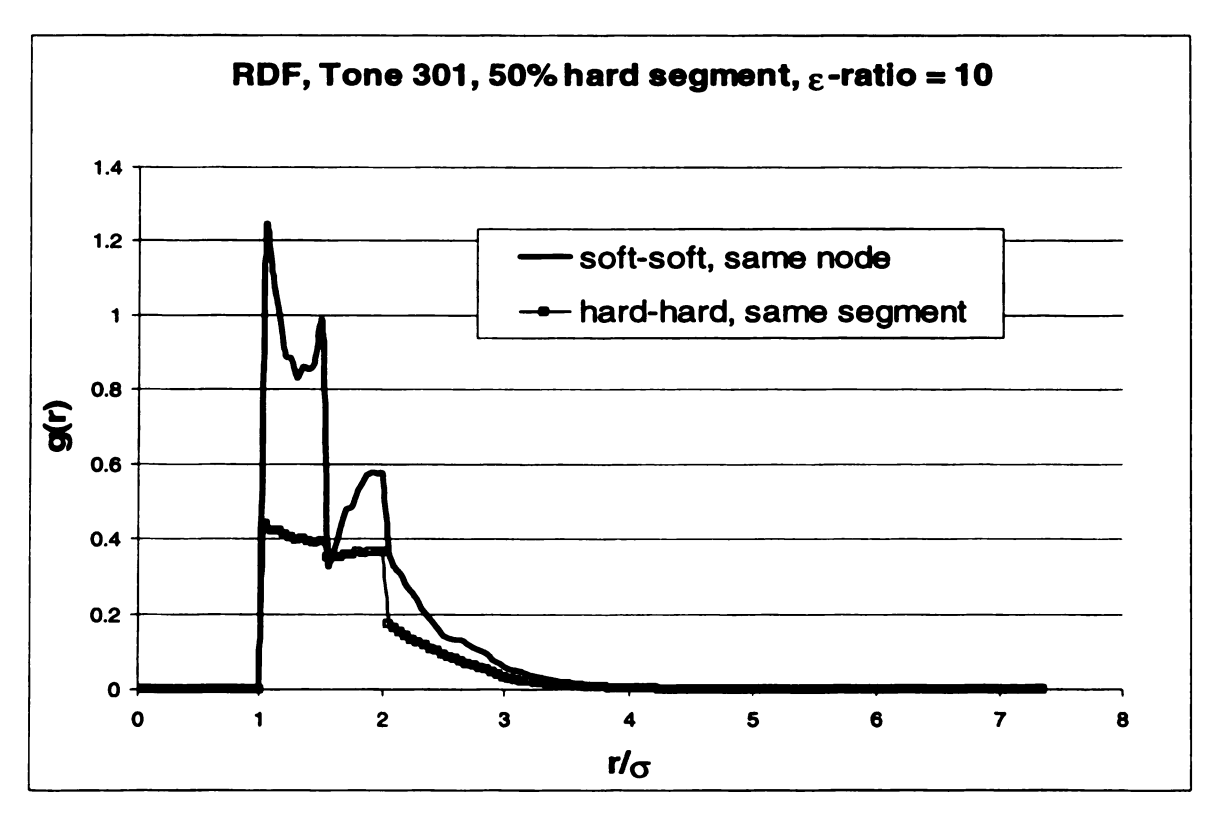


Figure A-26. RDF, Tone 310, 50% hard content, ε -ratio = 10, same chains

APPENDIX B

Listing of Additional System Parameters

Number of sites in each Cross-Link of fully linked systems:

Tone 301, 50% hard segment	2 soft sites, 3 hard sites, 5 sites total
Tone 301, 65% hard segment	2 soft sites, 5 hard sites, 7 sites total
Tone 305, 17% hard segment	4 soft sites, 1 hard site, 5 sites total
Tone 305, 50% hard segment	4 soft sites, 5 hard sites, 9 sites total
Tone 305, 63% hard segment	4 soft sites, 8 hard sites, 12 sites total
Tone 310, 13% hard segment	6 soft sites, 1 hard site, 7 sites total
Tone 310, 37% hard segment	6 soft sites, 4 hard sites, 10 sites total
Tone 310, 50% hard segment	6 soft sites, 7 hard sites, 13 sites total

Distribution of cross-link and dangling end lengths in partially linked systems:

Tone 305, 50% hard segment Longest Cross-Link: 10 sites

Shortest Cross-Link: 5 sites

Average Cross-Link: 5.5 sites

Longest Dangling End: 11 sites

Shortest Dangling End: 3 sites

Average Dangling End: 7.2 sites

Tone 310, 38% hard segment

Longest Cross-Link: 11 sites

Shortest Cross-Link: 7 sites

Average Cross-Link: 7.5 sites

Longest Dangling End: 11 sites

Shortest Dangling End: 3 sites

Average Dangling End: 6.6 sites

Tone 310, 50% hard segment

Longest Cross-Link: 10 sites

Shortest Cross-Link: 7 sites

Average Cross-Link: 7.4 sites

Longest Dangling End: 16 sites

Shortest Dangling End: 6 sites

Average Dangling End: 9.8 sites

APPENDIX C

Calculation of reduced Temperature and Pressure

$$k_B = 1.3806 \bullet 10^{-16} \bullet \frac{erg}{K}$$

Boltzmann Constant

P = 1 atm

chose atmospheric pressure, since Agrawal & Drzal

conducted experiments at this Pressure

T = 363 K

curing occurred at 90°C

Choice of site size:

 $\sigma = 3.8 \text{ Angstrom (A)}$ methylene beads

 σ = 4.812 A n-C₄H₁₀ [square well] σ = 5.339 A n-C₄H₁₀ [Lennard –Jones] σ = 5.27 A Benzene [Lennard – Jones]

 σ = 5.22 A Benzene [Sutherland] σ = 4.938 A Benzene [Kihara]

σ chosen:

 $\sigma = 5 A$

Choice of energy well depth:

 $\epsilon/k_B = 387 \text{ K}$ n-C₄H₁₀ [square well] $\epsilon/k_B = 309.74 \text{ K}$ n-C₄H₁₀ [Lennard – Jones] $\epsilon/k_B = 440 \text{ K}$ Benzene [Lennard – Jones]

 $\varepsilon/k_B = 1070 \text{ K}$ Benzene [Sutherland] $\varepsilon/k_B = 975.37 \text{ K}$ Benzene [Kihara]

An ε -value of ε = 400 K*k is chosen as a mean between the values for n-C₄H₁₀ and Benzene. Butane and benzene represent two significant backbones of the polyurethanes investigated by Agrawal & Drzal (1995a). The chosen ε corresponds to the hard-hard interaction energy (ε_{hh}) used in this work.

reduced Pressure:

$$P_R = \frac{P \bullet \sigma^3}{\varepsilon} = 2.294 \bullet 10^{-3}$$

reduced Temperature:

$$T_R = \frac{k_B \bullet T}{\varepsilon} = 0.908$$

APPENDIX D

TABLE D-1 SUMMERY OF AVERAGE ENERGY PER SITE

Tone	Hard Segment Content (%)	Energy per Site	Standard Deviation	
301	50	-1.572	∓ 1.54E-02	
301	65	-2.274	∓ 2.96E-02	
305	17	-0.228	∓ 2.42E-02	
305	50	-1.914	∓ 1.64E-02	
305	63	-2.772	∓ 2.87E-02	
310	13	-0.201	∓ 1.70E-02	
310	37	-1.232	∓ 1.67E-02	
310	50	-2.094	∓ 1.18E-02	

TABLE D-2 SUMMERY OF SYSTEM PACKING FRACTIONS

Tone	Hard Segment Fraction (%)	Packing Fraction	Standard Deviation	
301	50	0.186	∓ 1.22E-03	
301	65	0.138	∓ 9.83E-04	
305	17	0.103	∓ 2.56E-04	
305	50	0.206	∓ 4.91E-03	
305	63	0.278	∓ 6.65E-03	
310	13	.113	∓ 8.56E-04	
310	37	.216	∓ 5.27E-03	
310	50	.231	∓ 2.20E-03	

TABLE D-3 CROSS-LINK LENGTH AND PACKING FRACTION CORRELATION

Tone	Hard Segment Content (%)	Total Cross-Link Length	No. of Soft sites per Cross-Link	No. of Hard sites per Cross-Link	Packing Fraction
301	50	5	2	3	0.186
301	65	7	2	5	0.138
305	17	5	4	1	0.130
305	50	9	4	5	0.206
305	63	12	4	8	0.278
310	13	7	6	1	0.113
310	37	10	6	4	0.216
310	50	13	6	7	0.231

APPENDIX E



Figure E-1. Snapshot: Tone 305, 17% hard segment content



Figure E-2. Snapshot: Tone 305, 50% hard segment content



Figure E-3. Snapshot: Tone 305, 63% hard segment content

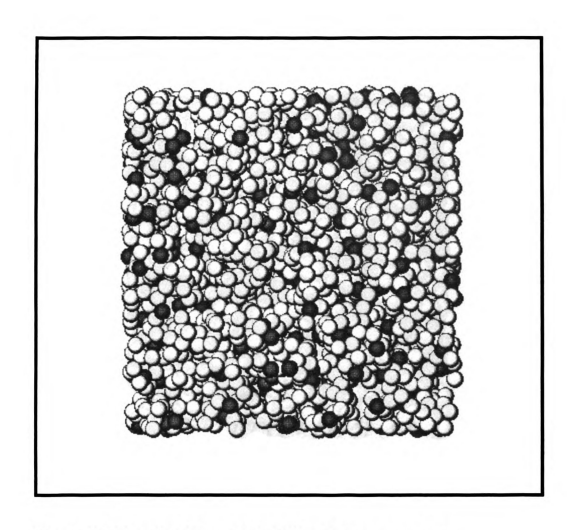


Figure E-4. Snapshot: Tone 310, 13% hard segment content



Figure E-5. Snapshot: Tone 310, 37% hard segment content

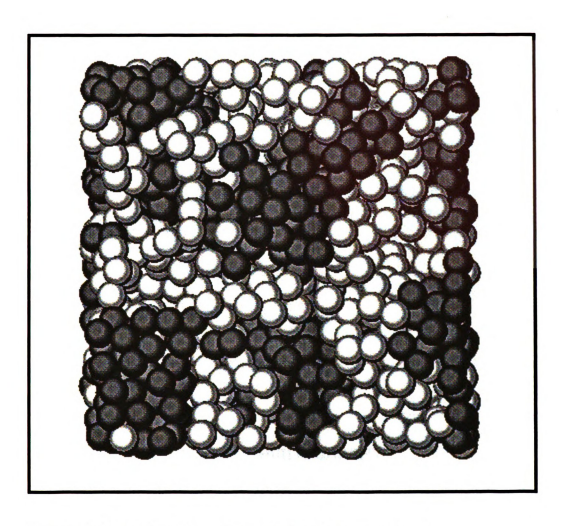


Figure E-6. Snapshot: Tone 310, 50% hard segment content

BIBLIOGRAPHY

BIBLIOGRAPHY

- Agrawal, R. K., & Drzal, L. T. (1995a). Adhesion Mechanisms of Polyurethanes to Glass Surfaces I. Structure-Property Relationships in Polyurethanes and Their Effects on Adhesion to Glass. Journal of Adhesion, 54, 79-102.
- Agrawal, R. K., & Drzal, L. T. (1995b). Adhesion mechanisms of polyurethanes to glass Surfaces. Part II. Phase separation in polyurethanes and its effects on Adhesion to glass. <u>Journal of adhesion science and technology</u>, 9, 1381-1400.
- Agrawal, R. K., & Drzal, L. T. (1996). Adhesion Mechanisms of Polyurethanes to Glass Surfaces III. Investigation of Possible Physico-Chemical Interactions at the Interphase. <u>Journal of Adhesion</u>, 55, 221-243.
- Binder, K. (Ed.). (1995). <u>Monte Carlo and Molecular Dynamics Simulations in Polymer Science.</u> New York: Oxford University Press.
- Benoit, H., & Hadziioannou, G. (1988). Scattering Theory and Properties of Block Copolymers with Various Architectures in the Homogeneous Bulk State. Macromolecules, 21 (5), 1449-1464.
- Dawson, J. R., & Shortall, J. B. (1982). The Impact Behavior of RRIM Polyurethane Elastomers. Cellular Polymers, 1, 41-51.
- De Gennes, P. G. (1979). Effect of cross-links on a mixture of polymers. <u>Le</u> <u>Journal de Physique</u>, 40 (4), 69-72
- De Pablo. J. J., Laso, M., & Suter, U. W. (1992). Simulation of polyethylene above and below the melting point. <u>Journal of Chemical Physics</u>, 96 (3), 2395-2403
- Duering, E. R., Kremer, K., & Grest, G. S. (1991). Relaxation of Randomly Cross-Linked Polymer Melts. <u>Physical Review Letters</u>, 67 (25), 3531-3534.
- Duering, E. R., Kremer, K., & Grest, G. S. (1993). Dynamics of Model Networks: The Role of the Melt Entanglement Length. <u>Macromolecules, 26 (12),</u> 3241-3244.
- Duering, E. R., Kremer, K., & Grest, G. S. (1994). Structure and relaxation of end-linked polymer networks. <u>Journal of Chemical Physics</u>, 101 (9), 8169-8192.

- Eberhart, J.G. (1966). The Surface Tension of Binary Liquid Mixtures. <u>Journal</u> of Physical Chemistry, 70 (4), 1183-1186.
- Escobedo, F. A., & de Pablo, J. J. (1995a). A new method for generating volume changes in isobaric-isothermal Monte Carlo simulations of flexible molecules. <u>Macromolecular Theory and Simulation</u>, 4, 691-707.
- Escobedo, F. A., & de Pablo, J. J. (1995b). Extended continuum configurational bias Monte Carlo methods for simulation of flexible molecules. <u>Journal of Chemical Physics</u>, 102 (6), 2636-2652.
- Escobedo, F. A., & de Pablo, J. J. (1996). Monte Carlo simulation of branched and crosslinked polymers. <u>Journal of Chemical Physics</u>, 104 (12), 4788-4800.
- Escobedo, F. A., & de Pablo, J. J. (1997a). Phase behaviour of model polymeric networks and gels. <u>Molecular Physics</u>, 90 (3), 437-443.
- Escobedo, F. A., & de Pablo, J. J. (1997b). Simulation and theory of the swelling of athermal gels. <u>Journal of Chemical Physics</u>, 106 (2), 793-810.
- Flory, P. J. (1953). <u>Principles of Polymer Chemistry.</u> Ithaca, NY: Cornell University Press.
- Grest, G. S., & Kremer, K. (1990a). Critical properties of crosslinked polymer melts. <u>Journal de Physique (France)</u>, <u>51</u>, 2829-2842.
- Grest, G. S., & Kremer, K. (1990b). Statistical Properties of Random Cross-Linked Rubbers. Macromolecules, 23, 4994-5000.
- Grest, G. S., Kremer, K., & Duering, E. R. (1992). Kinetics of End Crosslinking in Dense Polymer Melts. <u>Europhysics Letters</u>, 19 (3), 195-200.
- Grest, G. S., Kremer, K., & Duering, E. R. (1993). Kinetics and relaxation of end crosslinked polymer networks. <u>Physica A, 194,</u> 330-337.
- Hölzl, T., Trautenberg, H. L., & Göritz, D. (1997). Monte Carlo Simulations on Polymer Network Deformation. Physical Review Letters, 79 (12), 2293-1342.
- Kau, C., Hiltner, A., Baer, E., & Huber, L. (1989). Damage Processes in Reinforced Reaction Injection Molded Polyurethanes. <u>Journal of Reinforced Plastics and Composites</u>, 8, 18-39.

- Kenkare, N. R., Hall, C. K., & Khan, S. A. (1999). Pressure-volume properties of endlinked hard-chain polymer networks. <u>Journal of Chemical Physics</u>, 110 (15), 7556-7573.
- Kenkare, N. R., Smith, S. W., Hall, C. K., & Khan, S. A. (1998). Discontinuous Molecular Dynamics Studies of End-Linked Polymer Networks. Macromolecules, 31 (17), 5861-5879.
- Kroschwitz, J. I. et al. (Ed.). (1997). Urethane Polymers. <u>Kirk-Othmer</u>
 <u>Encyclopedia of Chemical Technology</u> (Vol. 24, pp. 695-726). New York: John Wiley & Son, Inc.
- Kumar, S. K., Vacatello, M., & Yoon, D. Y. (1988). Off-lattice Monte Carlo simulations of polymer melts confined between two plates. <u>Journal of Chemical Physics</u>, 89 (8), 5206-5215.
- Lay, S., Sommer, J., & Blumen, A. (1999). Comparison of structural properties of different polymer network types as obtained by computer simulation. <u>Journal of Chemical Physics</u>, 110 (24), 12173-12182.
- Li, X., & Chiew, Y. C. (1994). Monte Carlo simulation of Lennard-Jones chains. Journal of Chemical Physics, 101 (3), 2522-2531.
- Macosko, C. W. (1989). <u>RIM Fundamentals of Reaction Injection Molding.</u> New York: Hanser Publishers.
- Metropolis, N., Rosenbluth, A. W., Rosenbluth, M. N., Teller, A. H., & Teller, E. (1953). Equation of State Calculations by Fast Computing Machines. Journal of Chemical Physics, 21 (6), 1087-1092
- Nath, S. K., McCoy, J. D., Curro, J. G., & Saunders, R. S. (1995). Density Functional Theory of Polymer-Polymer Phase Separation Behavior. <u>Journal of Polymers Science: Part B: Polymer Physics, 33,</u> 2307-2317
- Plischke, M., & Barsky, S. J. (1998). Molecular dynamics study of the vulcanization transition. Physical Review E, 58 (3), 3347-3352
- Rosenbluth, M. N., & Rosenbluth, A. W. (1955). Monte Carlo Calculation of the Average Extension of Molecular Chains. <u>Journal of Chemical Physics</u>, 23 (2), 356-359.
- Schulz, M., & Sommer, J. U. (1992). Monte Carlo studies of polymer network formation. Journal of Chemical Physics, 96 (9), 7102-7107

- Schwarz, E.G., Critchfield, F.E., Tackett, L. P., & Tarin, P. M. (1979). Silane Effects and Machine Processing in Reinforced High Modulus RIM Urethane Composites. <u>Journal of Elastomers and Plastics</u>, 11, 280-300.
- Siepmann, J. I., & Frenkel, D. (1992). Configurational bias Monte Carlo: a new sampling scheme for flexible chains. <u>Molecular Physics</u>, 75 (1), 59-70.
- Sommer, J. U. (1994). Structural properties and swelling behavior of randomly crosslinked polymer networks: A Monte Carlo Study. <u>Macromolecular Symposia</u>, 81, 139-152.
- Sommer, J. U., Schulz, M., & Trautenberg, H. L. (1993). Dynamical properties of randomly cross-linked polymer melts: A Monte Carlo study. I. Diffusion dynamics. <u>Journal of Chemical Physics</u>, 98 (9), 7515-7520.
- Trautenberg, H. L., Sommer, J. U., & Göritz, D. (1995). Structure and Swelling of End-linked Model Networks. <u>Journal of the Chemical Society</u>. Faraday transactions, 91 (16), 2649-2653.
- Van Krevelen, D. W. (1990). <u>Properties of Polymers</u> (3rd ed.). New York: Elsevier Science Publishers.
- Vargas, E., & Barbosa, M. C. (1998). Phase diagram for irregular and non-symmetric cross-linked polymer blends. Physica A, 257, 312-318.
- Yang, P. C., & Lee, W. M. (1987). Fracture Mechanism Study of Flake Glass Filled RIM Urethane Systems. <u>Journal of Elastomers and Plastics</u>, 19, 120-146.

General References

- Frenkel, D., & Smit, B. (1996). <u>Understanding Molecular Simulation: From Algorithms to Applications.</u> San Diego, CA: Academic Press
- Rowley, R. L. (1994). <u>Statistical Mechanics for Thermophysical Property</u>
 <u>Calculations.</u> Englewood Cliffs, NJ: Prentice Hall.

